

**“Radical Clock Investigation with a MetalloPorphyrin
Enzyme Model”**

INAUGURAL DISSERTATION

zur

Erlangung der Würde eines
Doktors der Philosophie

vorgelegt der

Philosophisch-Naturwissenschaftlichen Fakultät



der

Universität Basel

von

Laura Sbaragli

aus Rufina

Italien

Basel 2005

Genehmigt von der Philosophisch-Naturwissenschaftlichen Fakultät der Universität Basel auf
Antrag der Herren:

Prof. Dr. Wolf-D. Woggon

Prof. Dr. Edwin. C. Constable

Prof. Dr. Urs Séquin (Chairman)

Basel, den 24.Mai 2005

Prof. Dr. Hans-Jacob Wirz (Dekan)

The work presented was initiated and guided by Prof. Dr. Wolf-D. Woggon at the Department of Chemistry of the University of Basel, during the period from August 2000 to October 2004.

This work is present in the following publications:

“Reactivity of a new class of P450 enzyme models.” Meyer, Dominik; Leifels, Tycho; Sbaragli, Laura; Woggon, Wolf-D. *Biochem. and Biophys. Research Communications* (2005), 338(1), 372-377.

“On the Mechanism of Cytochrome P450-Catalyzed Oxidations: Reaction of a New Enzyme Model with a Radical Clock” Sbaragli, Laura; Woggon, Wolf-D. *Synthesis* (2005), No.9, 1538-1542

“New synthetic models of cytochrome P450: how different are they from the natural species?” Kozuch, Sebastian; Leifels, Tycho; Meyer, Dominik; Sbaragli, Laura; Shaik, Sason; Woggon, Wolf-D. *Synlett* (2005), (4), 675-684.

“Design and synthesis of new P450 enzyme mimics. Cytochromes P450: Biochemistry, Biophysics and Drug Metabolism” Woggon, W.-D.; Leifels, T.; Sbaragli, L. *International Conference on Cytochromes P450, Prague, Czech Republic, (2003)*

I wish to thank:

- Prof. Dr. Wolf Woggon for his continuous support during the realization of this work, for many stimulating discussions and for his confidence to let me work in generous freedom,
- Prof. Dr. Antoinette Chougnat for experimental advices. Dr. Klaus Kulicke and Dr. Daniel Häussinger for their help with the interpretations of many NMR-spectra. Dr. Heinz Nadig for his MS-spectra.
- Prof. Dr. Edwin Constable for agreeing to co-referee this thesis
- All members of the Woggon's group for their help, the interesting discussions, the good atmosphere and the fun during work and spare time.

TABLE OF CONTENTS

Theoretical part

1. Introduction	1
1. 1. Heme Proteins	1
1.1.1 Classification of Cytochrome P450	5
1.1.2 CYP2B1 and CYP2E1	5
1. 2. The Catalytic Cycle of Cytochrome P450	6
1.2.1 The role of axial ligand in heme-based catalysis	8
1.2.2 Electrophilic Oxidative Species in the Catalytic Cycle	9
1. 3. P450 Oxidation Mechanism	10
1. 3. 1. From the Rebound Theory to the Two Oxidant Theory	10
1. 3. 2. Evidence from experiments with genetically engineered P450 enzymes	18
1. 3. 3. A theoretical approach of monooxygenation mechanisms by P450 enzymes.....	22
1. 3. 4. The Exact Nature of the Transition State.....	28
2. Description of the Problem and Aim of this Work	30
3. Porphyrin and Probe Synthesis.....	32
3. 1. Towards the Synthesis of a First Porphyrin Model.....	32

3. 2. Synthesis of porphyrins 38 and 39 - first models for mimicking the prosthetic porphyrin IX active site of P450.....	33
3. 3. Optimization of reaction conditions for radical clock experiments.....	48
3. 4. Synthesis of porphyrins 55 - novel model for mimicking the prosthetic porphyrin IX active site of P450.	49
3. 5. Synthesis of the cyclopropyl derivatives – slow and fast radical clocks.....	56
4. Radical Clock Experiments and Discussion.....	59
4. 1. Radical Clock Experiments	59
4. 1. 1. Slow Radical Clock Experiments	59
4. 1. 2. Fast Radical Clock Experiments.....	62
4.1.3. Proposed Mechanism	67
5. Future Directions.....	71
6. Summary	73

Experimental Part

7. Experimental Part.....	75
7. 1. General Remarks	75
7. 1. 1. Solvents and Reagents.....	75
7. 1. 2. Materials & Instruments	75

7. 1. 3. Chromatographic Methods	76
7. 1. 4. Spectroscopic Methods	77
7. 2. Syntheses	79
7. 2. 1. Cyclopropyl Derivatives and Related Synthetic Studies	79
7. 2. 2 Pivaloyl Porphyrins	89
7. 2. 3. Dichloroporphyrin.....	104
7.3. Porphyrin catalyzed oxidations.....	110
7.3. 1. General procedure for catalytic oxidation of probe 45	110
7.3. 2. Qualitative Enzymatic Experiments with Rat Liver Microsomes, CYP 2B1 and 2E1. ..	112
7.3. 3. General procedure for catalytic oxidation of probe 10	114

Appendix

8. References	119
9. Curriculum Vitae.....	127
10. Eidesstattliche Erklärung	12

THEORETICAL PART

1. Introduction

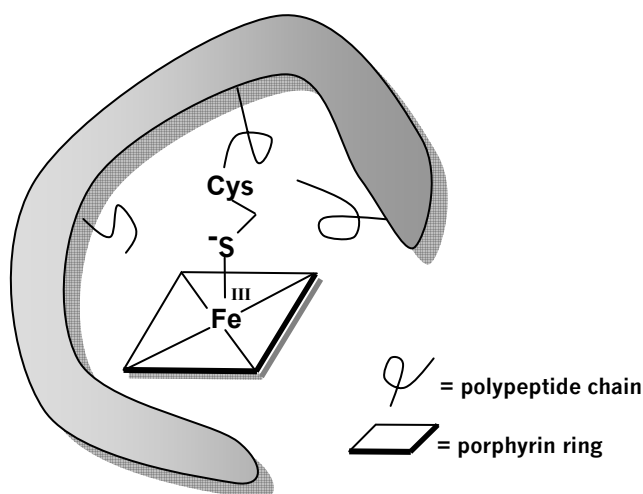
1.1 Heme Thiolate Proteins

Heme thiolate proteins belong to a class of heme proteins where the heme iron fifth ligand is a thiolate group (typically of a Cys residue). These proteins are found in organisms from all domains of life and are major catalysts in the oxidative biotransformation of a structural diversity of endogenous and exogenous compounds.^{1,2}

A distinctive feature of heme-thiolate proteins is a Soret absorption band at around 450 nm in the CO difference spectrum of reduced forms.³ The class includes the following families:

- Heme chloroperoxidase
- Nitric oxide synthase
- P450 enzymes (P450s), also known as cytochromes P450

Figure 1. Representation highlighting the sulfur atom / Cys residue of the heme-thiolate porphyrin inside the largely hydrophobic enzyme pocket.

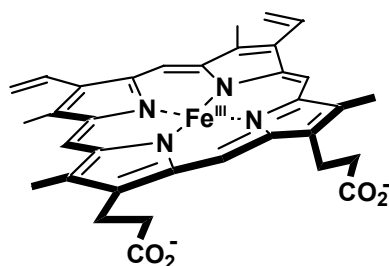


The 3D-structure of a protein can provide valuable insights into its function. Ideally, experimental techniques such as X-Ray crystallography, nuclear magnetic resonance (NMR) spectroscopy, and electron microscopy are used to determine the 3D-structure of proteins. Regrettably, the majority of proteins are currently not open to these techniques as they are difficult to crystallize, insufficiently soluble, or too large for NMR studies. One of the best alternative methods developed to determine the 3D-structure is the comparative (or homology) modeling technique.⁴

To date structural models of human P450s were based on known, distantly related, bacterial P450s.⁵ Yet the recent determination of the crystal structure of the more closely related rabbit CYP2C5⁶ has improved the reliability of comparative models for human P450s.⁷ Also, the availability of crystal structures of human CYP2C9^{8, 9} and CYP2C8¹⁰ can help in the determination of the structures of the major CYP2 metabolizing forms (CYP2A6, 2C19, 2D6, and 2E1). Two distinct research groups¹¹⁻¹³ have recently independently determined the crystal structure of truncated forms of CYP3A4. Cytochrome P4503A4 is highly expressed in human liver, it is able to oxidize a large number of structurally diverse substrates and contributes extensively to human drug metabolism.

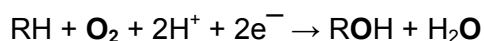
For the chloroperoxidase from *Caldariomyces fumago*^{14,15} and murine iNOS oxygenase domain¹⁶ the X-Ray structures were determined circa 10 years ago. Surprisingly the active site of all these enzymes is extraordinarily simple, with an iron protoporphyrin IX buried deep in a hydrophobic, substrate-binding pocket of the protein scaffold.

Figure 2. Iron(III)-protoporphyrin IX



Iron(III) protoporphyrin IX

Cytochromes P450 are oxidoreductases that activate molecular oxygen (O_2) and incorporate one of the oxygen atoms into a large variety of biological substrates, with concurrent two electron reduction of the other oxygen atom to H_2O .



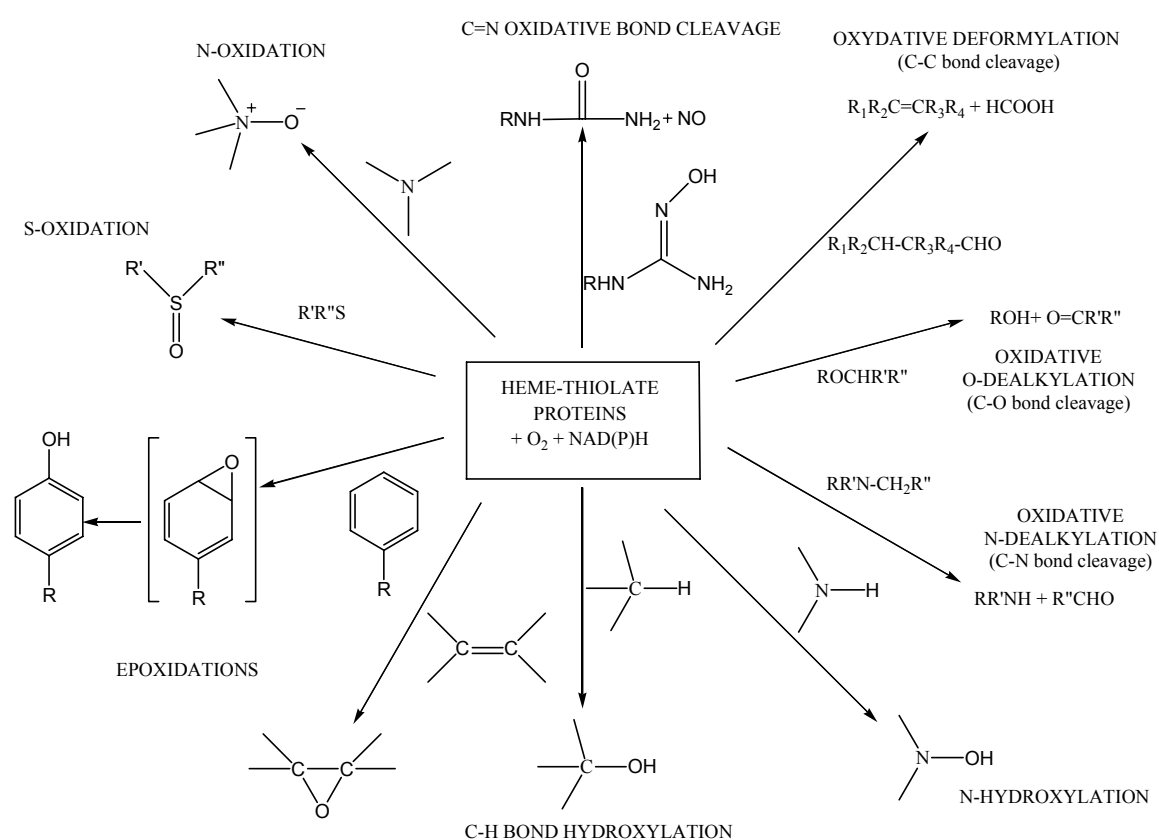
In many, but not all P450 enzymes, and in the biomimetic systems, it is possible to circumvent the stepwise activation of molecular oxygen by providing H_2O_2 or another small peroxide as a co-substrate in what is termed the “shunt” oxidation mechanism (*Scheme 2*). However, the catalytic turnover, supported by peroxides, can give product distributions that differ from those obtained under normal catalytic conditions^{17,18} and results in accelerated degradation of the prosthetic heme group.¹⁹

Cytochromes P450, of course, do not function only as monooxygenases but also as reductases. For example the CYP101 (cytochrome P450_{cam}) from *Pseudomonas putida*, which naturally catalyses the oxidation of camphor,¹⁷ has been shown to catalyze the

reductive dehalogenation of haloaliphatic compounds.^{20,21} And P450nor, found in the denitrifying fungus *Fusarium oxysporum*,²² can reduce NO_3^- and NO_2^- to N_2O .

The P450 structure, biochemistry and molecular biology have been extensively reviewed in the last decade.^{23,24} Such enzymes have been extracted and isolated from almost every mammalian tissue (e.g. liver, kidney, lung, intestine and adrenal cortex), as well as insects, plants, yeast and bacteria. As monooxygenases they are known to catalyze hydroxylations, epoxidations, N-, S- and O-dealkylations, heteroatom oxidations and oxidative cleavage of C-C bonds (see Scheme 1).

Scheme 1. General Oxidative Metabolic Activity Scheme of diverse Heme Thiolate Proteins

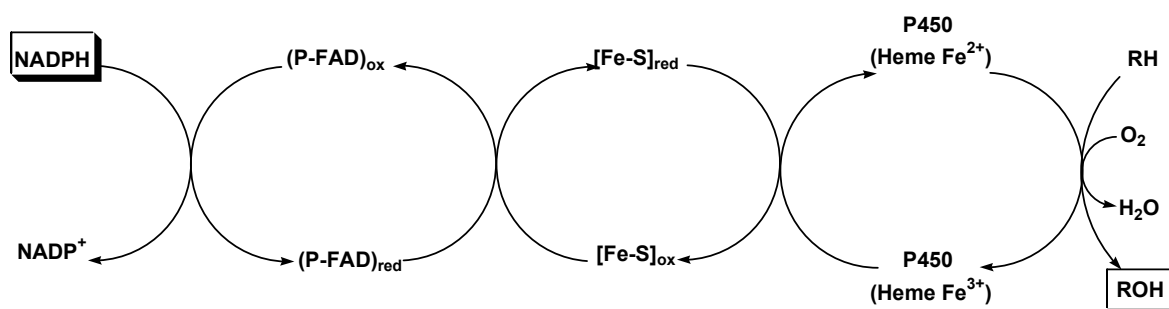


These oxygenation reactions play, for example, an essential role in drug metabolism and xenobiotic detoxification, carcinogen activation and steroid and prostaglandin biosynthesis.

As already mentioned above, for cytochrome P450s to function, they also need a source of electrons. The addition of two electrons (reduction) to the heme iron makes the difficult chemistry of breaking the oxygen-oxygen bond possible. The electrons are donated by another protein that binds to the P450 and passes an electron from a prosthetic group. There are two different kinds of electron transfer chains for cytochrome P450s both of which depend on the location of the enzyme in the cell.

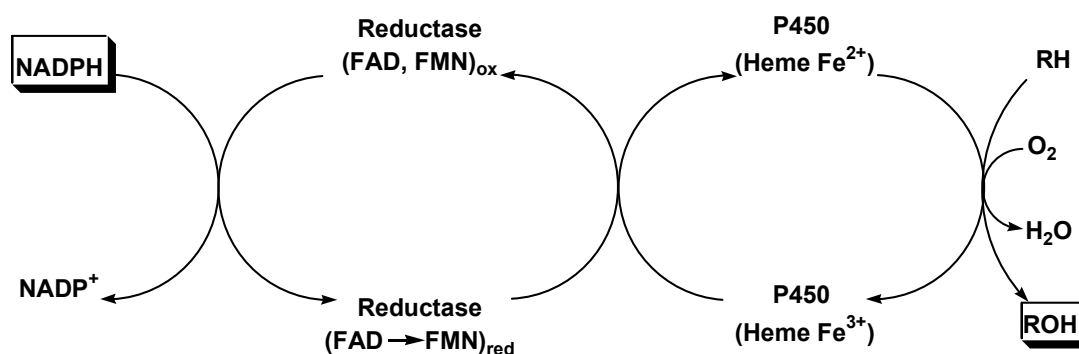
For the P450s found in the mitochondrial inner membrane or for the bacterial P450s, the electron transfer chain consists of a three protein system (**Type I**).²⁵ Ferredoxin (called adrenodoxin in the adrenals, but exactly the same gene codes for both proteins) is the immediate donor of electrons to the P450s in mitochondria. Ferredoxin has an iron sulfur cluster instead of a flavin, however, ferredoxin is reduced by ferredoxin reductase (or adrenodoxin reductase in the adrenals) that does contain a flavin. NADPH is the source of electrons that flow from ferredoxin reductase to ferredoxin and then to P450.

Figure 3. Electron chain for Type I P450s



For microsomal P450s situated in the endoplasmic reticulum (ER) the NADPH-cytochrome P450 reductase is again the electron source (**Type II**).^{26,27} This reductase is a membrane bound protein by an N-terminal tail that crosses the ER membrane once and it has two domains each containing one flavin. Two electrons are acquired from NADPH and migrate from FAD to FMN, then to the P450 heme iron. In some special cases of the microsomal P450s reactions the participation of NADH-cytochrome b5 reductase/cytochrome b5 electron transport system was observed.²⁸

Figure 4. Electron chain for Type II P450s



Type III enzymes do not require an exogenous source of electrons, as they already employ oxygen-containing substrates.²⁹ **Type IV** enzymes receive electrons directly from reduced pyridine nucleotides, without the intervention of an electron carrier.³⁰

1.1.1. Classification of Cytochrome P450

The P450 proteins are categorized into families and subfamilies by their sequence similarities. Sequences that are greater than 40% identical at the amino acid level belong to the same family. Sequences that are greater than 55% identical are in the same subfamily. There are now more than 2500 cytochrome P450 sequences known.

The nomenclature for the P450 gene superfamily is based on evolutionary relationships. **CYP** is the abbreviation for Cytochrome P450, the first numeral **n** signifies the gene-family, the capital letter for the gene-subfamily and the last numeral **m** is the gene number.³¹⁻³³

1.1.2 CYP2B1 and CYP2E1

Typical **CYP2B** substrates are 7-benzyloxyresorufin, 7-ethoxy-4-trifluoromethylcoumarin, benzphetamine, and testosterone. An intriguing aspect of many P450 enzymes, especially those of family **CYP2**, involves the differential regio- and stereoselectivity among structurally related proteins.³⁴ The phenobarbital inducible rat cytochromes **P450 2B1** and **2B2** are 98% identical, differing by only 13 amino acids. **P450s 2B1** and **2B2** have similar substrate specificities; however, in most cases **P450 2B1** has significantly higher catalytic activity than **P450 2B2**. The critical residues involved in substrate binding and catalysis by **P450 2B1** have been extensively studied using site-directed mutagenesis, susceptibility to inhibition by mechanism-based inactivators, and homology modeling based on the crystal structures of bacterial P450s and **P450 2C5**.³⁵⁻³⁹

The cytochrome **2E1** was discovered in rabbit liver microsomes and purified and characterized by *Koop, Morgan and Tarr*.⁴⁰ **CYP2E1** possesses the peculiar characteristic of being an ethanol-inducible cytochrome P450. **CYP2E1** displays the highest activity of the rabbit isozymes in the oxidation of ethanol to acetaldehyde and can also oxidize other alcohols, aniline, and several drugs.⁴¹ Although this "microsomal ethanol-oxidizing system"⁴² may not be a major pathway for alcohol oxidation under most circumstances, the increased levels of **2E1** resulting from the diabetic state, fasting, and exposure to ethanol and several other diverse agents, is a cause for concern because of resulting toxicities.⁴³ In particular, acetaminophen, a widely used antipyretic and analgesic drug, is normally non toxic, but in large doses it produces acute hepatic necrosis when converted to its active metabolite. Of a series of P450 isozymes examined, **2E1** was one of the most active in producing this metabolite.³⁹

The mechanism of action of these enzymes has captivated researchers in this area for many years. The oxidative metabolic catalytic cycle performed by cytochrome P450 has been partially determined and will be examined in the following chapter.

1. 2. The Catalytic Cycle of Cytochrome P450

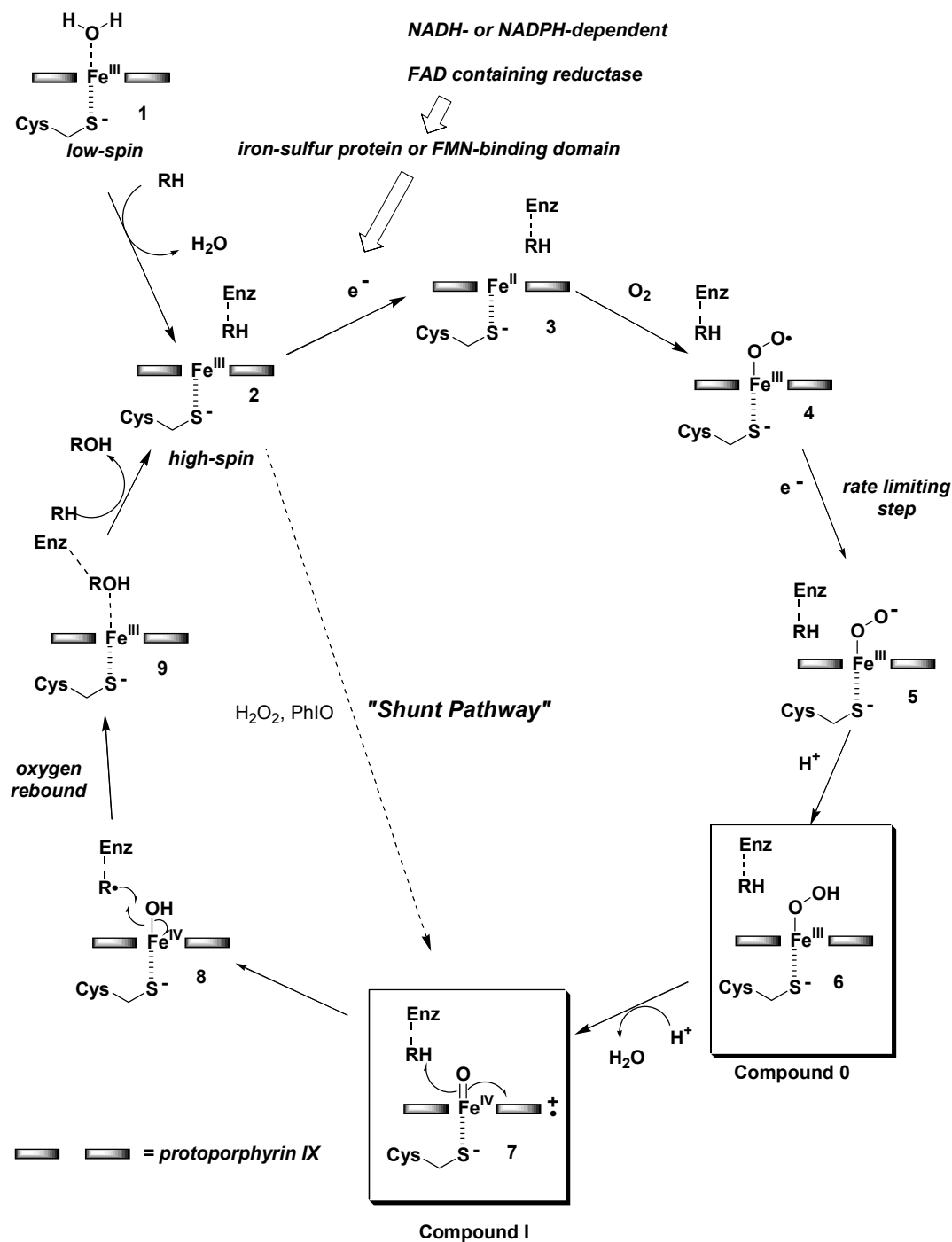
A conventional consensus on the mechanism of P450s,⁴⁴ the rebound mechanism in *Scheme 2*, has been attained from crystallographic and spectroscopic studies of different forms of P450_{cam} jointly with mechanistic studies with labeled substrates and substrate analogues. Nonetheless, several mechanistic features still remain unresolved.

The binding of a substrate⁴⁵ to the low spin ferric (Fe^{III}) resting state **1** causes a lowering of the redox potential,⁴⁶ which makes the transfer of an electron favourable from the cytochrome P450 reductase. This is accompanied by a change in the spin state of the heme iron at the active site, with a shift of the spin equilibrium from predominantly low-spin to almost completely high-spin of the enzyme-substrate complex **2**. This spin equilibrium sets off the entry into the catalytic cycle. It has also been suggested that the binding of the substrate brings about a conformational change in the enzyme which triggers an interaction with the redox component.

The next stage in the cycle is the reduction of the (Fe^{III})-complex **2** to give the ferrous (Fe^{II}) substrate complex **3** by an electron from the reductase. Subsequently an oxygen molecule binds to form the low spin, diamagnetic (d⁶, S = 0) intermediate **4**. Previous spectroscopic techniques alluded to a ferric superoxide (Fe^{III}-O₂⁻) species as opposed to a ferrous species (Fe^{II}-O₂).^{47,48} Only recently “time-lapse” study of the catalytic cycle of P450_{cam} using trapping techniques and cryocrystallography by *Schlichting* provided a high resolution structure (1.8 Å) of the dioxygen complex **4**.⁴⁹

A second mono-electron reduction gives ferric peroxo complex (Fe^{III}-OO⁻) **5**. This has been determined to be the rate-determining step of the reaction.⁵⁰

Scheme 2. The consensus mechanism of P450 hydrocarbon hydroxylations



It is difficult to define correctly the next steps of the catalytic cycle (**5-9**) due to the instability of the intermediates formed. Groves *et al.*⁴⁴ put forward a rebound mechanism. Accordingly the distal oxygen atom of the peroxo complex **5** is protonated to give a hydroperoxide complex (Fe^{III}-OOH) **6**. A subsequent protonation on the same oxygen atom brings about a heterolytic O-O bond cleavage which results in water release and the generation of the oxo-ferryl (Fe^{IV}) porphyrin radical intermediate Por⁺ (Fe^{IV}=O) **7**. This

intermediate is equivalent to the high-valent iron-oxo species of peroxidase enzymes, commonly known as Compound I.⁵¹ Groves suggested that this species **7** Por⁺ (Fe^{IV}=O) abstracts a hydrogen atom from the enzyme bound substrate providing a carbon-centered radical with a finite lifetime and hydroxo ferryl complex **8**. In the subsequent *oxygen rebound* step a transfer of the oxygen atom to the enzyme-bound substrate radical is proposed. This results in the formation of the low-spin ferric enzyme-product complex **9**. The catalytic cycle is closed once the oxidized product dissociates from the active site.

1.2.1 The role of axial ligand in heme-based catalysis

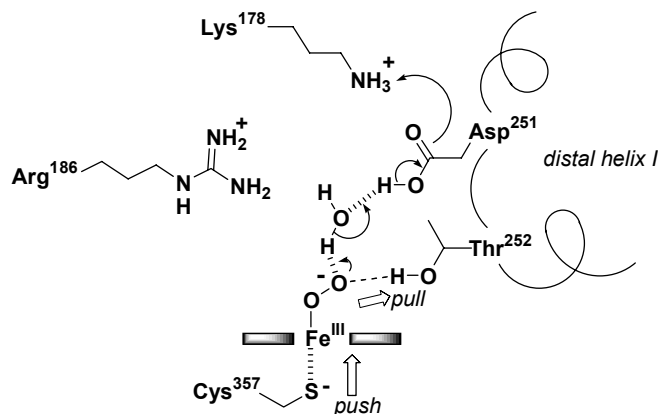
As already mentioned in the introduction, the common structural characteristic of these enzymes is the heme-thiolate (Fe-S-) coordination in their active sites.¹⁷

The strong electron-releasing character of the thiolate ligand has been assumed to serve as the “push” effect that enables the heterolytic O-O bond scission to generate the activated iron (IV)-oxo species commonly called Compound I.⁵² Furthermore, the electronegative thiolate group should determine the redox potential of the heme in these enzymes to accept electrons from their redox partners and to stabilize the electron-deficient active species.¹⁷ However, the regulation mechanism of these functions by the thiolate ligand has not been fully clarified. It has been previously stated that the conserved NH-S hydrogen bonds, between the thiolate ligand and the protons from the surrounding polypeptide amides, have been assumed to control the functions of the heme thiolate enzymes by neutralizing the negative charge on the thiolate.⁵³ Density functional calculations⁵⁴ have been used to explore the nature of this *push effect*. The calculations confirmed its existence and proved that this force is energetically a significant quantity.

Nevertheless, the *push effect* of the cysteinate ligand cannot, by itself, carry out the cleavage of the O-O bond. In fact it requires a proton source to permit the distal (outer) oxygen of the bound peroxide of **5** (Fe^{III}-OOH) to be released as a water molecule. Using crystallographic and kinetic isotope studies on the wild-type and D251N mutant of P450_{cam}, *Sligar* proposed a proton shuttle system.^{55,56} This proton delivery scheme involved two water molecules in the active site and two distal site amino acids, Asp251 and Thr252. In this proposal Thr252 and Asp251 construct a proton relay network that facilitates, in tandem with two other charged residues (Arg186 and Lys178), the network's arrival at the surface solvent thus supplying a conduit for protons (Figure 5). This *push-pull mechanism*, which is also

found in horse radish peroxidase (HRP),⁵⁷ is sustained by crystal structures seen in the “snap-shot” study of *Schlichting et al.*⁴⁹

Figure 5. Proton delivery system



1.2.2 Electrophilic Oxidative Species in the Catalytic Cycle

In the P450 reaction scheme, two potential oxidants with electrophilic reactivity are formed. These are designated the ferric-hydroperoxo species ($\text{Fe}^{\text{III}}\text{-OOH}$) or **Compound 0** and the high-valency ferryl-oxo π -cation radical Por^+ ($\text{Fe}^{\text{IV}}=\text{O}$) or **Compound I** (6 and 7 in *Scheme 2*). As these intermediates are short-lived in nature, their isolation and characterization has proven to be an elusive task.

Hoffman, Sligar and co-workers⁵⁸⁻⁶⁰ have lately used γ -radiation to generate hydrated electrons in situ at low temperatures to reduce oxyferrous D251N, T252A, and wild-type CYP101. EPR, ENDOR and electronic absorption spectroscopy were then used to directly observe the peroxo and hydroperoxo states.⁵⁸⁻⁶² Using the same radiolytic reduction of the oxy-ferrous horseradish peroxidase (HRP) at 77 K, *Sligar*⁶³ observed the formation and decay of the putative intermediate hydroperoxo-ferric complex (Cpd0). EPR and UV-visible absorption spectra showed that protonation of the primary intermediate of radiolytic reduction, the peroxo-ferric complex ($\text{Fe}^{\text{III}}\text{-OO}^-$) **5**, to form the hydroperoxo-ferric complex ($\text{Fe}^{\text{III}}\text{-OOH}$) **6** is completed only after annealing at temperatures 150–180 K. This approach has sadly not led to direct detection of the elusive P450 Cpd I species, yet its involvement in catalysis could be inferred.⁵⁸ *Schlichting et al.*⁴⁹ reported the low-temperature X-ray crystallographic characterization of oxyferrous P450 under conditions known to produce hydrated electrons. They witnessed a form of the enzyme that was cautiously identified as P450 Compound I, even if other species could not be excluded. *Kellner* have also inferred Cpd I existence by using transient electronic spectroscopy and decay kinetics.⁶⁰

More solid kinetic analysis of Cpd I formation and decay was given by *Ishimura, Sligar* and their co-workers using stop-flow experiments.^{64, 65} By mixing substrate-free ferric P450 with *m*-chloroperoxybenzoic acid, both groups observed a transient derivative with an absorption spectrum that showed a good similarity to that of *C. fumago* chloroperoxidase Compound I.

Further evidence for the participation of a second electrophilic oxidant in P450-catalysed reactions has come from studies of substrate oxygenations by P450 active-site mutants with impaired hydroxylase activity (see chapter 1.3.2.).^{44, 66-69}

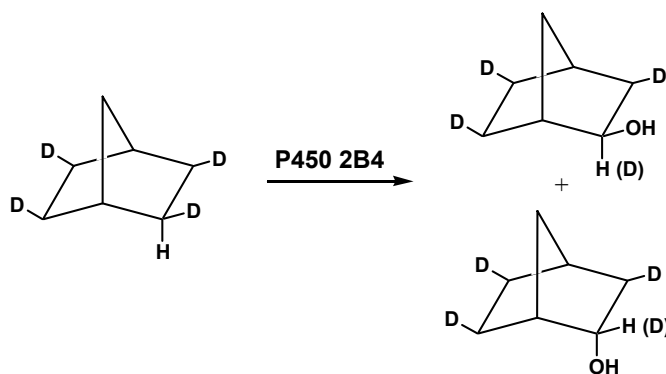
1. 3. P450 Oxidation Mechanism

1.3.1. From the Rebound Theory to the Two Oxidant Theory

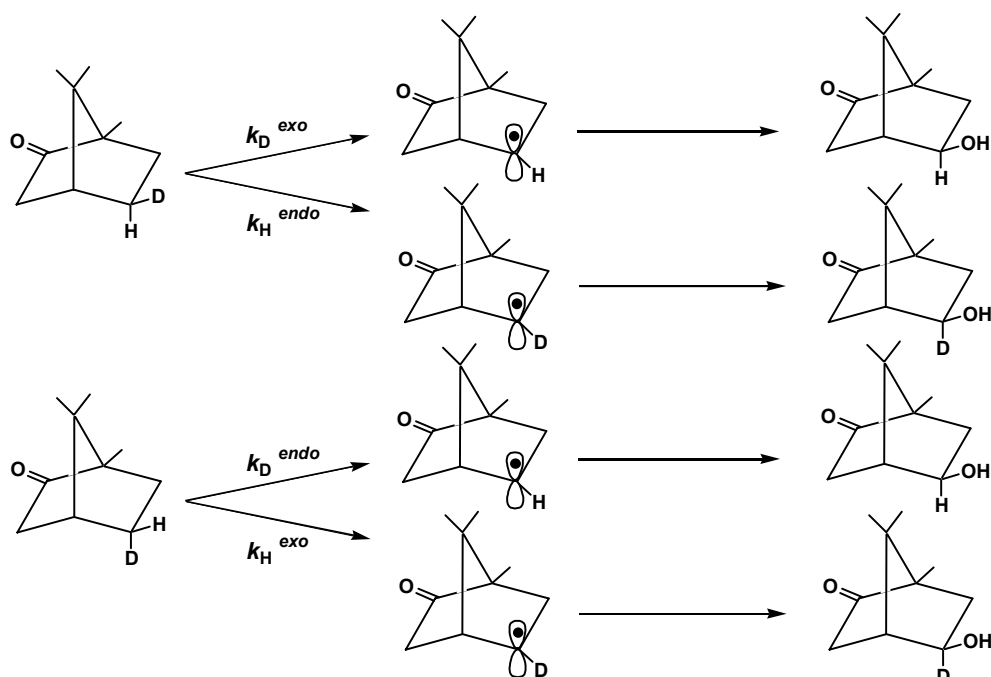
The rebound mechanism formulated in the original studies of *Groves*⁴⁴ (see chapter 1.2) has gained support by the results from a variety of experiments favoring the existence of a discrete radical intermediate.⁷⁰⁻⁷⁹

One example is the strong kinetic intramolecular isotopic effects ($k_H/k_D > 11$) observed for the first time by *Hjelmeland*⁷⁰ and by *Groves*⁷¹ respectively for benzylic and aliphatic hydroxylation performed by P450s. The lack of a carbocation rearrangement and the extremely low acidity of typical aliphatic C-H bonds suggested a two step radical mechanism. Additional proof of the existence of a radical intermediate was attained when stereochemical scrambling, for example, in cytochrome P450-2B4 hydroxylation of the *exo-d*₄ norbornane was detected⁷¹ (*Figure 6*).

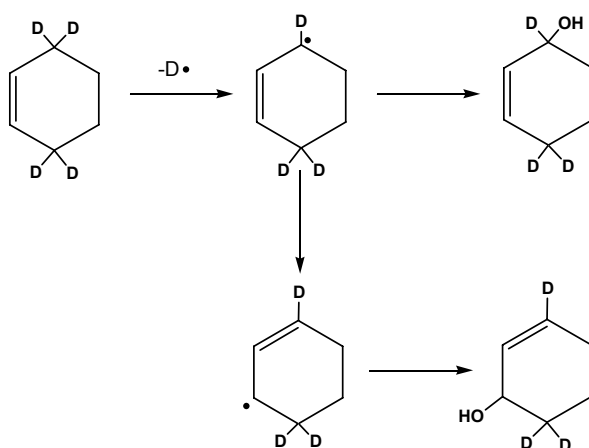
Figure 6. Stereochemical scrambling in the P450 hydroxylation of *exo-d*₄ norbornane



This scrambling phenomenon was also observed by *Sligar et al.* in the camphor hydroxylation with P450cam (CYP101), which had the ability to extract either an *exo* or *endo* hydrogen but delivered the oxygen solely to produce the *exo*-hydroxy isomer (*Figure 7*).⁷²

Figure 7. Stereochemical scrambling in P450 camphor hydroxylation

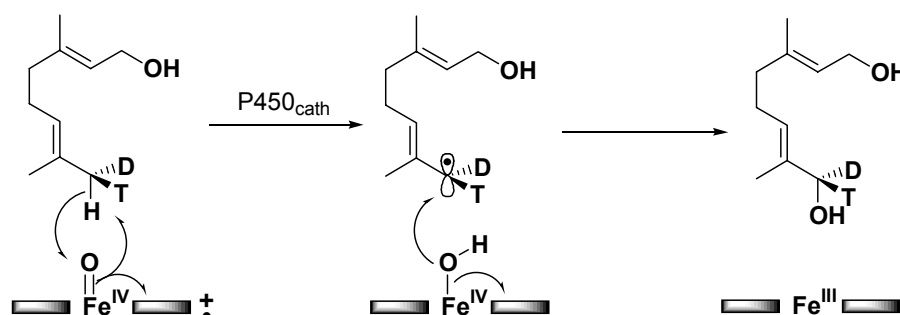
In another publication *Groves*, in the P450-2B4 hydroxylation of (3,3,6,6- d_4) cyclohexene, reported an allylic rearrangement of the hexene double bond.⁷⁴ This allylic shift was attributed to a hydrogen atom abstraction from the allylic site and a subsequent geminate, cage recombination of the incipient allylic free radical (*Figure 8*).

Figure 8. Allylic rearrangement in the P450 hydroxylation of (3,3,6,6- d_4) cyclohexene.

Nevertheless, *Woggon et al.*⁸⁰ alleged that this allylic rearrangement was faster than the trapping by the hydroxyl radical delivered by the PorFe^{IV}-OH **8** (see *Scheme 2*) due to the cyclic nature of the substrate. In support of this statement they performed an allylic enzymatic oxidation of an open system. P450_{Cath}-catalyzed hydroxylation of both enantiomers of

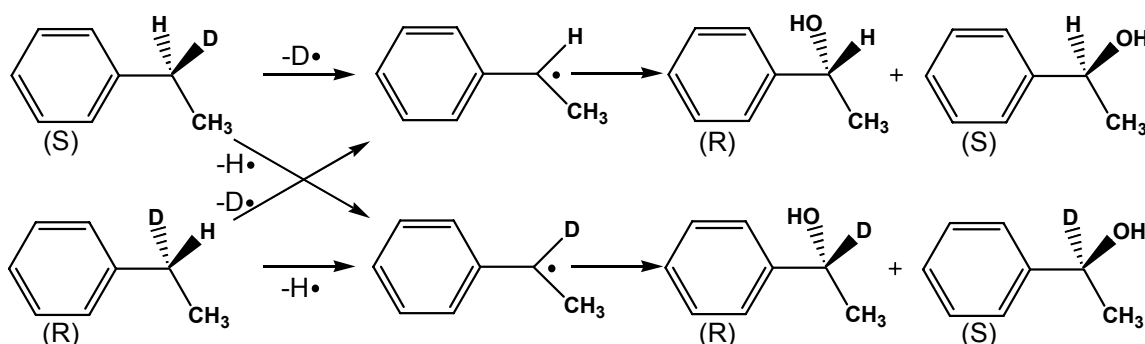
geraniol, which is chiral by virtue of isotopic substitution on the terminal methyl group (see *Figure 8b*), showed a very high level of regio- and stereospecificity, indicating that the radical intermediate was short-lived.

Figure 8b. P450_{Cath}-catalyzed hydroxylation of chiral geraniol.



White et al. determined that the *S* and *R* enantiomers of (1-*d*₁) ethylbenzene were hydroxylated by P-450_{LM2} with very high regioselectivity at the benzylic position and that a moderate preference (4:1) was exhibited for pro-*S* hydrogen removal.⁷⁵ *White* noticed also that an appreciable fraction (25-40%) of the hydroxylation events involved crossover of stereochemistry between the hydrogen-abstraction and oxygen-delivery steps (*Figure 9*). This observation required that a tri-coordinate benzylic carbon atom had to have been a discrete intermediate.

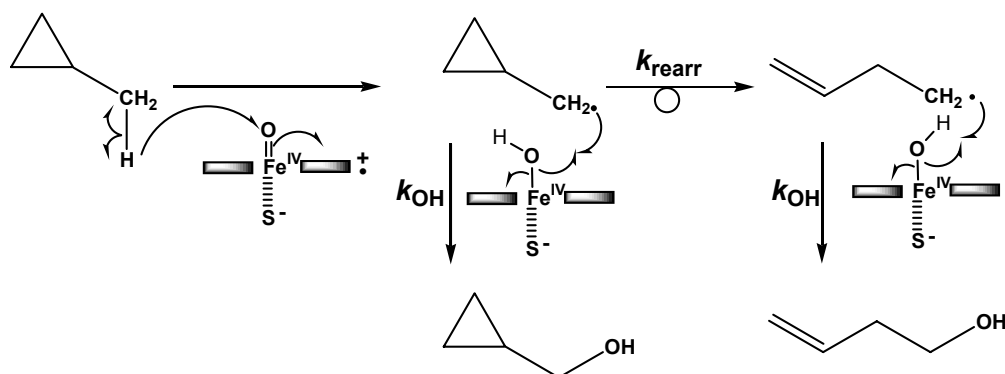
Figure 8. Regioselectivity in the P450 hydroxylation of *S* and *R* enantiomers of (1-*d*₁) ethylbenzene.



Dinnocenzo and Jones et al.^{76, 77} provided more indirect evidence for this rebound mechanism using KIE measurements. They found that for several aryl methanes the KIE's of P450 hydroxylation equate to those of an equivalent hydrogen abstraction reaction by *tert*ial butoxyl radical. Both processes necessitate isostructural transition states. All these results suggested that an intermediate species, most probably a radical, was formed in the hydroxylation reaction.

To verify the existence of the hydrocarbon radical intermediate and explore its lifetime “radical clock” experiments were undertaken. The pioneering experiments were performed with a radical clock consisting of a cyclopropyl ring bonded to the carbon that is proposed to become a radical centre during the course of the reaction. The three-membered rings have an inherent strain which causes such cyclopropyl carbonyl radicals to quickly and essentially irreversibly rearrange⁸¹ to the corresponding homoallylic radical. The ratio of products derived from the cyclopropyl carbonyl radical *versus* the homoallylic radical is thus determined by their relative magnitudes of the rate constants for radical quenching ($k_t = k_{OH}$, Figure 10) and rearrangement ($k_r = k_{rearr}$, Figure 10).

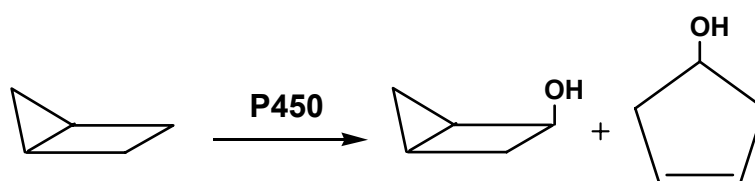
Figure 10. Measurement of k_{OH} of a cyclopropyl radical clock



Since the rate of rearrangement can be independently measured, the ratio of unrearranged to rearranged product allows the determination of both the rate of radical quenching (oxygen rebound) and the lifetime of the radical intermediate. Initial experiments with a variety of substrates containing relatively simple cyclopropyl rings ($k_r = 1\text{--}4 \times 10^8 \text{ s}^{-1}$ at 37°) yielded only unrearranged product.^{78, 79, 82} Thus, either a radical intermediate was not present or its rebound rate was much faster than that of the rearrangement.

Bicyclo[2.1.0]pentane (Figure 11) was then subjected to P450-catalyzed hydroxylation by *Ortiz de Montellano and Sterns*⁸³ since this hydrocarbon would yield a radical which was known from studies by *Jamieson et al* to rearrange ($k_r = 2.4 \times 10^9 \text{ s}^{-1}$) more rapidly than cyclopropylmethyl radical.⁸⁴

Figure 11. P450-catalyzed hydroxylation of Bicyclo [2.1.0] pentane



Due to the extra strain of the system the rearrangement rate is faster than the recombination rate and the P450 oxidation reaction produced rearranged and unrearranged products that allowed a rebound rate of $1.4 \times 10^{10} \text{ s}^{-1}$ to be calculated.⁸⁵ Similar oxidation experiments performed much later with norcarane and spiro[2, 4]octane gave comparable values to that above in the range of 10^{10} s^{-1} . In this case the oxidation of norcarane and spiro[2, 4]octane with P450cam (CYP101), P450BM3 (CYP102), CYP2B1 and CYP2E1⁸⁶ afforded products indicative of a radical intermediate with a lifetime ranging from 16 to 52 ps.

For fully probing the rebound mechanism more sophisticated probes were devised. Phenyl substituted cyclopropyl probes produced cyclopropyl carbinyl radicals which were found to rearrange at a rate up to 1000 times faster than the parent probes seen above.⁸⁷ The two ultrafast probes used in these experiments, *trans*- 1-methyl-2-phenylcyclopropane **10** and 1-methyl-2,2-diphenyl-cyclopropane **11** (Figure 12), gave alcohol products ratios which yielded unexpected high values for k_{OH} ca. $1.5 \times 10^{12} \text{ s}^{-1}$ and ca. $7 \times 10^{12} \text{ s}^{-1}$, respectively.⁸⁸

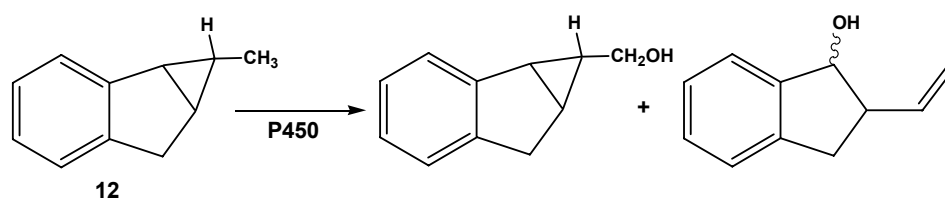
Figure 12. Ultrafast radical clock probes *trans*- 1-methyl-2-phenylcyclopropane and 1-methyl-2,2-diphenyl-cyclopropane.



With the phenyl-substituted cyclopropylcarbinyl radicals corresponding to **10** and **11**, *Atkinson* and *Ingold* believed that there was a likelihood that the enzyme enforced conformations where the π -electron system of the phenyl ring(s) could not overlap fully with the bond which breaks in the cyclopropane ring, and thus induce a “slowing down” of the ring-opening. This possibility had been considered by *Liu et al.* (1993) in their study of the oxidations of **10** and **11** by methane monooxygenase from *Methylococcus capsulatus* (Bath).⁸⁹ This explanation was in full agreement with the experimental results obtained with bicyclo[2.1.0]pentane, where *Ortiz de Montellano*⁸³ witnessed limited mobility also for this smaller substrate. Nevertheless this rationalization of high k_{OH} values based on the steric constraints in the enzyme pocket was dismissed by the subsequent *Atkinson* experiment performed with both enantiomers of **10**. Regardless of the fact that two enantiomers should give different results due to their different diastereomeric complexes with the enzyme, both gave, upon microsomal P450 hydroxylation, quite similar results in terms of their overall reactivity, the observed KIEs, and, most importantly, the product distributions.⁹⁰

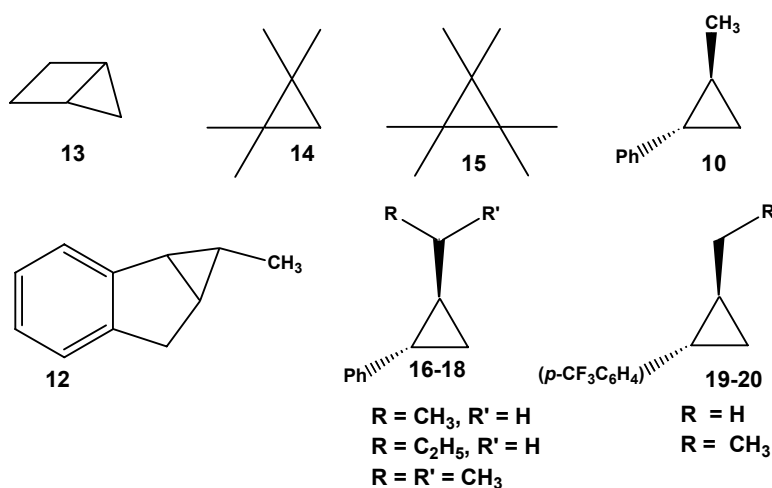
Newcomb believed that a definitive answer to the high k_{OH} values could be found employing an ultrafast clock **12** ($k_r = 3 \times 10^{11} \text{ s}^{-1}$)⁹¹ (Figure 13) having an accelerating substituent that was conformationally locked with respect to the cyclopropane ring.⁹² This probe was unlikely to be subjected to steric constraint. Surprisingly, the rebound constant calculated from the distribution of the rearranged and unrearranged alcohols had the value $1.4 \times 10^{13} \text{ s}^{-1}$ which was on the order of a vibrational rate constant and not of a chemical rate constant (Figure 13). The generally accepted upper limit lifetime of a radical intermediate in the transition state theory is 170fs.

Figure 13. Ultrafast radical clock probe with $k_r = 3 \times 10^{11} \text{ s}^{-1}$



At this stage *Newcomb* felt it necessary to carry out a systematic study on the hydroxylation of ten probes (Figure 14) by P450 2B1 and 2B4 in order to verify if a linear correlation with a slope of 1 existed in a log-log plot of the ratio of rearranged to unrearranged alcohol product *versus* the radical rearrangement rate constant.⁹³

Figure 14. P450 hydroxylations of ten key probes



The lack of a consistent trend in the set of “quantitative” data⁹⁴ together with the results of kinetic isotope studies⁹⁵ and the outcomes of experiments performed with P450-mutants on the same set of probes by *Coon* (see next paragraph), lead *Newcomb* to conclude that the overall mechanistic picture was incomplete. *Newcomb* cast doubts about the general accepted hydrogen abstraction-rebound mechanism⁴⁴ and suggested that an unidentified process might be occurring in competition with or as a part of the hydroxylation sequence. Because a radical and a cationic intermediate would suffer the same skeletal

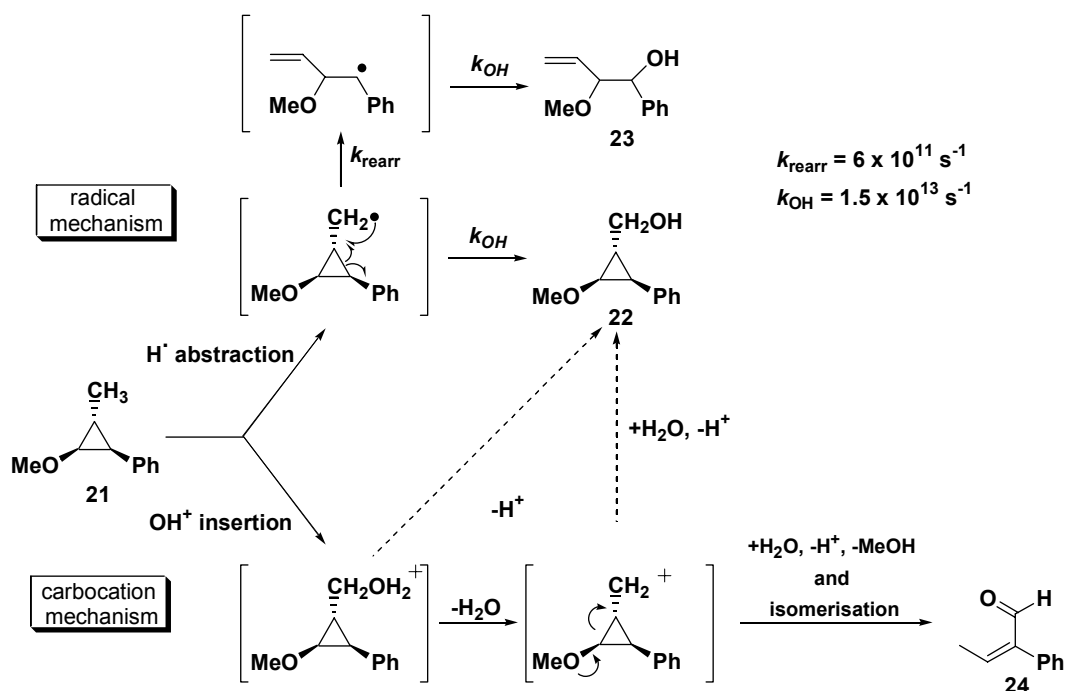
reorganization in each probe for which rearranged products were found, the possibility of a side reaction involving a cation could not be excluded.

His attempted solution was to use hypersensitive radical probe substrates that could distinguish between radical and carbocation intermediates on the basis of the identity of the rearranged products (*Scheme 3*). Production of a radical at the methyl group in this probe gives highly regioselective cleavage, favoring the benzylic radical product (>50:1), and production of a cation at the methyl position results in ring opening towards the alkoxy group to the limit of detection (>1000:1).⁹⁶⁻⁹⁸

Oxidation of *trans,trans*-2-methoxy-3-phenylmethylcyclopropane **21** with six cytochrome P450 isozymes gave cation derived rearrangement products, disproving the assumption that such rearrangements arose exclusively from radical species. Variable partitioning between the radical and carbocation mechanisms thus was concluded to explain the wide range of measured k_{OH} values.⁹⁹

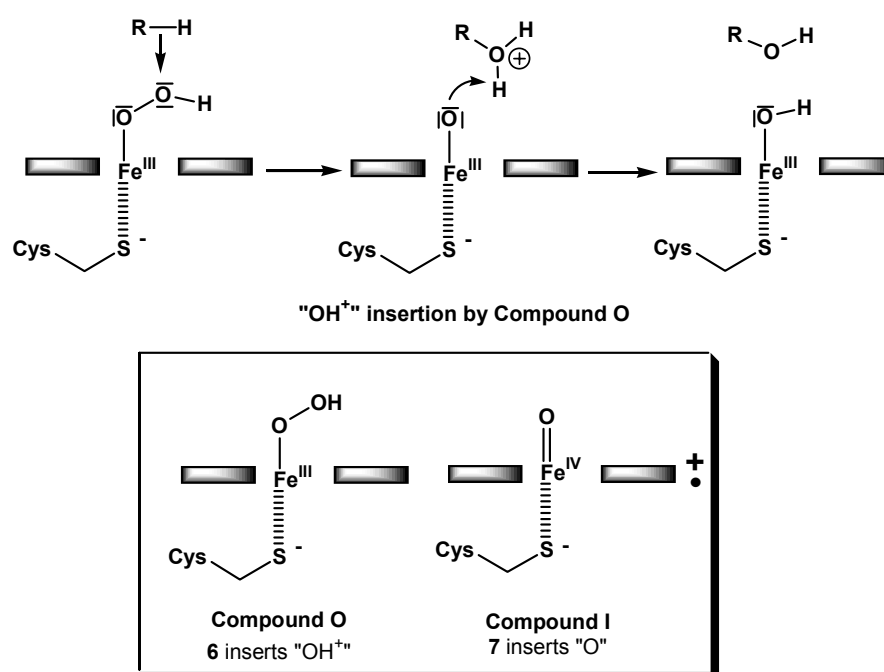
From the small amounts of radical rearrangement products generated from the hypersensitive probes, the radical lifetimes in the P450-catalyzed reactions could be calculated to range from 70 to 200 fs^{98,99} which are again too short for true radical intermediates, but rather correspond to the decomposition rate of a transition state. The occurrence of cationic intermediates necessitated another mechanistic model (*Scheme 3*).

Scheme 3. The carbocation model proposed in fast radical clock experiments



In this regard, the most plausible premise was insertion of OH^+ into a C-H bond to generate protonated alcohol species that could undergo solvolysis-type reactions to yield cationic rearrangement products.^{94,99} This route required heterolytic O-O bond fission of the hydroperoxo-iron state (Compound 0) of P450 (*Scheme 3b*) to insert OH^+ .^{98,99} The new mechanism as shown in *Scheme 3*, was therefore based on a “two oxidant” paradigm whereby both oxo-ferryl-(FeIV) Cpd I and its precursor hydroperoxo-(FeIII) Cpd O are good electrophiles and can respectively react through a radical and a cationic mechanism (*Scheme 3b*). Variable partitioning between the radical and carbocation mechanisms thus was concluded to explain the wide range of measured k_{OH} values.

Scheme 3b. Involvement of Compound 0 in the catalytic cycle



However, density functional analysis of mechanisms involved in ethylene epoxidation by a Fe(III)–OOH model disclosed barriers for the model pathways, detailed by *Shaik*, of 37–53 kcal/mol.¹⁰⁰ This was taken to indicate that hydroperoxo-iron (Cpd 0), as such, could not be the ultimate oxidant, in line with its significant basicity and poor electron-accepting capabilities.¹⁰⁰

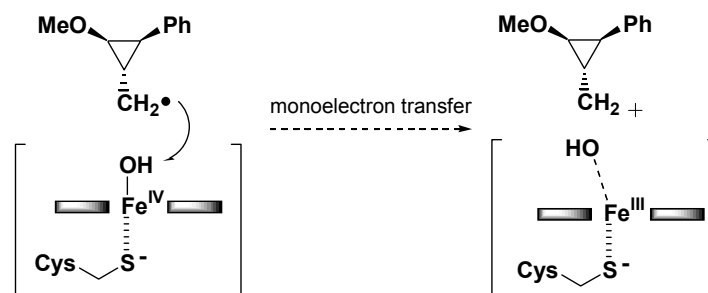
Furthermore this hydroxylation reaction effected by hydroperoxo iron species (Compound 0) was not a viable alternative since *Loew* calculated that protonation of the distal oxygen in the reduced ferrous dioxygen unit $[\text{Fe}-\text{O}-\text{O}]^{2-}$ triggers Fe-O bond weakening¹⁰¹ and *Kamachi* determined that the subsequent conversion of the protonated

PorFe^{III}-OOH₂⁺ to Por⁺Fe^V=O (CpdI) involves a barrierless reaction pathway with a significant energy release of 50 kcal/mol.¹⁰²

It is noteworthy that the percentage of cationic rearrangement products observed in these experiments does not correspond to the stability of the cation involved. One example of this is seen in a series of probes,⁶⁶ with either a hydrogen or *para*-trifluoromethyl substituent on the phenyl and an ethyl, propyl, or isopropyl group replacing the methyl on the cyclopropane ring (*Figure 14*). Even though ring opened products were again observed the overall results were contradictory. In fact the cation stabilizing groups resulted in *less* rather than more rearrangement, the opposite to what would be expected should a protonated alcohol have been the initial oxidation product.⁶⁶ Unfortunately this result does not sustain the production of a protonated alcohol, which should ionize and rearrange more readily with increasing stability of the carbocation, and thus these findings weigh heavily against the participation of an Fe^{III}-OOH species.⁶⁶

The alternative *Ortiz de Montellano's* proposal^{86,103} of a carbocation formation through a monoelectronic oxidation of the radical intermediate requires that this oxidation reaction proceeds at higher rates than usual radical rearrangement.¹⁰⁴

Scheme 3c. Proposed monoelectron oxidation of cyclopropylcarbinyl radical



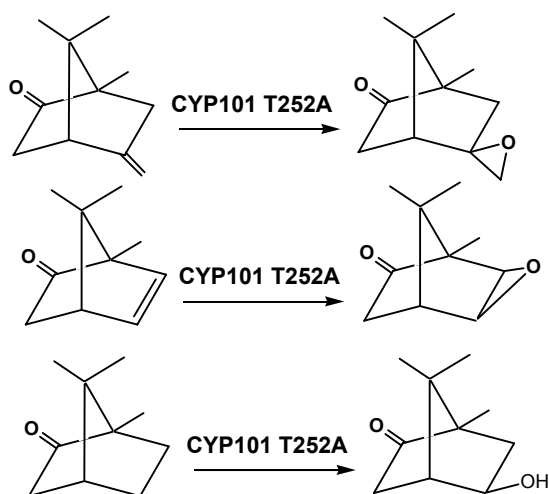
Unfortunately there are no experimental data that could prove or disprove this proposition. Factors which could influence the rate of electron transfer include the relative proximity of the electron donor and acceptor and the redox potential difference between them. At this point it was clear that there was no general consensus on the oxidative power of the Fe-OOH intermediate claimed by *Newcomb* to be the second electrophilic species acting in the P450 hydroxylation mechanism.

1.3.2 Evidence from experiments with genetically engineered P450 enzymes

A contribution to this debate came from studies with mutated P450s. The crystal structures of bacterial CYPs 101, 102 and 108 contain a highly conserved active-site threonine within H-bonding distance to the peroxo-iron unit.¹⁷ Of particular interest, attenuated camphor and laurate hydroxylation was observed, when T252/268 in the CYP101 and CYP102 polypeptide, respectively, were replaced with alanine.^{68,105} In the opinion of *Sligar* and *Ishimura* the production of less than 0.1% of hydroxycamphor implied that this mutant makes a minimal amount of oxo-ferryl $\text{Por}^+\text{Fe}=\text{O}$ (CpdI).

Nevertheless, the T252A variant was found to accept electrons from NADH and reduce dioxygen to H_2O_2 ¹⁰⁵ via the intermediacy of hydroperoxo-iron.⁹² Mutation was considered to disrupt a key step in H^+ delivery, presumably introduction of the second proton to hamper O-O bond dissociation.⁵⁸ Therefore, P450 mutants devoid of the active-site threonine were regarded as ideal means for testing the direct involvement of hydroperoxo-iron (Cpd0) in epoxidations. *Sligar*, in a series of oxidation reactions, showed that T252A, a form of the enzyme that produces none or very little of the hydroxylated product with the normal substrate, 1R-camphor, is however, capable of catalyzing the epoxidation of olefins. Indeed, a drastic increase in the ratio of epoxide to hydroxy products derived respectively from two camphor analogues (5-methylenecamphor and 5-norbornen-2-one) and 1R-camphor during catalysis by the T252A congener of CYP101 could be demonstrated in comparison to the wild type parent by *Sligar et al.*⁶⁴ (Figure 15)

Figure 15. Epoxidation of two camphor analogue by the T252A congener of CYP101

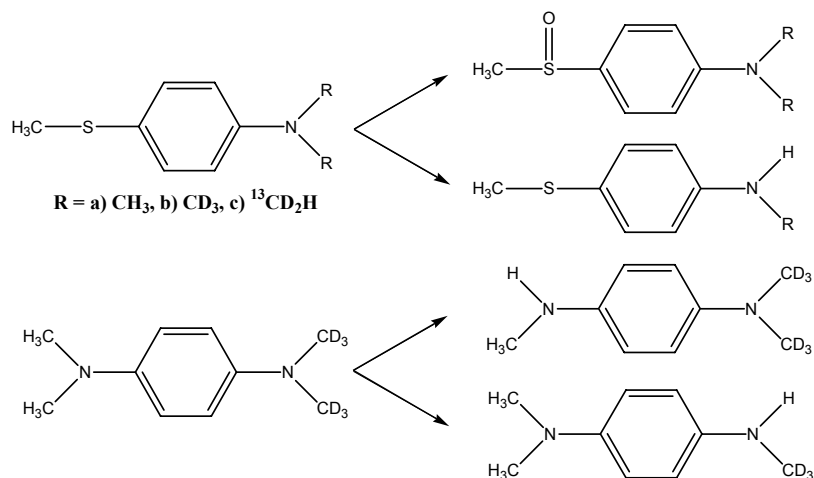


These two alkenes, however, were epoxidised by the mutant T252A at a rate only 15-20% compared to that of the wild-type CYP101. In summary, while it seems that the hydroperoxoferric P450 intermediate Cpd 0 is capable of epoxidising alkenes, the Cpd I state is still probably the major catalyst for alkene epoxidation in the wild-type enzyme.

Similar findings were made with truncated CYP2E1 lacking the active-site threonine. Vaz *et al.* showed that the 2E1 mutant T303A mediated the metabolism of cyclohexene, *cis*-but-2-ene and *trans*-but-2-ene at an increased ratio of epoxidation to allylic hydroxylation.¹⁰⁶ On the other hand, when CYP2B4 T302A was employed on the same substrates the results were different. A reduction of the rates of both allylic hydroxylation and epoxidation was registered. The failure to observe similar changes with the CYP2B4 mutant to those seen with CYP2E1 was disappointing, but could be rationalized assuming that the mutation causes changes in the active site and not only eliminates the hydrogen bond that is used to promote O–O bond cleavage.

Jones *et al.* assessed the participation of an alternative electrophilic intermediate in heteroatom oxygenation by employing the T268A mutant of CYP102. The engineered enzyme fostered sulfoxidation of *p*-(*N,N*-dimethylamino)thioanisole relative to *N*-dealkylation of the substituted amine function (*Figure 16*).¹⁰⁷ Nevertheless this research was inconclusive since, even if the KIE data and products distribution seemed to demonstrate the involvement of two separate oxidants, it was impossible to determine which reaction was catalyzed by which specific oxidant.

Figure 16. Sulfoxidation vs *N*-dealkylation of *p*-(*N,N*-dimethylamino)thioanisole.



A mutant of truncated CYP2B4 with exchange of alanine for threonine at position 302 turned out to have decreased ability to catalyze NADPH-dependent N-oxide formation from N,N-dimethylaniline, questioning an obligatory hydroperoxo-iron-promoted mechanism.¹⁰⁸ However, when the measurements were conducted with iodobenzene in place of NADPH/O₂ to directly generate the favored Por⁺Fe^{IV}=O entity (CpdI),¹⁰⁹ the enzyme variant still mediated N-oxygenation of the tertiary arylamine at a rate less than half that of the wild-type-catalyzed reaction¹⁰⁷ so that reasonable interpretation of the data seemed difficult.

Using the same wild-type and engineered P450s pairs, the potential involvement of Fe(III)-OOH in hydroxylation reactions was inferred from mutant-induced changes in regioselectivity during the oxidation of cyclopropyl probes (previously mentioned) designed to give different rearrangement products with radical and cationic intermediates.^{66 95 97, 110} The results of these investigations provided evidence supporting the existence of a second (or altered) oxidant in the mutant enzyme and the formation of (carbo)cationic species as minor, non critical intermediates in certain oxidations.

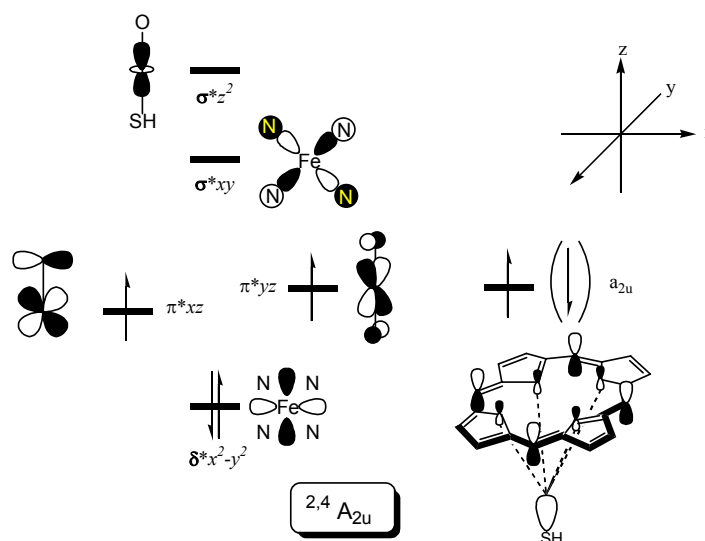
Both *Coon* and *Newcomb* results suggested that the oxidizing species produced when the distal threonine is mutated to an alanine in CYP2E1, but probably not in CYP2B4, may vary to some extent from that formed in the intact enzyme. What these results did not discover was whether or not this species is in fact the PorFe^{III}-OOH intermediate. The authors also acknowledge the possibility that the reported results of the mutation could be due to physico-chemical changes, which affect the reactivity of the ferryl species. Thus there is no concrete indication that the ferric hydroperoxy species is an oxidant in C-H hydroxylations by P450 enzymes.

1.3.3 A theoretical approach of monooxygenation mechanisms by P450 enzymes.

Density functional theory (DFT) together with quantum mechanical/ molecular mechanics) calculations (QM/MM) are capable of supplying chemists with a tool that can provide, at least qualitatively, reliable and detailed descriptions of bioinorganic reaction mechanisms.¹¹¹ Indeed, *Shaik's* DFT calculations^{73, 112} have attempted to offer a simple resolution of the mechanistic dilemma, posed by studies of C-H P450-hydroxylation,⁹⁴ in terms of a two-state reactivity (TSR) of Cpd I alone; namely, one reagent with two different pathways.

Prior to a detailed description of these two different pathways, it is necessary to elucidate how *Shaik et al.* describe, by the use of DFT and of the QM/MM calculations, all known model and enzymatic Cpd I species as tri-radicaloid.^{73, 86, 95, 98, 107, 110, 112, 113} **Scheme 4** shows the key orbitals of Cpd I: five d-block orbitals, labeled as $\delta_{x^2-y^2}^*$, σ_{xy}^* , $\sigma_{z^2}^*$, π_{xz}^* , and π_{yz}^* , and one porphyrin sulfur mixed orbital, labeled as a_{2u} .

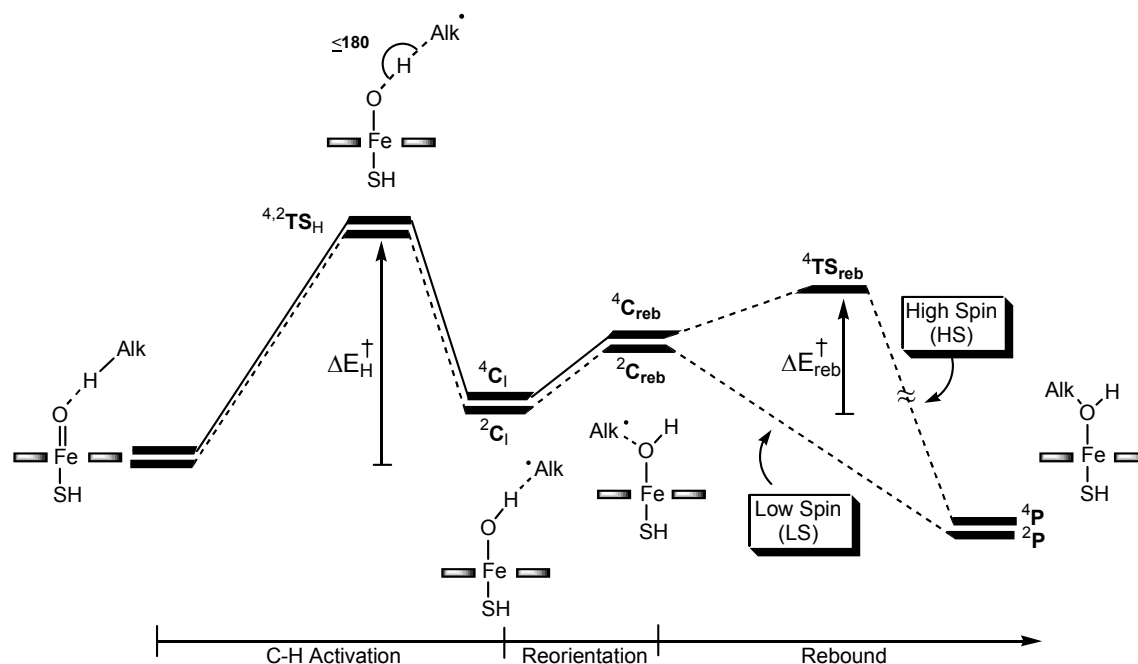
Scheme 4. Key orbitals of Cpd I of P450. Origin of the degenerate state of CpdI ($^{2,4}A_{2u}$)



Of the d orbitals, only the δ orbital is pure nonbonding, while the rest have antibonding interactions with the ligands.⁹⁹⁻⁹⁴ The species Cpd I possesses three odd electrons in the π^* and a_{2u} orbitals. The coupling between the electron in a_{2u} and the π^* triplet is very weak, since the π^* and a_{2u} orbitals are virtually disjointed. As a result the ferromagnetic state, with all spins up, and the antiferromagnetic state, where the electron in a_{2u} possesses an opposite spin to those in π^* , are close in energy. DFT calculations show the close proximity of the two states.⁷² Clearly, therefore, Cpd I has a virtually degenerate ground state $^{2,4}A_{2u}$ and is accordingly a two-spin--state oxidant. Hereafter, the two states are referred to as the high-spin (HS) and low spin (LS) states.

In the light of the TSR theory, *Shaik* has re-examined the experimental results obtained by various research groups relative to the diverse P450-oxidative reactions as epoxidation, heteroatom oxidation, (N,S,O)-dealkylation and C-H hydroxylation. In the specific case of a C-H bond hydroxylation of an alkane (Alk-H), the energy profile along the reaction coordinates resulted in the following (Scheme 5):

Scheme 5. Energy profile for C-H hydroxylation of Alk-H by Cpd I of P450.



A two-spin state mechanism is outlined above with HS and LS pathways that begin from the degenerate states $^{2,4}A_{2u}$ of Cpd I (the 2, 4 superscripts relate to the doublet, antiferromagnetic, and quartet, ferromagnetic, spin states of Cpd I). During the C-H bond activation phase both reaction profiles stay in close proximity up to the iron-hydroxo radical species ($^{4,2}C_I$). At the point where the alkyl radical is released from the weak $OH\cdots Alk$ interaction to take up a rebound position ($^{4,2}C_{reb}$), the two states split. Two scenarios can then occur:¹¹²

1. The rebound on the LS surface is barrierless and thereby the LS route is characteristic of a concerted mechanism. Along this pathway leading to the formation of the LS ferric-alcohol complex (^{2}P) no radical intermediate is formed.
2. The HS route, leading to the HS ferric-alcohol complex (^{4}P) is stepwise with discrete lifetimes for the radical intermediates.

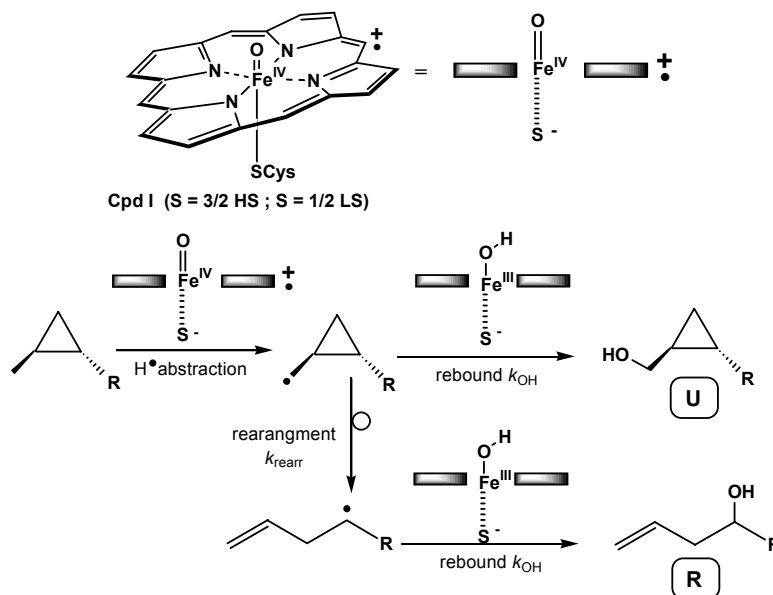
The interplay of a concerted (LS) and a stepwise process (HS), *spin crossover*, produces the “illusion” of two different oxidants and is, in *Shaik’s* view, the cause of the controversy over the exact nature of the oxidant species involved in the P450 hydroxylation.^{73, 112}

This two state scenario has a direct impact on how radical lifetimes are determined. In the radical clock experiments this separation of states sees the radical in the HS state having sufficient time to rearrange. Conversely the radical in the LS state, with a lifetime approaching zero, will collapse to give the ferric-alcohol product. The rearranged product thus formed originates only from the HS state while the unrearranged product is due to both LS and HS states with the largest contribution coming from the LS.¹¹⁴ Therefore, the radical lifetime, which is quantified from the ratio $[U/R]$, (Scheme 6) is not a “legitimate” lifetime, since it also reflects the relative yields of the HS and LS processes. As a consequence, since the LS surface in C-H hydroxylation lies below the HS, the quantity $[U/R]$ will yield apparent lifetimes that are shorter than the real ones.

An important indication emerging from these theoretical studies demonstrates that, not only is Cpd I a chameleon species (with its two spin state nature) but, it is also a chameleon oxidant that tunes its reactivity and selectivity patterns in response to the protein environment in which it is accommodated and in dependence of the substrate.¹¹⁵⁻¹¹⁸

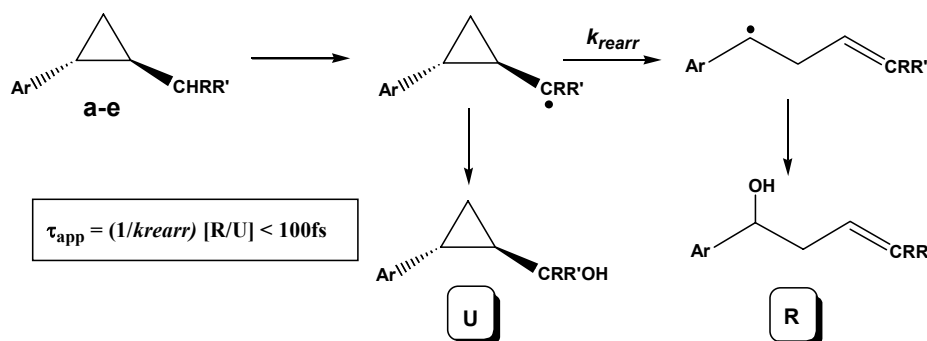
TSR^{73, 119} describes a two-state rebound mechanism, which on one hand supports the KIE evidence indicative of a hydrogen abstraction-like transition state in the bond activation and on the other hand reveals how a two-state rebound step can lead to apparently controversial lifetimes. This occurs if one starts from the assumption that the $[U/R]$ quantity is a result of a single radical intermediate that is rapidly partitioned between instant rebound and rearrangement followed by rebound, as in *Scheme 6*.

Scheme 6. One radical intermediate which divides between instant rebound and rearrangement followed by rebound to produce both U and R products.



In order to confirm the effectiveness and legitimacy of this complex theoretical-computational creation, *Shaik* tried to rationalize a set of “quantitative” results obtained in *Newcomb’s* laboratories in experiments performed with the substrates **a-e** and P450 enzymes (*Scheme 7*) (see chapter 1.3.1, *Figure 14*).

Scheme 7. A mechanistic scheme for determining the apparent lifetime (τ_{app}) of a radical intermediate, using the ratio of rearranged (R) to unrearranged (U) alcohol products derived from P450 oxidation of the probes a-e.⁹⁴



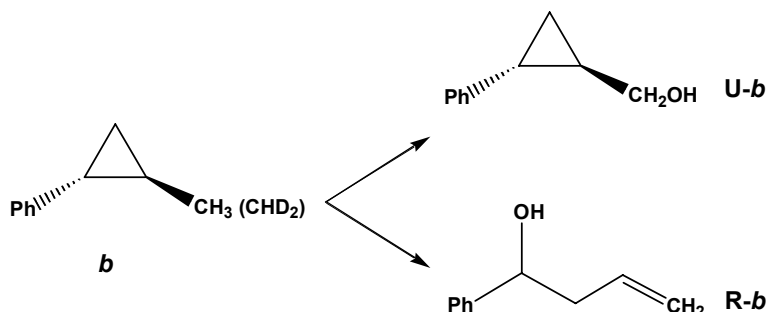
probe	Ar	R, R'	IP _{alk}	[U/R]
a	pCF ₃	H, H	highest ↑ lowest	4
b	pH	H, H		4.3
c	pCF ₃	H, CH ₃		12
d	pH	H, CH ₃		25
e	pH	CH ₃ , CH ₃		>100

The ratio (U/R) in the above table, obtained in *Newcomb's* enzymatic experiments, lead to the calculation of rebound rate constants that exceed the decomposition rate for a transition state and showed no correlation to each other. These data brought *Newcomb* and *Toy*⁹⁴ to put forward their two oxidant theory.

The TSR scenario, with rearrangement occurring only on the HS manifold, could give order to the experimental data. An examination of the rebound barrier for the HS manifold^{73, 112} led to the estimation that as the radical becomes a better electron donor (lower ionization potential, IP, or oxidation potential), so should the rebound barrier decrease until it would completely cease to exist. Therefore the first two probes **a** and **b** should produce large quantities of the rearranged product. On the other hand probe **e**, which produces the radical with the lowest IP, exhibits virtually no rearrangement (<1%). DFT calculations¹²⁰ confirmed that indeed **b** should produce a considerable amount of rearranged product, estimated as 20–30% based on the relative HS and LS barriers, while **e**, which also reacts by TSR, should yield no rearranged products, since its LS and HS pathways are both effectively concerted. It can be concluded from this that *Shaik's* TSR theory could predict accurately the product ratio (U/R).

Another example how the TSR theory can find a rationale behind the kinetic isotope effect (KIE) is shown below. *Shaik* again reinterpreted the findings of *Newcomb et al.*⁹⁵ that the two alcohols **U-b**, and **R-b** (*Figure 17*) exhibit different sensitivities to isotopic substitution of the scissile C-H bond in the substrate, trans-2-phenyl-methylcyclopropane **b**, such that the reaction is characterized by the product isotope effect (PIE) that is significantly different from unity, namely $\text{PIE}(\mathbf{U-b}/\mathbf{R-b}) > 1$.

Figure 17. Kinetic isotopic studies



This finding proposes that **U-b** and **R-b** cannot be formed from a single intermediate that partitions into **U-b**, and **R-b**; the finding requires two different mechanisms, and the applicability of TSR was again put to the test.

In the TSR model the **U-b** alcohol is produced mainly on the LS manifold and the **R-b** on the HS route. Since the HS and LS hydrogen-abstraction transition states (${}^{4,2}\text{TS}_\text{H}$) in *Scheme 5* are not theoretically equal the subsequent kinetic isotope effects (KIE) will unavoidably be distinct. This then equates to $\text{KIE}_\text{LS} \neq \text{KIE}_\text{HS}$. From this an intrinsic product isotope effect (PIE_int)¹²⁰ for the rearranged (R) and unrearranged (U) products, can then be described by the following equation (Eq.1):

$$\text{PIE}_\text{int} = \text{PIE}_\text{TS} = (\text{U}_\text{H}/\text{U}_\text{D}) / (\text{R}_\text{H}/\text{R}_\text{D}) = (\text{KIE}_\text{LS}/\text{KIE}_\text{HS}) \quad (\text{Eq.1})$$

It is quite tricky to compare theoretical KIE values to experimentally determined ones, since the latter may be masked and may not reflect the intrinsic KIE values.^{76, 121, 122} Nevertheless, *Jones et al.*¹²¹ demonstrated that, in this specific case, the PIE observed (PIE_obs) coincided with the PIE_int . This allowed *Shaik* to directly compare the DFT calculated PIE values with the *Newcomb*'s experimental PIE values and a perfect match could be revealed.

Both the examples above show how the TSR theory accommodates some of *Newcomb*'s experimental results. *Shaik*'s calculations accommodate nearly all the outcomes of various oxidations performed by P450 enzymes/ mimics and it is thus a unifying theory that could potentially resolve any final debate in this area. A large number of chemists believe that his calculations carry a lot of weight to rationalize the results coming from a plethora of different reactions.

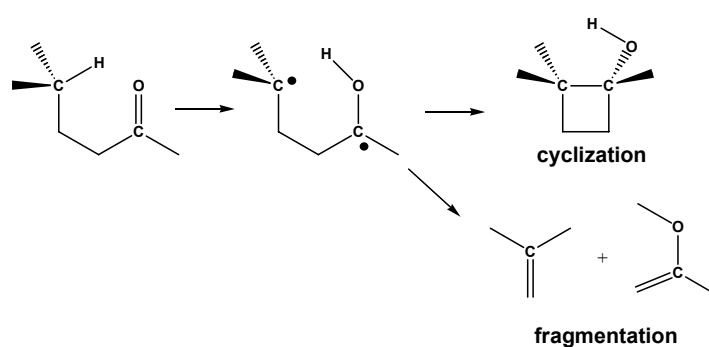
The TSR theory is also a good starting point for developing an interpretation of the experimental results of this thesis work described in the following chapters.

1.3.4. The Exact Nature of the Transition State

It is necessary, when discussing the activity of the enzyme cytochrome P450 to take into account the true definition or modern day consensus as to what classifies a “transition state” or “reaction intermediate”. As it is impossible to categorically define what exact species are formed in the latter part of the catalytic cycle, an insight could be provided by examining what constitutes a “transition state” as defined by *Newcomb*. He argues that since the measured rate constants k_{OH} for radical trapping are on the order of vibrational rate constants and not chemical rate constants,⁹² thus the radical lifetimes approach those of a transitional state, about 100-170 fs at ambient temperature.

Recent advancements in physical chemistry have brought a new insight into reactive intermediates by the use of compact ultra-fast laser pulse techniques.¹²³⁻¹²⁵ As the technique becomes widely used a wealth of findings are emerging. *Zewail* has produced a breakthrough by taking *femto*-second snapshots of reactions with exposure time measured in *femtoseconds*.¹²⁶ This has revolutionized the understanding of how reactions proceed and redefined what chemical intermediates can be properly identified. From *Zewail* 's study of Norrish type-II reactions (*Scheme 18*) with this revolutionary technique a first glimpse of carbon-hydrogen homolytic cleavage at a femtosecond scale was observed.^{127 128-131}

Figure 18. Norrish type II reaction



The time scale for the ultrafast hydrogen atom transfer (70 ± 90 fs) and diradical closure and cleavage (400 ± 700 fs) are obtained from the time evolution of the mass gated species. The observed vastly different reaction times indicate the non concerted nature of the two steps. This is of vital importance as it redefines how species with finite lifetimes as short as 70 fs can be categorized as reaction intermediates and not simply “transition states” as previously imagined. In this context it is necessary to reevaluate *Newcomb*'s need to introduce a new oxidant.^{66, 93} This new definition of an intermediate with such short lifetimes

makes it necessary to raise the question how it is possible to reconcile the experimental results of *Newcomb* with the calculations of *Shaik*.

2. Description of the problem and Aim of this Work.

As already mentioned in chapter 1.3.3 opposing conclusions were reached from the experimental findings of *Newcomb* (with his two oxidant theory)^{66, 98, 110} and the calculations of *Shaik* (he postulates a one oxidant theory).¹¹³ *Shaik* questions *Newcomb's* interpretation whether or not the observed short “radical lifetimes” invalidate the existence of radical intermediates.

Yet it was felt necessary to re-examine the experimental work of *Newcomb* in detail to determine how, exactly, he evaluated the lifetimes of the radical formed during the course of his experiments. If alkane hydroxylation is indeed initiated by hydrogen abstraction then the lifetimes of carbon radical can only be calculated indirectly by first deducing the rate at which the radical can be hydroxylated. This rate constant of the oxidation step can, in turn, only be calculated by knowing two specific measurements; firstly the ratio of rearranged (ROH) and un-rearranged (UOH) products formed and, secondly, the rate constants of the radical rearrangements. (see Eq.2 and Eq.3)

$$\text{Life time (fs)} = 1/k_{\text{OH}} \text{ (Eq.2)} \quad \text{and} \quad k_{\text{OH}} = k_r \times [\text{UOH}]/[\text{ROH}] \text{ (Eq.3)}$$

From Eq.2 it is obvious that the rate of hydroxylation is directly proportional to the rate of rearrangement and, herein, is found a fundamental problem with how *Newcomb* evaluates and projects his results. It is apparent that any misinterpretation of the k_r values could have a fundamental impact on the rate of hydroxylation and conversely the lifetime of the radical species formed. It is only since accurate values of rate constants for hydrogen atom transfer became available that it has been possible to show an indirect method for measuring rearrangement rate constants in archetypal fast radical reaction, i.e. the cyclopropylcarbinyl radical ring opening. These experiments, conducted by *Ingold*,¹³² *Newcomb* and others¹³³⁻¹³⁷ have provided a powerful and convenient method for measuring the rate constants of these rearrangements at intermediate and warm temperatures.

It would be reasonable to propose that a substantial change in the environment where the radical formation takes place would have considerable influence on the rate of rearrangement. This “effect” has already been noted in several examples where some “fast” radical clocks have yielded less rearrangement than slower clocks.^{88, 91, 93} *Shaik's* DFT calculations have attempted to account for such confusing results by again demonstrating

the “chameleon” like character of Cpd I, with its HS and LS states, but his theoretical calculations only offered a qualitative explanation of the short lifetimes observed by *Newcomb*.

These new radical clock experiments, reported in this thesis and based on novel porphyrin mimics, have certain advantages:

1. The experimental work on P450 mimics is important because, in these new experiments oxidation rates (k_{OH}) can be calculated for reactions performed under similar conditions used to determine k_r rates in previous trapping experiments.
2. The novel experiments have the advantage of producing radical species in a simple environment without the influence of outside factors. This is in contrast to previous P450 experiments with microsomes or purified isozymes, which gave k_{OH} values influenced by substrate-protein interactions.

The next chapter outlines the reasoning behind the porphyrin mimic synthesis as well as its design and also discusses the implications of the results of the new radical clock experiments.

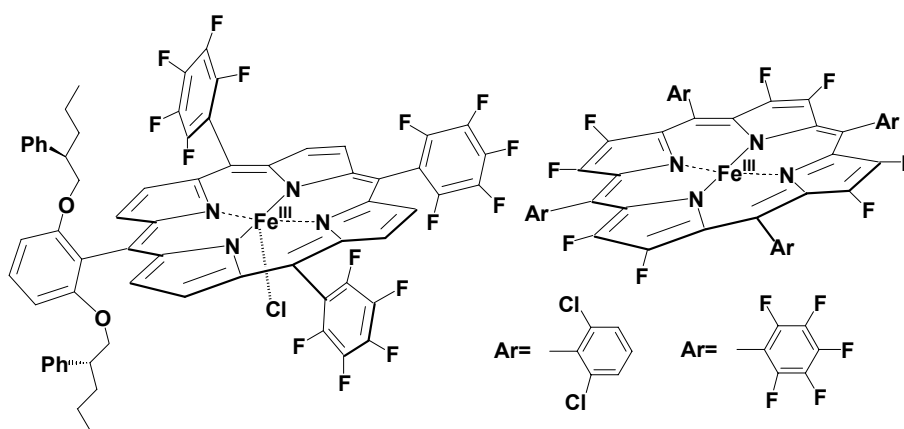
3. Porphyrin and Probe Synthesis.

3. 1. Towards the Synthesis of a First Porphyrin Model

Studies using synthetic metalloporphyrins as models for P450 have afforded important insights into the nature of the enzymatic reactions. Their use to mimic metallo-enzyme has long been shown to be an effective strategy in elucidating the sophisticated mechanisms of biological processes.¹³⁸ Experiments with synthetic P450 enzyme models are still today contributing to the understanding of the mechanism of the P450 action and providing information on the possible structure and electronic nature of iron porphyrin intermediates of the catalytic cycle.

When designing a porphyrin synthesis two fundamental characteristics of the model should be taken into account: stability and reactivity. The stability of the porphyrin chromophore is especially important in the presence of powerful oxidants. In order to have robust porphyrins and simultaneously control the spin- and oxidation state of the iron many research groups employ *face sheltered* and/or *electron deficient* iron porphyrins (Figure 19).¹³⁹⁻¹⁴³ The structural-electronic aspects that modulate the reactivity of the porphyrin are not well defined. Certain rules, though, are applicable irrespective of the porphyrin involved. The catalytic efficiency and the reactivity of the porphyrin can, for example, be enhanced by introducing halogens on the aryl groups of *meso*-tetraarylporphyrins and on the β -pyrrolic positions of the macrocycle ring¹⁴⁴⁻¹⁴⁶ 139, 140 (Figure 19).

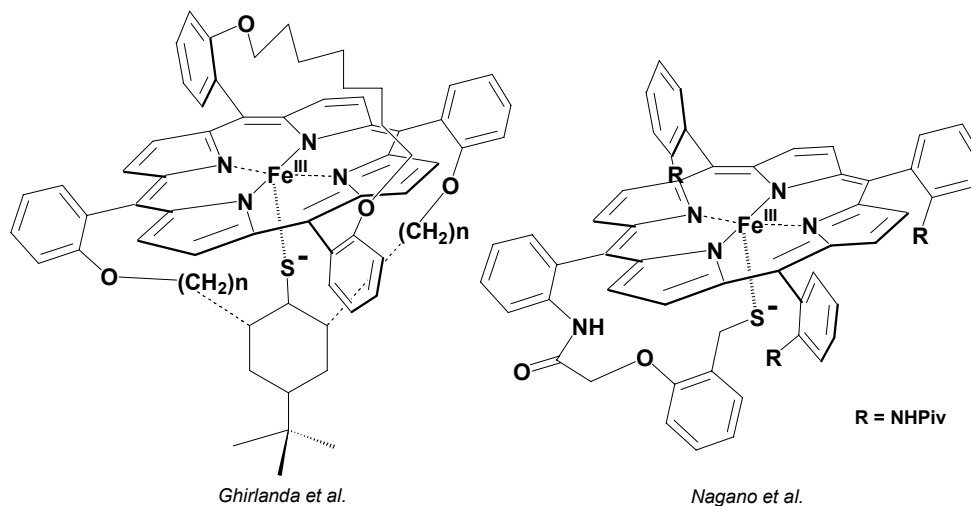
Figure 19. Examples of metalloporphyrins



Any good active site analogues of P450s should aim to reproduce as much as possible the structural features found in the enzyme itself. A good design of a structural mimic has to take into account the characteristic coordination of the sulfur to the central iron

of the heme-thiolate protein. Examples of synthesized porphyrins which follow this reasoning are given below (Figure 20).

Figure 20. Metalloporphyrin analogues of P450 active site.



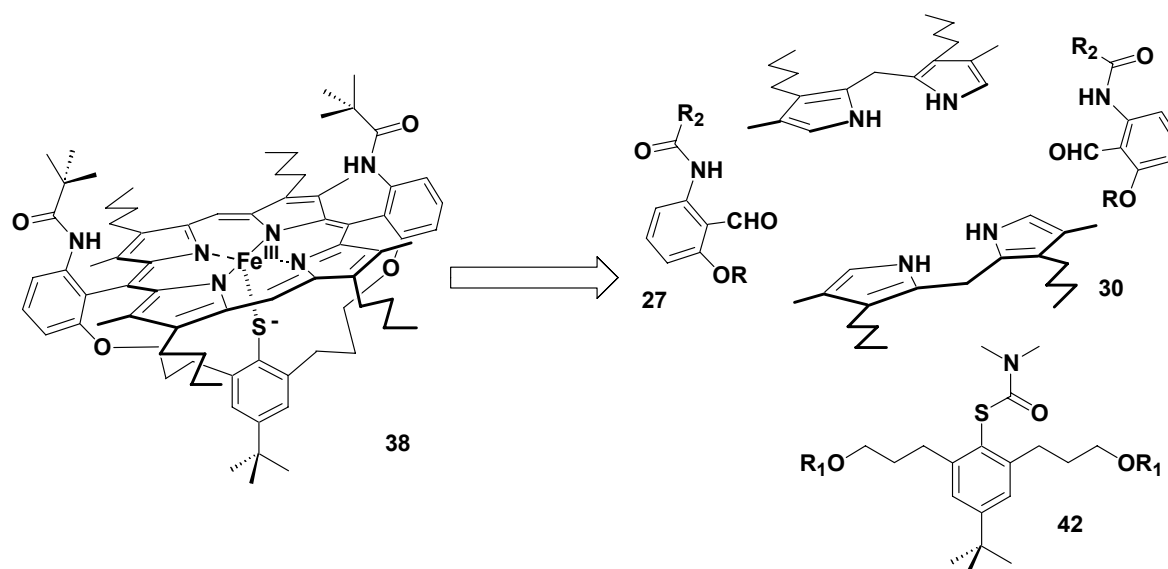
In both porphyrin models described in the next chapters the cysteine like coordination found in the natural enzyme is reproduced by the thiolate or thiophenolate groups coordinated to the iron. Furthermore, in the second model, the introduction of electronwithdrawing groups increases the activity of the porphyrin mimic. In the following paragraph the methodology used for the synthesis of two novel porphyrins is described.

3.2 Synthesis of porphyrins **38** and **39** - first models for mimicking the prosthetic porphyrin IX active site of P450.

The target compound **38**¹⁴⁷ is a *face-protected* iron(III) diphenyl porphyrin carrying a thiophenolate ligand attached to a bridge tightly spanning the porphyrin plane such that the sulfur is forced into coordinating to the iron, and its decomplexation from the iron is prevented for steric reasons.¹⁴⁸ The substrate binding site is protected against porphyrin–porphyrin interactions by means of two pivalylamido groups (“picket-fences”)¹⁴⁹ that also provide H-bonding to ligands coordinating to the iron. The complex compound **38** was prepared keeping in account established procedures.^{147, 148, 150 151}

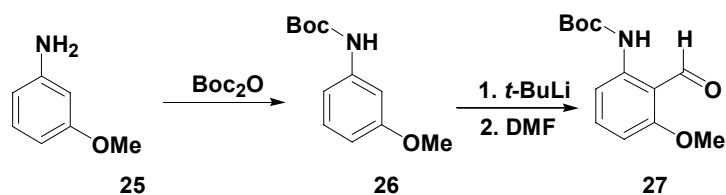
A retrosynthetic analysis of the iron(III)-porphyrin **38** (Scheme 8) leads to three main building blocks: the dipyrromethane derivative **30**, the 2,6-substituted benzaldehyde **27** and the protected thiophenyl bridge **42**.

Scheme 8. Retrosynthetic analysis of methylcarbamoyl iron porphyrin model 38.



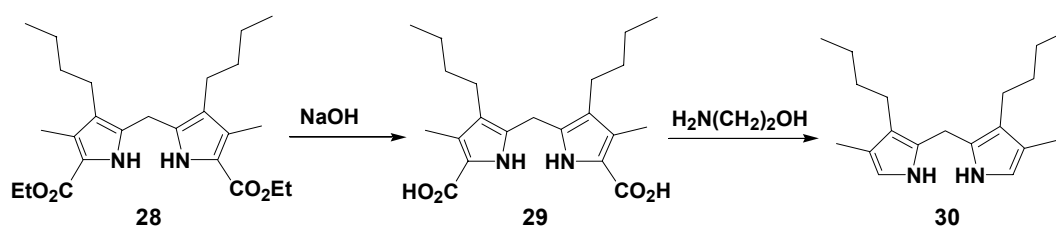
The salicylaldehyde derivative **27** was synthesized in two steps by performing a prior protection of the aniline and a subsequent formylation directed in the 2-position by the methoxy (R = Me) and carbamate groups (*Scheme 9*).¹⁵²

Scheme 9. Synthesis of salicylaldehyde derivative 27



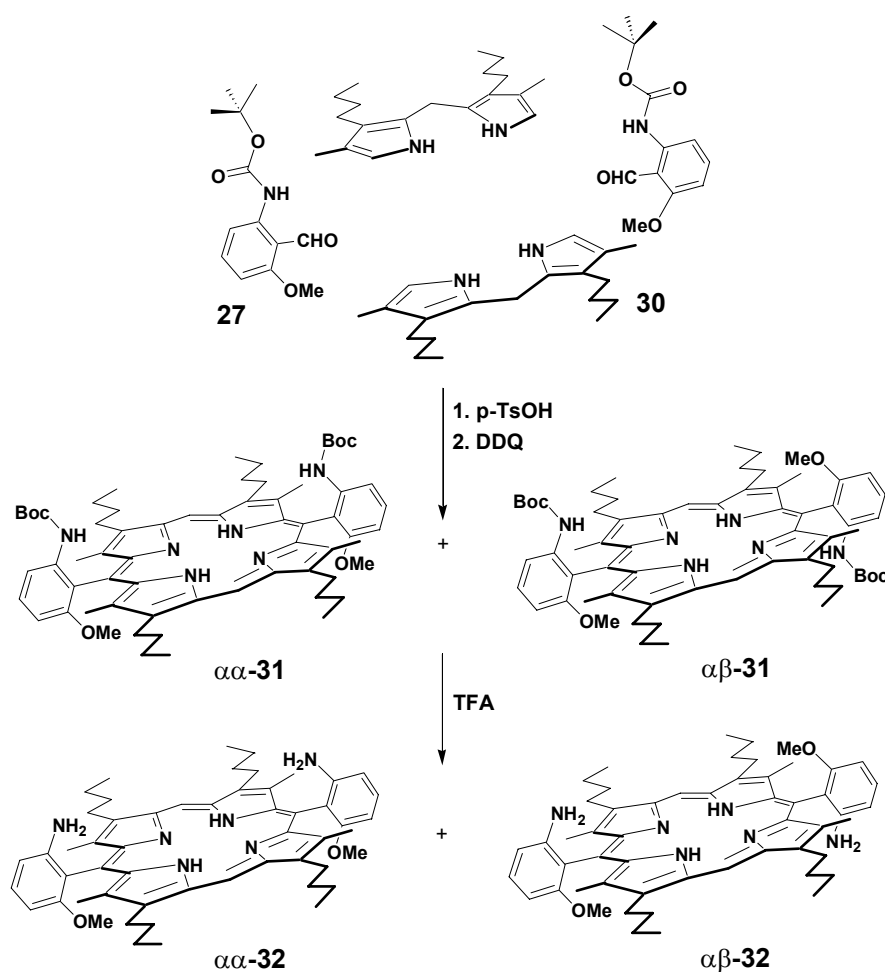
The second fragment for the porphyrin condensation was the dipyrromethane **30**. It was synthesized from diester **28** which was already on stock in our group. Saponification of the diester **28**¹⁵³ and subsequent decarboxylation of the resulting diacid **29** yielded α -unsubstituted, air and light sensitive dipyrromethane **30** which was immediately used in the next step (*Scheme 10*).

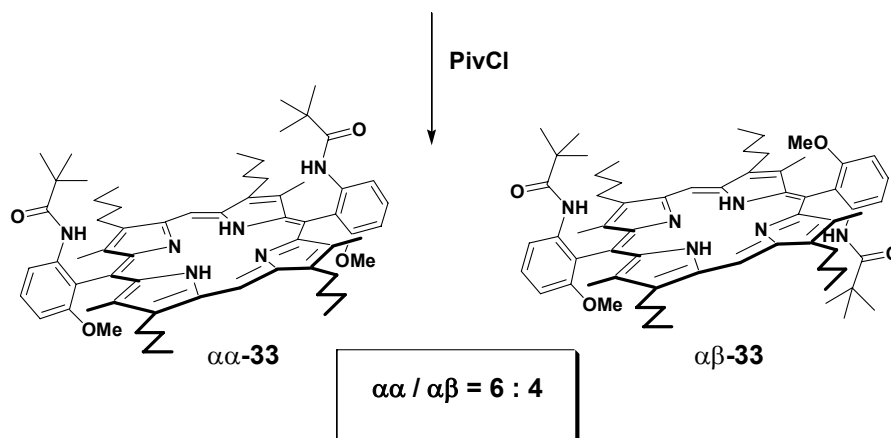
Scheme 10. Synthesis of dipyrromethane 30



Classical MacDonald [2+2]-type porphyrin condensation¹⁵³ of dipyrromethane **30** and benzaldehyde **27** under acid catalysis with *p*-toluenesulfonic acid gave the porphyrinogen compound with the characteristic UV-vis band at 486 nm. The reduced chlorin form of the porphyrin was subsequently oxidized with DDQ providing a mixture of two atropisomers, $\alpha\alpha$ -**31** and $\alpha\beta$ -**31**, in $\sim 35\%$ yield that is perfectly in agreement with the values reported in literature for this kind of reaction.^{154, 155} This mixture was then treated with trifluoroacetic acid to remove the N-protecting groups in a quantitative way. The rationale behind the use of a N-Boc protected benzaldehyde (**27**) at the MacDonald condensation stage is based on the know-how, acquired earlier in our research group, with experiments where the direct [2+2] addition of the N-Piv benzaldehyde and the dipyrromethane derivative gave considerable lower yields (see Mu Linjing, Report 2001).

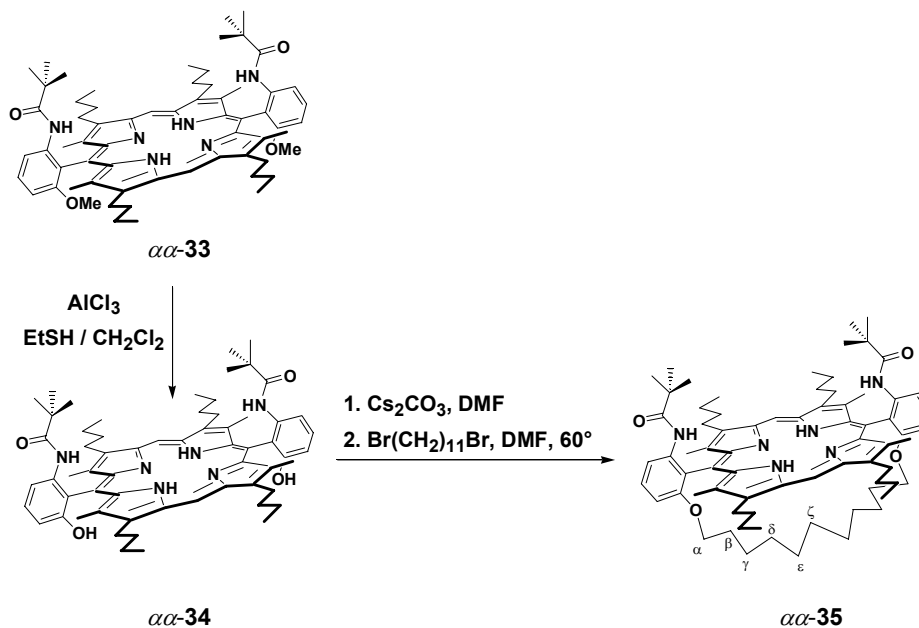
Scheme 11. From the MacDonald condensation to the atropisomers separation





The synthesis proceeded with the protection of the amino function of $\alpha\alpha$ -32 and $\alpha\beta$ -32 with the pivaloyl group. For obvious polarity reasons the separation of the two atropisomer ($\alpha\alpha$ and $\alpha\beta$) by flash chromatography was attempted at this stage rather than in the following step, after the cleavage of methyl ethers. The atropisomers of this porphyrin, due to steric overcrowding between the substituents at the β -pyrrole and 2'- and 6'-positions of the phenyl rings, are configurationally stable during manipulation or purification. Since the atropisomers cannot interconvert at high temperatures used in the bridging step, it necessitated the use of pure $\alpha\alpha$ -isomer cleanly to avoid formation of side products during the coupling step with sulfur bridge 42.

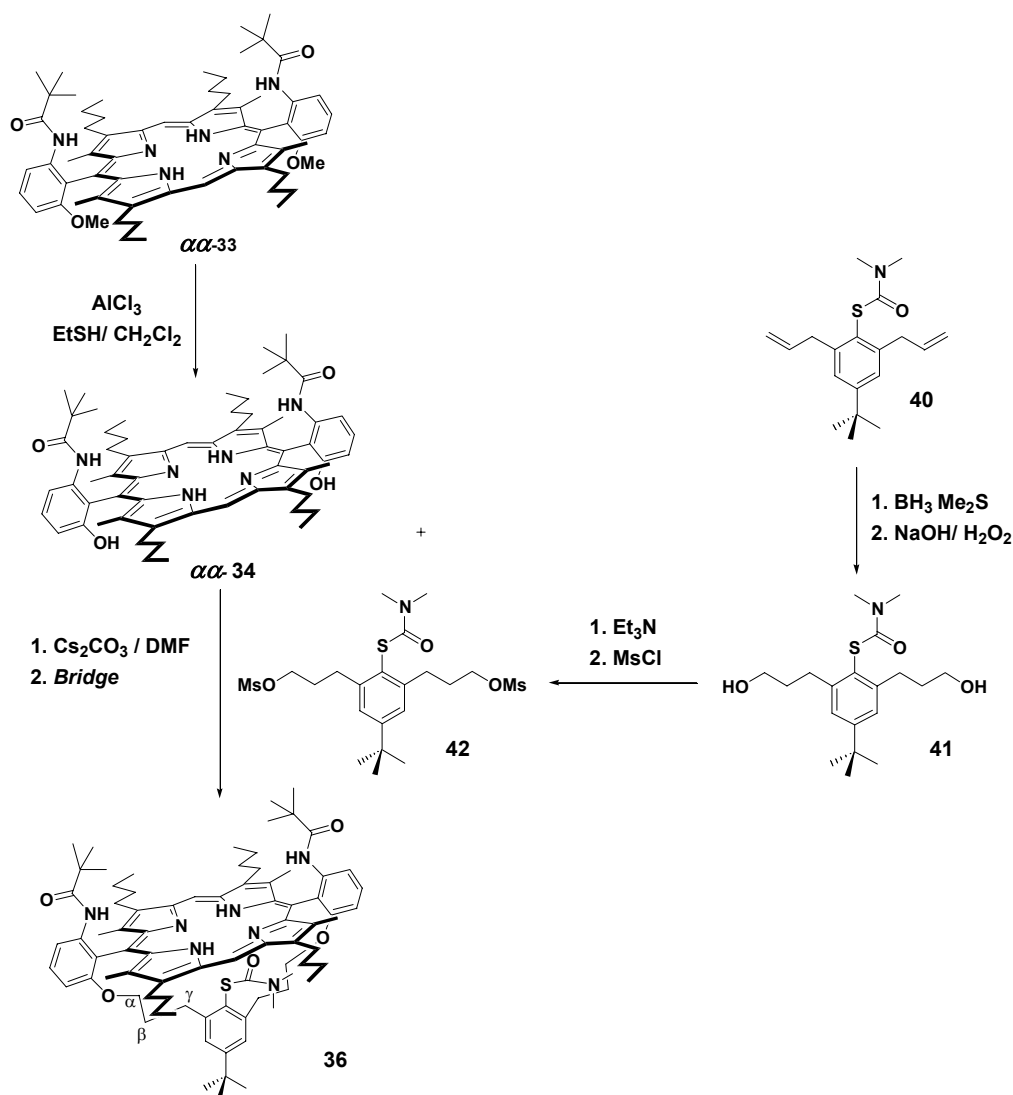
The purification on silica gel yielded $\alpha\alpha$ -33 in 44% as the more polar fraction and $\alpha\beta$ -33 in 29% as the less polar compound. The ratio of the two atropisomers $\alpha\alpha/\alpha\beta \sim 6:4$ was slightly in favor of the desired product $\alpha\alpha$ -33 with an overall yield of 25% for both $\alpha\alpha$ and $\alpha\beta$ from benzaldehyde 27. The correct assignment of the atropisomers of 34, product obtained from the cleavage of the methylether, was based not only on NMR investigations but also on the analysis of the products of the reaction of the supposed $\alpha\alpha$ -34 with 1, 11-dibromoundecane in the presence of Cs_2CO_3 in hot DMF under high-dilution conditions (Scheme 12).

Scheme 12. Chemical derivatisation of bisphenol porphyrin $\alpha\alpha$ -34 for atropisomer assignment.

The $^1\text{H-NMR}$ spectrum of **35** displayed high-field shifted signals for the methylene groups of the undecanyl chain due to the ring current of the porphyrin and proved the atropisomers identification to be right.

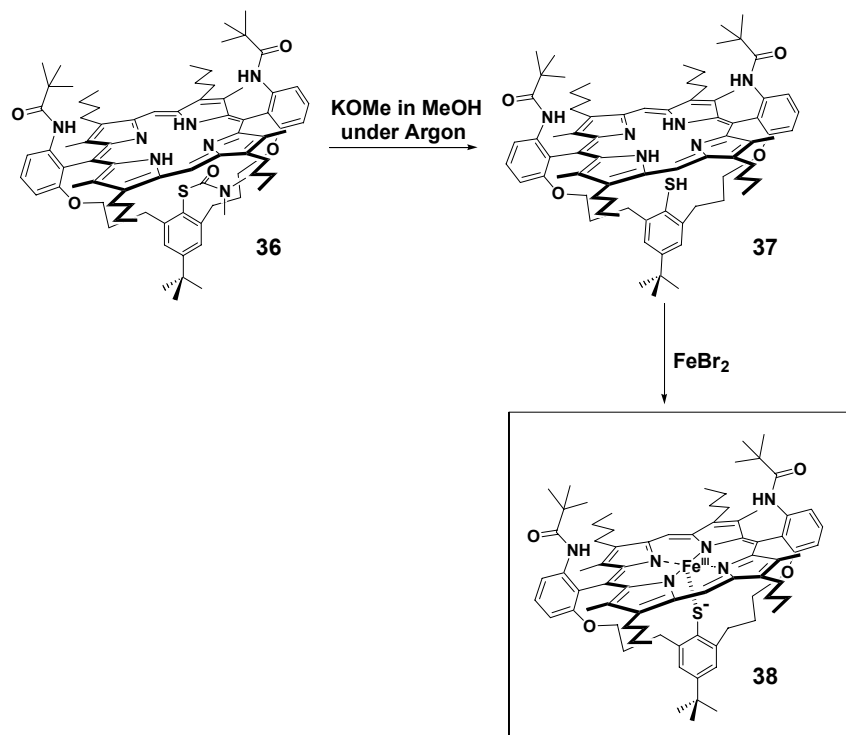
The synthesis was continued with the $\alpha\alpha$ -atropisomer of **33** and cleavage of the methyl ethers was carried out with anhydrous aluminum chloride in a solvent mixture of CH_2Cl_2 and EtSH to give $\alpha\alpha$ -**34**.

Scheme 13. Cleavage of the methyl ether and synthetic route to bridged bis-(methyl carbamoyl)-porphyrin **36.**



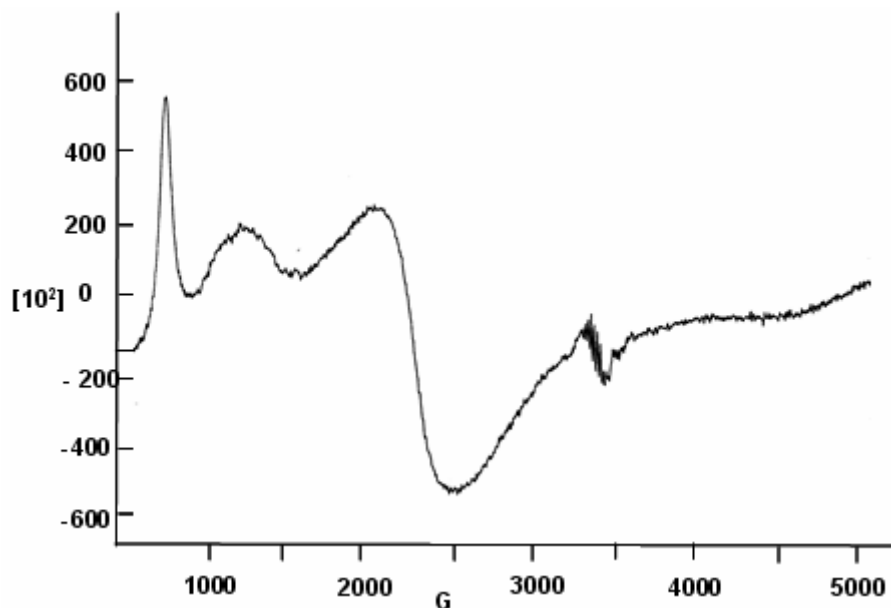
This gave bisphenol porphyrin $\alpha\alpha$ -**34** in good yield (Scheme 12 and 13). The more commonly used de-methylation method with BBr_3 at -78°C was not employed due to the unwanted removal of pivaloyl N-protecting groups and the low efficiency of phenol formation. The activated and protected thiophenylene **42** was then slowly added to the $\alpha\alpha$ -**34** under high-dilution conditions in hot DMF in the presence of Cs_2CO_3 . The dimesylate **42** used in the bridging was synthesised from the corresponding diol **41** which was obtained *via* the hydroboration reaction of diallylthiophenol carbamate **40**¹⁴⁸ that was on stock in our group (Scheme 13).

Cleavage of the thiocarbamate protecting group of **36** liberated the thiophenol function and subsequent iron insertion using FeBr_2 in the presence of 2,6-lutidine as base in refluxing toluene completed the synthesis of bis (methyl carbamoyl) model **38**.

Scheme 14. Completion of the synthesis of the porphyrin **38**.

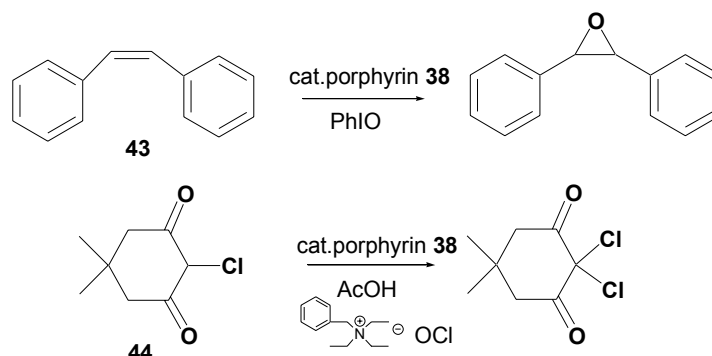
Upon iron insertion the *Soret* band in the UV/vis blue-shifts from 413 nm for **37** to 404 nm for iron (III) compound **38**. Furthermore, the correct mass of the isolated iron(III) porphyrin model compound **38** was confirmed by ESI-MS and MALDI-TOF-MS. It is essential to carry out the deprotection reaction of **38** and the iron insertion under strict exclusion of dioxygen as it is known from previous work in our group that the sulfur of the thiophenolate is prone to oxidation to give the phenylenesulfonate compound [T.R.Leifels, Synthese von Modellverbindungen–PhD Dissertation-Uniiversität Basel 2001]. In practice, the deprotection reaction of **36**, the work up and the purification of **37** was done under argon with degassed solvents and reagents. The iron insertion and all further reactions with the iron(III) porphyrin **38** were performed in a glove box with an inert atmosphere, degassed solvents and reagents.

The cw-EPR spectrum of **38** in dry toluene at low temperature showed g-values (8.30, 5.29, 3.10, 2.05 and 2.00) characteristic of pure high-spin iron(III) porphyrins with a strong rhombic distortion (Figure 21).

Figure 21. cw-EPR spectrum of **38** in toluene

It has already been observed that porphyrin **38** is an adequate P450¹⁴⁸ and CPO¹⁴⁷ mimic respectively in epoxidation reactions (i.e. of *cis*-stilbene **43** and in the chlorination reaction of monochlorodimedone (MCD) **44** (Scheme 15).

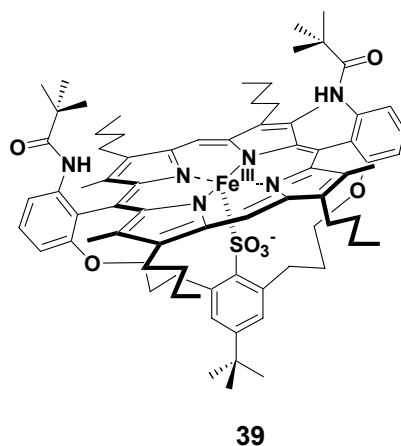
The halogenation of MCD performed using 1.5% mol of porphyrin **38**, together with the transfer-catalyst benzyltriethylammonium hypochlorite as the chlorine source and the AcOH as proton supply, gave the dichlorodimedone in 75% yield and a turnover equal to **45**. The epoxidation of *cis*-stilbene was carried out with iodosylbenzene (PhIO) as an oxygen-donor and 1.1% mol of porphyrin **38** as catalyst and it proceeded in almost quantitative manner.

Scheme 15. Epoxidation of stilbene **43** and chlorination of MCD **44**.

A major problem with porphyrin **38** is its lack of stability during aerobic reaction conditions which makes its handling quite problematic and time consuming. Despite considerable steric congestion at the thiolate ligand in complex **38**, oxidants used for the 'shunt pathway' such

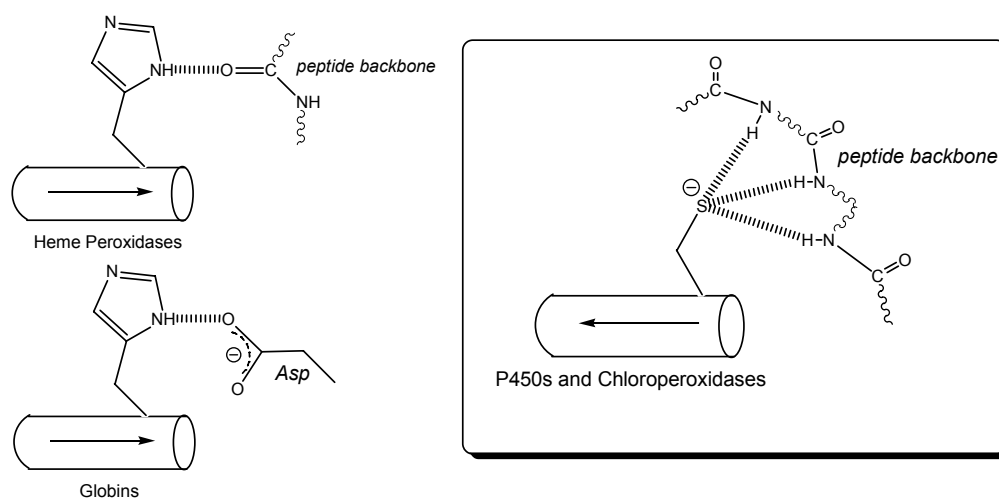
as PhIO , PhF_5IO , and H_2O_2 and in particular O_2 oxidize the thiolate slowly via $-\text{SO}-$, $-\text{SO}_2-$ to SO_3- creating an undesired mixture of porphyrin oxidants during reactions. In order to avoid this problem, the model compound **39** was considered as an alternative to the thiolate ligand (Figure 22). Although it was initially difficult to visualize how the new sulfonate ligand could replace the thiolate ligand and still genuinely mimic the naturally occurring enzyme, this new sulfonate iron(III) porphyrin **39** has some important features of note.

Figure 22. Iron(III) porphyrin **39**.



The synthesis of the sulfonate iron porphyrin $[\text{Fe}-\text{SO}_3(\text{H})]$ was prompted from data relating to unusual characteristics of the local environment of the proximal Cys-ligand in the P450s. As clearly represented in the illustration below, extracted from a paper of Poulos⁵³ (Figure 23), the thiolate ligand of the P450 is at the positive N-terminal end of a helix and accepts three hydrogen bonds, one of which has the optimal orientation, from peptide NH groups.

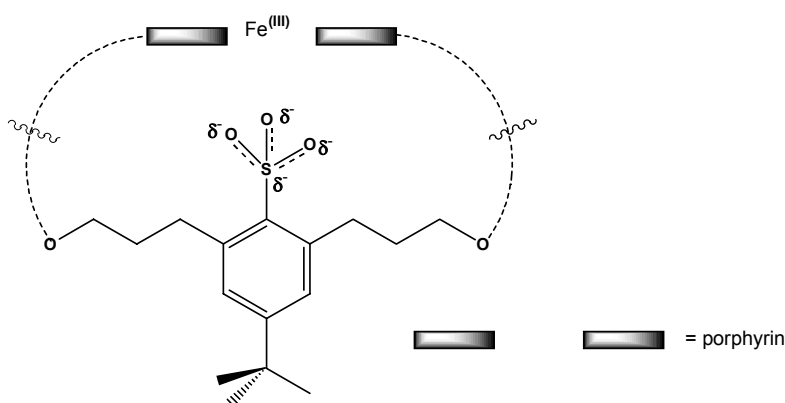
Figure 23. (H-bonding) - Schematic diagram showing the H-bonding interactions between the proximal heme thiolate ligand in P450.



The conservation of these H-bonds in structurally unrelated thiolate-iron proteins like chloroperoxidase CPO¹⁴ and nitrogenase¹⁵⁶ emphasizes the importance of these interactions. Thus, in thiolate iron proteins, the sulfur atom is surrounded by an electropositive environment, exactly the opposite to what is found for the His ligand in peroxidases and globins. This hydrogen network appears necessary to decrease the negative charge on the thiolate ligand in P450/CPO and increase the negative charge on the His in peroxidases. One can speculate that this is required to increase the redox potential of heme-thiolate proteins and decrease the redox potential in peroxidases relative to the non-H-bonded situation.

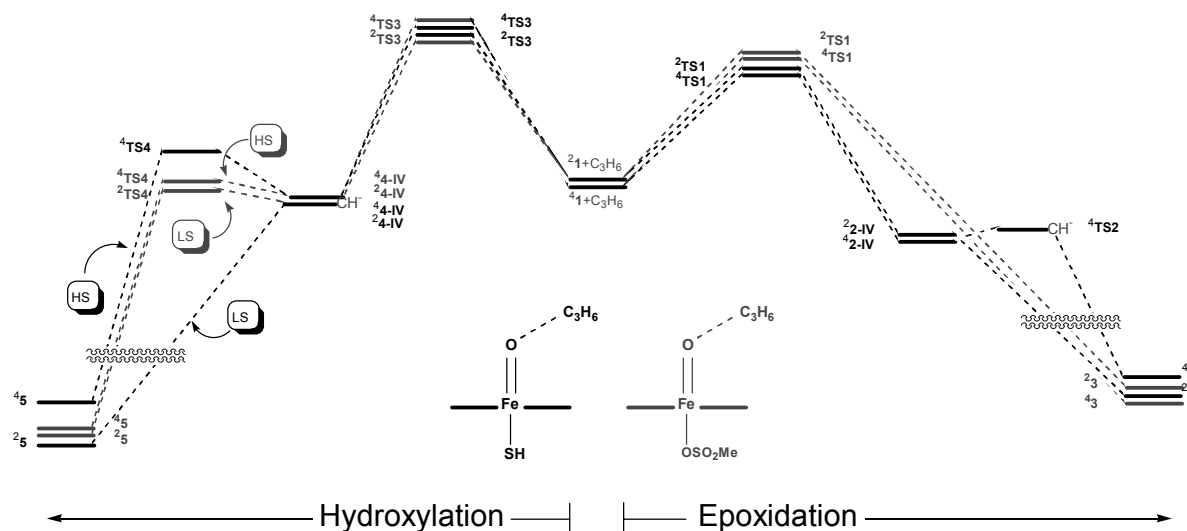
Our porphyrin model is somehow able to mimic the H-bonding of the thiolate to the amino acid residues of the protein backbone, since the negative charge is not merely located on the sulfur atom, but it is delocalized over the three oxygen atoms. The *inverted umbrella* shape of the sulfonate group functions as the hydrogen-bonds set (*Figure 24*).¹⁵⁷

Figure 24. Umbrella-Sulfonate-porphyrin model



Additionally, even though no systematic studies with this sulfonate type compound **39** have been previously conducted in our group¹⁴⁸ a theoretical DFT study of its reactivity was initiated in collaboration with the laboratory of Prof. *Shaik*. The results of these DFT calculations were surprising and, as elucidated in *Figure 25*, the comparison between the reactivity of the first (SH) model **38** with that of the SO₃-type **39** suggested a very strong equivalence.

Figure 25. Energy profile of propene oxidations by Cpd I (in black) versus Cpd I - SO₃ (in red)- obtained with DFT calculation.¹⁵⁷



From the examination of the energy profile diagram above, representing the conclusions of these theoretical studies, the existence of a solid analogy between the activities of the two porphyrins **38** and **39** is rather evident. By comparing the hydroxylation coordinates of the **CpdI-SO₃** and **Cpd I-SH** profiles a difference is observed particularly at the rebound stage. In the **Cpd I-SH** profiles the low spin surface is barrierless which contrasts sharply to the **CpdI-SO₃** profile where both HS and LS states approximate each other. This is important for the following reasons:

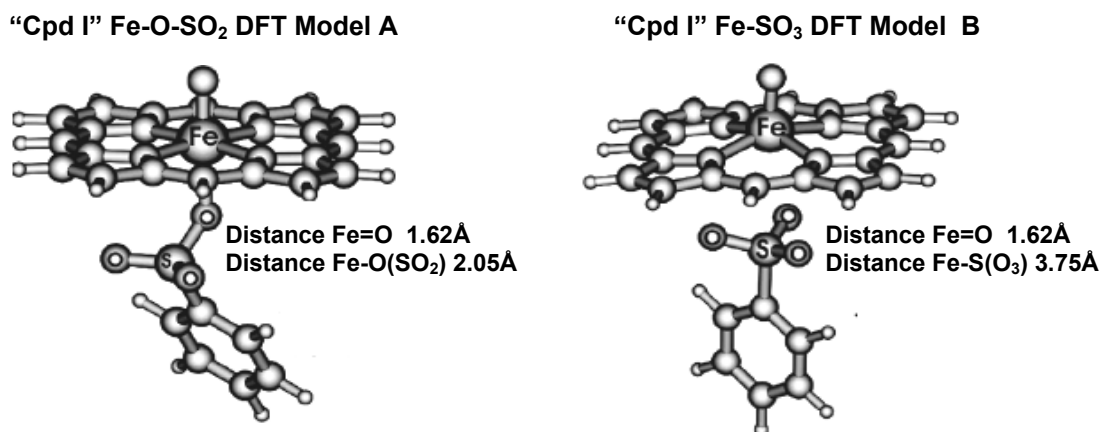
- The concerted LS manifold seen in the **Cpd I-SH** profile will alter the lifetime of the only transition state (HS) giving the false perception of a very short lifetime.
- In the second profile (**CpdI-SO₃**) two defined transition states are observed which offer a truer reflection of the actual lifetime since both the LS and HS states approximate each other. In this scenario the “observed lifetime” has a higher probability of being the “actual lifetime” making this **CpdI-SO₃** a better porphyrin probe.

In addition, the synthetic model shows a small preference for C-H hydroxylation over C=C epoxidation, while the natural species has an opposite slight preference.

The DFT calculations supported a proposal that one of the oxygens from the SO₃⁻ ligand coordinates to the iron instead of the S⁻. This is shown in *Figure 25b* where the iron-oxo porphyrin species **39_{DFT}** which acts as a model for **39**, is described in two different coordination modes, one with an Fe-O bond between the heme and the RSO₃⁻ ligand **39_{DFT-A}**, and the other with an Fe-S bond **39_{DFT-B}**. The second option (model B) is unfavorable, the Fe-S

bond is too long and the species is positioned at an energy level 19-31 kcal/mol higher than the corresponding Fe-O bond (mode A). In addition, frequency calculations have demonstrated that **39**_{DFT-B} (B) are not stable minima but are in fact saddle points for the exchange of three different Fe-O bonds.

Figure 25b. Porphyrin Models **39**_{DFT-A} and **39**_{DFT-B} obtained by DFT calculations.¹⁵⁷

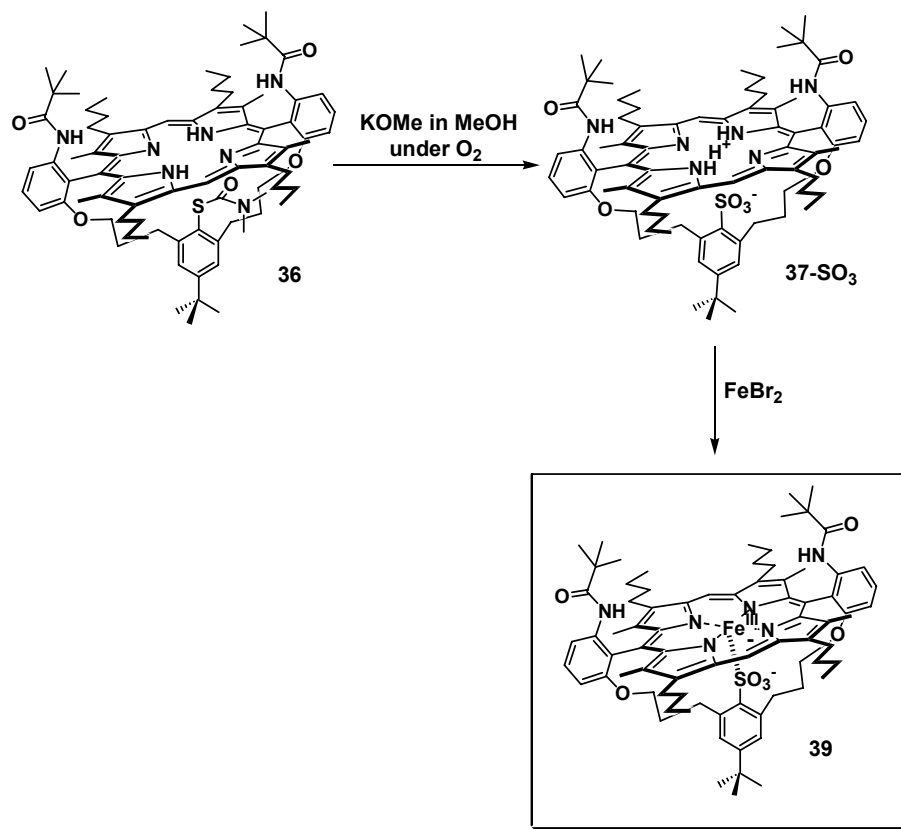


Thus calculations have shown that the new sulfonate porphyrin possesses an equivalent reactivity to its thiolate precursor even though the nature of the 5th ligand is very different -the “hard” oxygen of the Fe-O-SO₂ ligation in this case replaces the “soft” sulfur of the Fe-S (thiolate) ligation. It should be noted that *Shaik* calculated both energy profiles and bond distances only with an optimized Cpd I SO₃ species. Thus, although these DFT calculations proposed a certain structure and reactivity of the new porphyrin mimic, it was hoped that both UV, EPR analysis and eventually X-Ray analysis would properly define the structure of **39**. The attainment of the X-Ray structure was particularly important as it would help identify the nature of the Fe-SO₃ ligation and the actual bond distances in the porphyrin resting state.

At this point, therefore, it was necessary to find a good procedure for obtaining compound **39**. Several attempts in oxidizing the thiolate functional group of the porphyrin with or without iron already inserted (**37** and **38** respectively) have been made. Reaction conditions like TBHP or *m*-CPBA in dichloromethane, H₂O₂ together with a micro-emulsion of Na₂MoO₄ and sodium dodecylsulfate in BuOH¹⁵⁸ gave low yields and numerous side products. KMnO₄ and 18-crown-6 ether in benzene or KMnO₄ alone in acetone was found to be the most efficient system even if the yield was very modest at 25%. Finally it was found that the cleavage of the thiocarbamate protecting group of **36** using aerobic conditions was the shorter and most effective way to produce compound **39**. The solution of **36** in dioxane was bubbled with O₂ before the addition of KOMe and the reaction mixture was then left refluxing for 30 hours in an atmosphere enriched in molecular oxygen. With this procedure

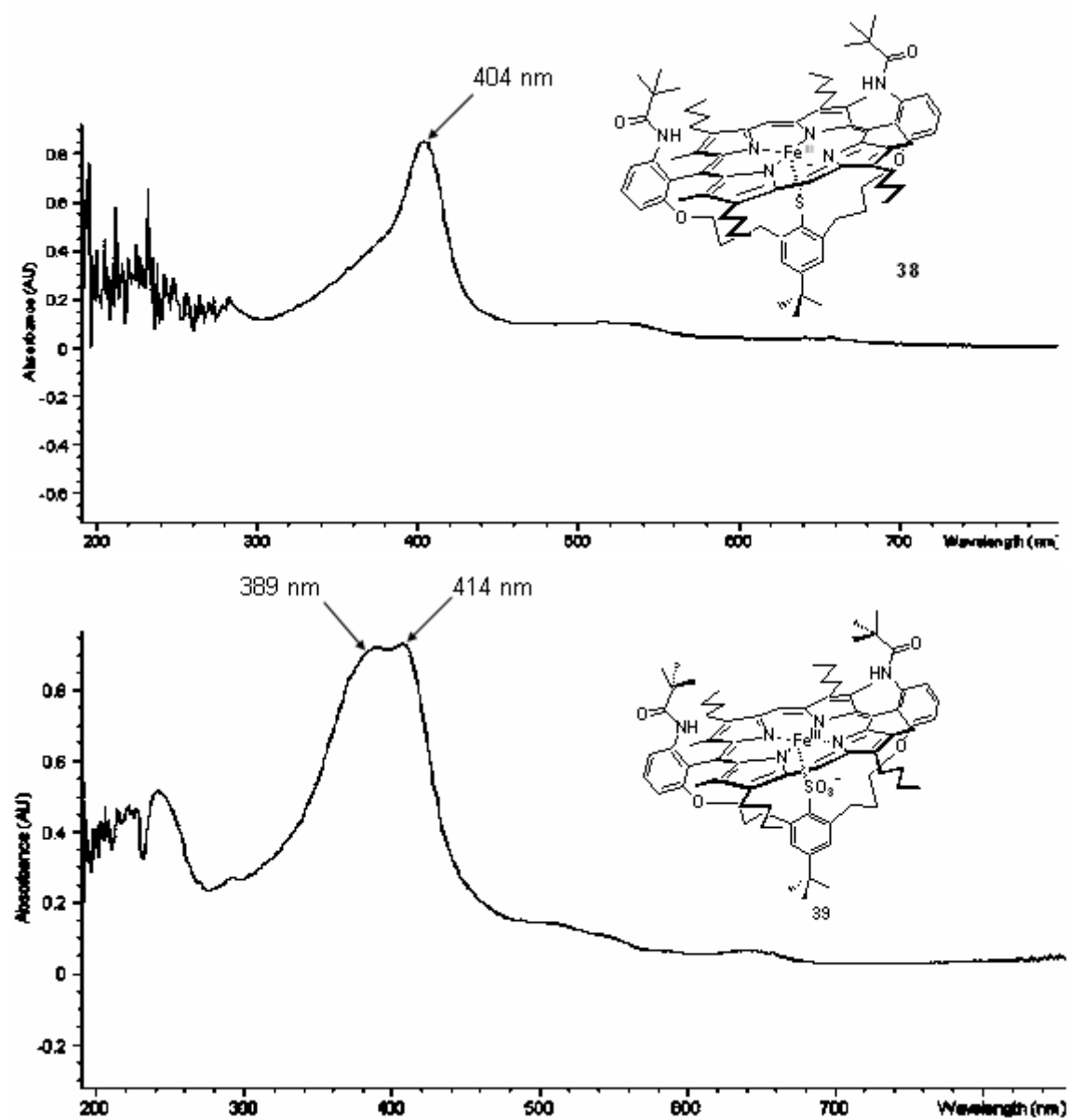
there is no need to isolate the thiolate porphyrin and the overall yield of compound **37-SO₃** was between 35-40 %. Upon iron insertion, the porphyrin **39** was then obtained.

Scheme 16. Completion synthesis ironsulfonate porphyrin **39**

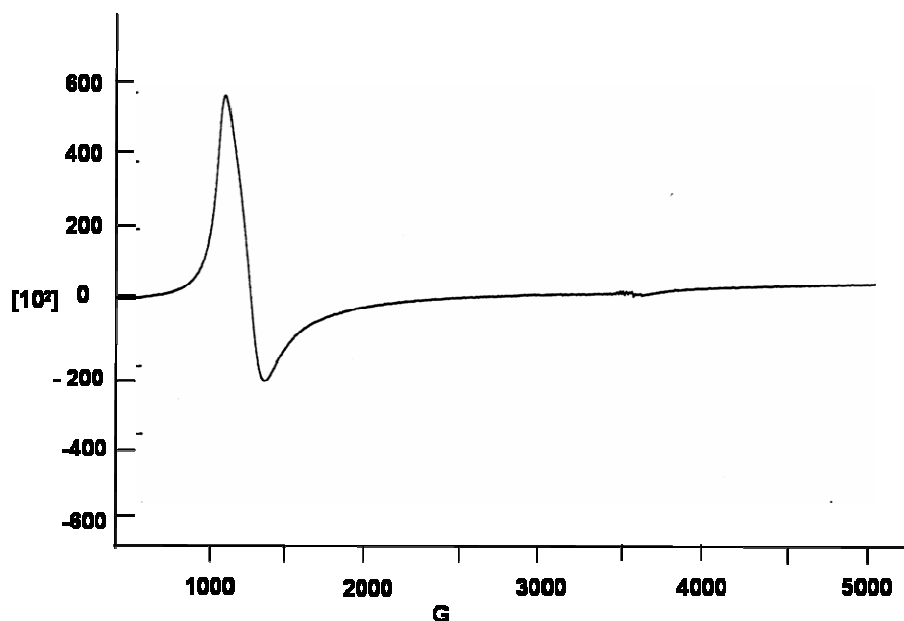


A considerable difference was observed between the UV-*vis* spectrum of thiolate iron-porphyrin **38** and the sulfonate iron porphyrin **39**. The *Soret* band of **38** has a $\lambda_{\text{max}} = 404$ nm and **39** presented, on the other hand, a split *Soret* band with maxima at $\lambda_{\text{max}} = 389$ and 414 nm (*Figure 26*).

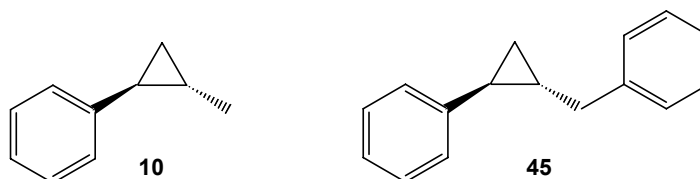
Figure 26. UV-visible spectrum of **38** in chloroform and **39** in methanol



The cw-wave EPR spectrum of porphyrin **39** is axial distorted with g-values characteristic of a high spin Fe^{III} system (toluene, 94K, g-factor: 5.6) (Figure 27).

Figure 27 cw-wave EPR spectrum of porphyrin **39** in toluene

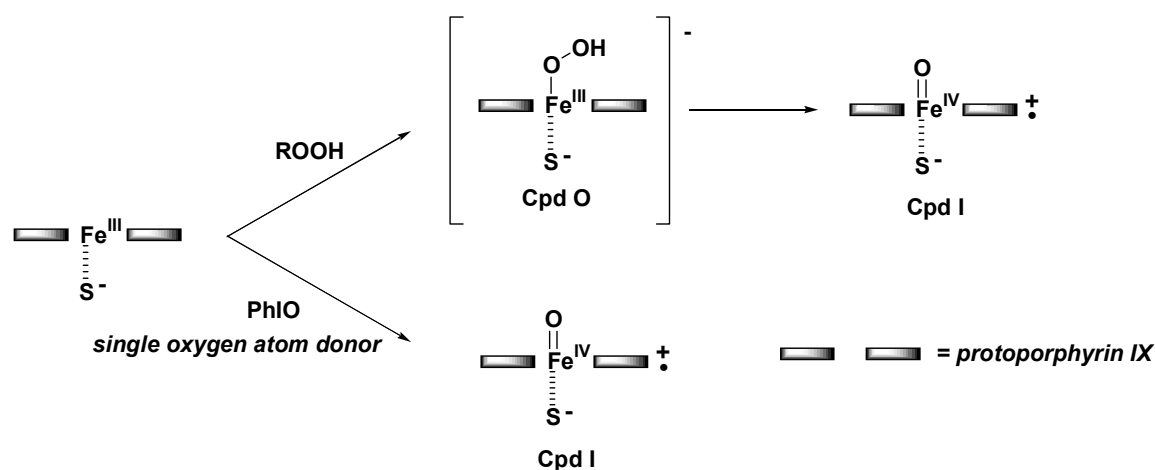
On finishing the original synthesis the new porphyrin mimic **39** was utilized for finding the correct conditions for substrate oxidation and subsequent analysis. As already mentioned in the previous experimental work we attempted to examine the definition of radical lifetimes of the intermediate predicted by the rebound mechanism. The compounds chosen as substrates for C-H hydroxylation were the cyclopropyl radical clocks used extensively for this purpose.^{137,87,159} The ultimate objective of this work was to examine the behavior of the *trans*-methyl-phenyl cyclopropane **10** (Figure 28) in the so called *shunt pathway* (see *Shunt pathway* in section 1.2), involving our porphyrin mimic and a suitable oxygen donor. Yet, as a primary non activated C-H bond is very prohibitive to oxidation, the correct conditions needed to successfully perform this reaction had to be found using a similar but more activated cyclopropane derivative. *Trans*-benzyl-phenyl cyclopropane **45** (Figure 28) was designed as the required substrate analogue since the C-H benzylic position of the ethyl benzene was reported by Groves¹⁶⁰ to be easily hydroxylated in a reaction employing a metallo porphyrin catalyst and oxygen donors.

Figure 28. Substrates use in the oxidation performed with metallo porphyrin and oxygen donor

3. 3. Optimization of reaction conditions for radical clock experiments

Since the overall yield of the oxidation products of **10** was expected to be low, it was necessary that the reaction conditions were maximized. This required optimal solvent, time, oxidizing reagent, and temperature to be found along with a suitable porphyrin/ substrate ratio. The decision of which oxidant to use was based on its ability to produce an unambiguous oxidative species. In order to avoid the formation of a synthetic Cpd 0 (*Figure 29*) all peroxide oxidants were excluded.^{161, 162} Iodosyl benzene was chosen since, as a mono oxygen donor, it can give the synthetic analogue of Cpd I but not the hydroperoxide form (equivalent to Cpd 0).^{163 164, 165}

Figure 29. Comparison between single oxygen atom donors and peroxides



This oxidant had the added bonus, in that its degradation product, iodobenzene, has a very low retention time during GC analysis and therefore, does not interfere with the alcohol product signals. This preference for PhIO then limited the solvent selection, used in the oxidation reaction as iodosyl benzene is known to be partially soluble only in CH_2Cl_2 .¹⁶⁶ This oxygen transfer reagent has been, for several years, incorrectly adjudged to be soluble in MeOH. In fact the high solubility of iodosylbenzene in methanol is due to a solvolysis reaction that forms iodobenzene dimethoxide, $\text{PhI}(\text{OMe})_2$.¹⁶⁶ Dry CH_2Cl_2 on the other hand is an ideal solvent for these radical clock experiments as it could reproduce a similar environment to that experienced by the probe inside the hydrophobic surroundings of the enzymatic pocket. The temperature range in which the reaction could be carried out was quite restricted. At low temperatures (around 0°C) PhIO was found to precipitate out of solution. All the oxidation reactions were eventually carried out at 20°C , in CH_2Cl_2 using 1 equivalent of PhIO. An assessment of the ratio of porphyrin mimic to substrate was also important. Various trial reactions were conducted using 1-10% porphyrin to detect how this ratio affected the quantity of product formed. There was found to be no increase in the

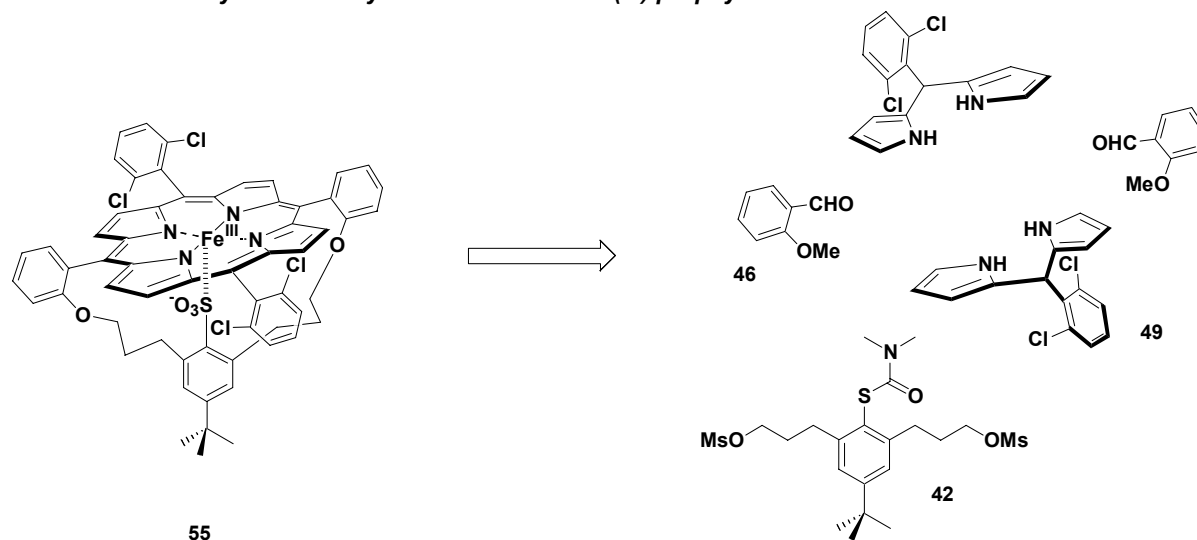
quantity of products produced using an amount greater than 2.5% porphyrin mimic. The actual duration of the oxidation reaction was also short - typically it was found that there was no increase in yield after a 30 minute time period.

3.4 Synthesis of porphyrins **55** - novel model for mimicking the prosthetic porphyrin IX active site of P450.

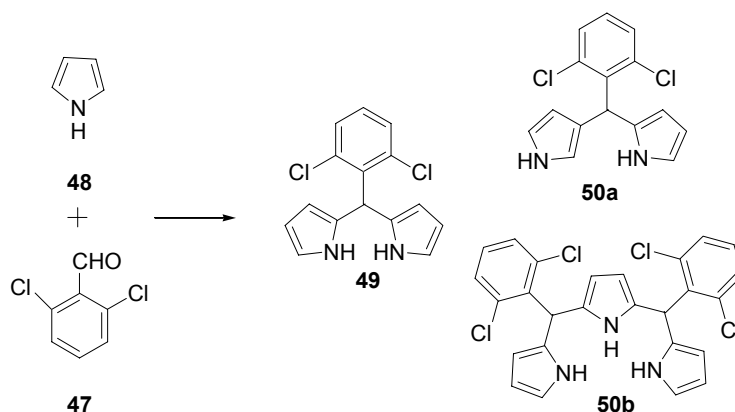
During the course of these trial experiments a second porphyrin mimic was synthesized. The reasoning behind this decision were

- A new porphyrin with all *meso* positions locked was thought to be a more stable alternative to **39**. The stability of the porphyrin could also be improved by incorporating EWD groups that reduce the electron density on the porphyrin ring.¹⁶⁷⁻¹⁶⁹
- The overall length and yield of the original synthesis were prohibitive to producing the quantities of porphyrin required to conduct several oxidation reactions. The choice of a C₂ symmetry porphyrin core was deemed a better alternative and had the bonus of avoiding the time consuming separation of the atropisomer intermediates formed after the MacDonald condensation (see Paragraph 3.2.).
- As another member of the research group was attempting the synthesis of an analogous porphyrin it was thought valuable to produce a similar species for comparative analysis.

The synthesis of this novel porphyrin was then undertaken. A retrosynthetic analysis of the iron (III)-porphyrin **55** leads to three main building blocks: the dipyrromethane derivative **49**, the commercially available 2-methoxybenzaldehyde **46** and the protected thiophenyl bridge **42** (*Scheme 17*).

Scheme 17. Retrosynthetic analysis of the novel iron (III) porphyrin model 55.

5-Substituted dipyrromethanes are important precursors for the synthesis of meso-substituted porphyrins.^{155, 170} The method for obtaining the dipyrromethane **49** is a one-flask synthesis in which the aldehyde is dissolved in a 80-fold excess of pyrrole **48** with a catalytic amount of the acid (0.1 equiv. of TFA) at room temperature in the absence of any other solvent.¹⁷⁰ The reaction is performed in the dark and it goes to completion after only five minutes. The crude solution was a complex mixture of six compounds. The desired **49** compound was the main product with two of the side products almost certainly were the N-confused 5-phenyldipyrromethane **50a**, and 5,10-diphenyltripyrane **50b** as suggested previously by Lindsey (Scheme 18).¹⁷¹

Scheme 18. Synthesis of 5-Substituted dipyrromethane 49.

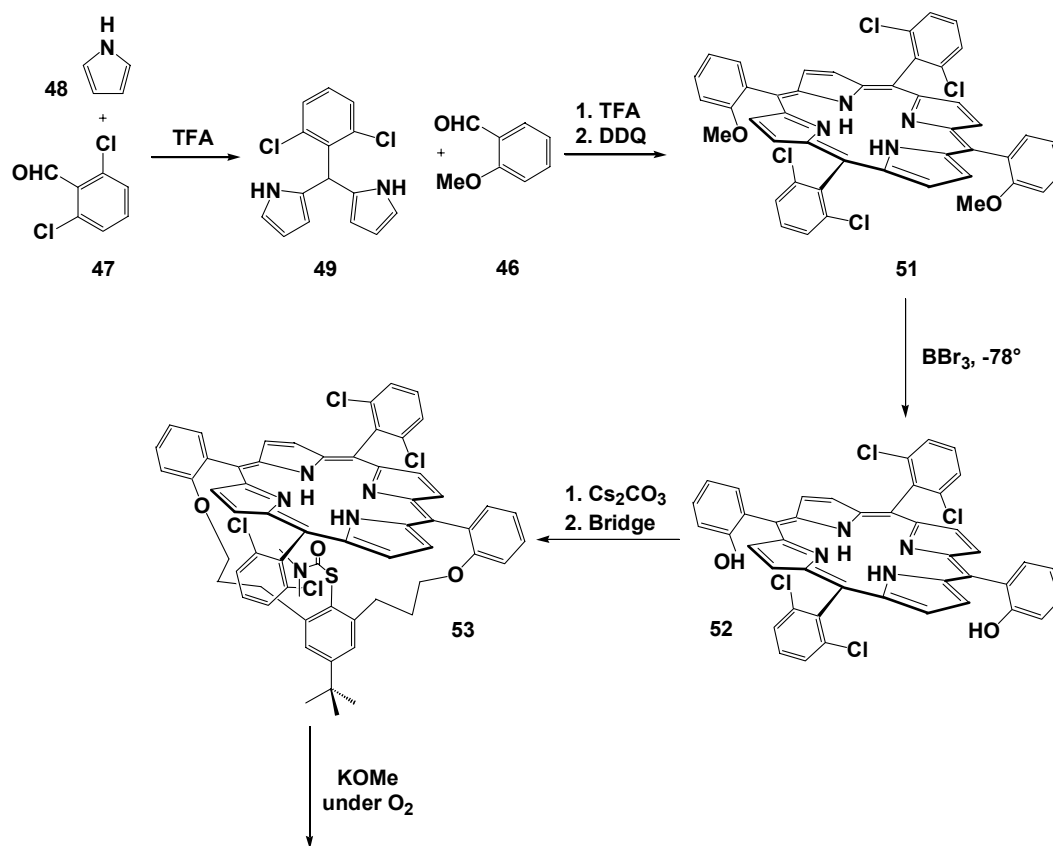
This synthetic procedure followed by flash chromatography purification and subsequent crystallization provided a yield of pure 5-(2,6-dichlorophenyl)dipyrromethane of around 30%, that it was in full agreement with the literature values.¹⁷¹

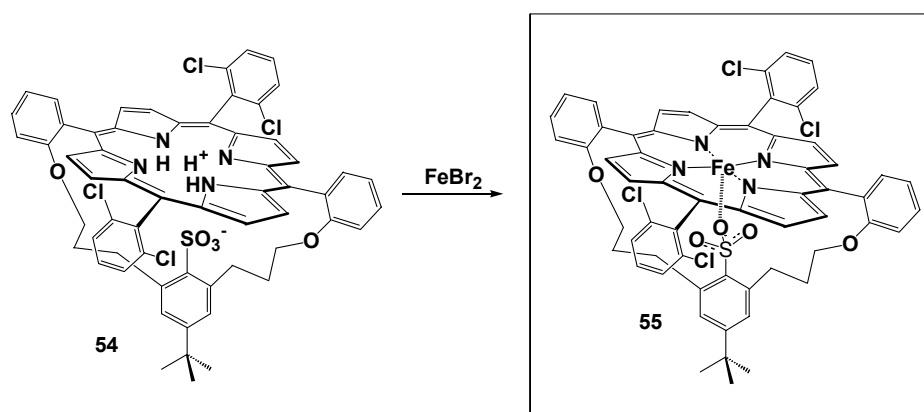
The synthesis of the A₂B₂-porphyrin was completed using the optimized conditions reported by Lindsey *et al.*¹⁷¹ The condensation is performed in dilute solution at room

temperature. The **49** and 2-methoxybenzaldehyde **46**, in ratio 1:1, have a concentration around 10 mM in CH_2Cl_2 . TFA was used as the acid of choice, rather than $\text{BF}_3\cdot\text{Et}_2\text{O}$, since the degree of scrambling with the latter increases dramatically. The porphyrinogen species formed with a UV absorption at 485 nm is then oxidized with DDQ to give the pure porphyrin **51** characterized by a *Soret* band at 418 nm in 30% yield.

The cleavage of the methyl ethers was carried out following the commonly used demethylation method with BBr_3 at -78°C . The reaction course was followed by ESI-MS in order to verify when the transformation of **51** into the bisphenol porphyrin **52** was accomplished. The synthesis continued with the bridging of **52** with activated and protected thiophenylene **42** under high-dilution conditions in hot DMF in the presence of Cs_2CO_3 to give porphyrin **53**. (Scheme 19).

Scheme 19. Synthetic route to the porphyrin 55

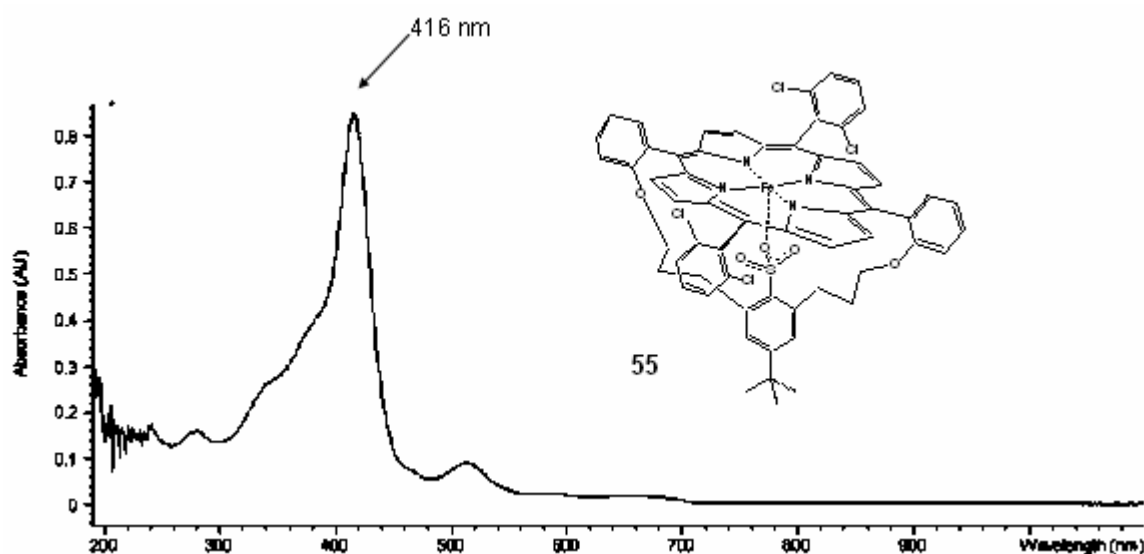




Finally the cleavage of the thiocarbamate protecting group of **53** in aerobic conditions produced compound **54** with an overall yield around 35%. Subsequent iron insertion using FeBr₂ in the presence of 2,6-lutidine as base in refluxing toluene completed the synthesis of model **55** (Scheme 19).

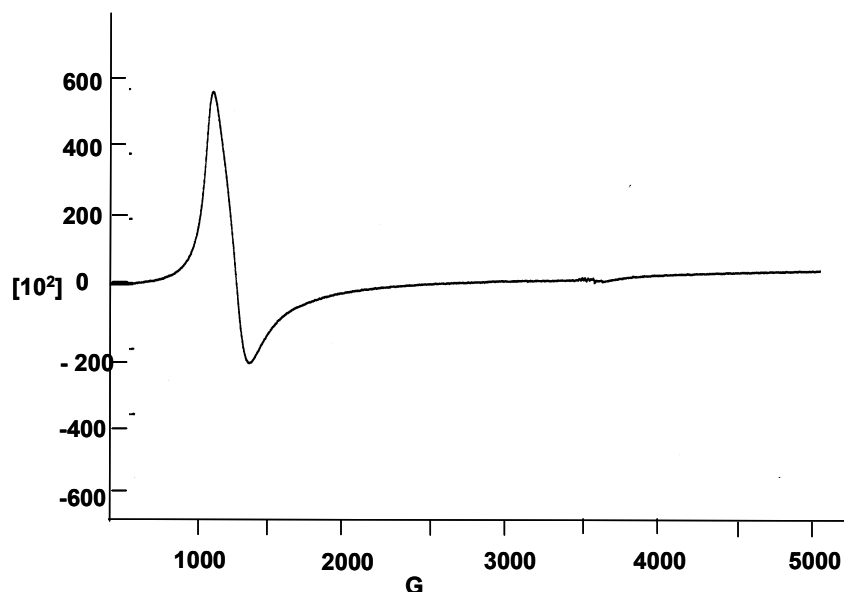
The UV-visible spectrum of **55** presents a Soret band at $\lambda_{\max} = 416$ nm.

Figure 30. UV-vis spectrum of **55** (in CH₃Cl)



The EPR analysis of compound **55** displayed a high spin axial distorted spectrum, indicative of a slightly strained system with the iron protruding out of plain towards the fifth ligand and typical of a oxygen- iron coordination (*Figure 31*).¹⁷²

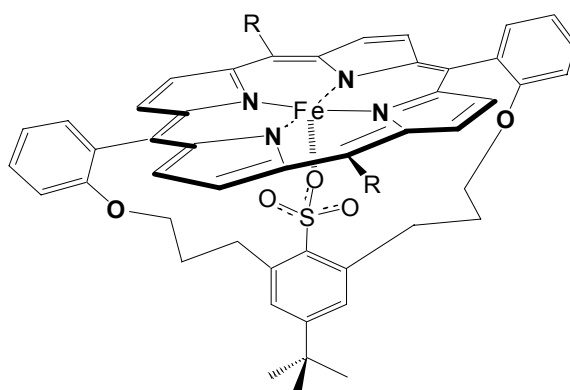
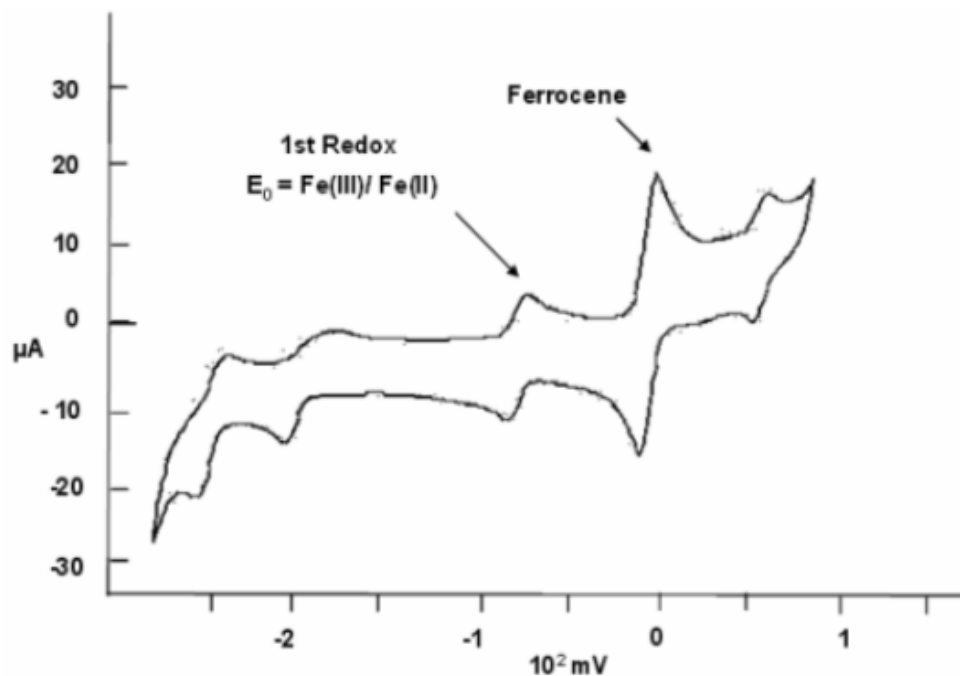
Figure 31. cw-wave spectrum of porphyrin 55 in toluene



Cyclovoltammetry revealed a distinctive feature of these Fe-SO₃-type porphyrins. The results showed the porphyrin mimic redox potential E_0 is comparable to that of heme thiolate proteins. In fact, as is shown in *Figure 32*, measurements done by Meyer using porphyrin **55** and a second porphyrin **55b**, illustrated below, provided values of $E_0(\mathbf{55}) = -280$ mV and $E_0(\mathbf{55b}) = -340$ mV respectively, that correspond, for example to the P450 cam $E_0 = -290$ mV.¹⁷³

It is noteworthy that previous cyclovoltammetry experiments conducted with Fe-SH porphyrins, synthesized in our research group, gave redox potentials of ≈ -600 mV. In this context the anodic shift can be rationalized in terms of a negative charge which is no longer localized on the sulphur atom, as in the Fe-SH mimic, but is redistributed in the SO₃ conical volume.

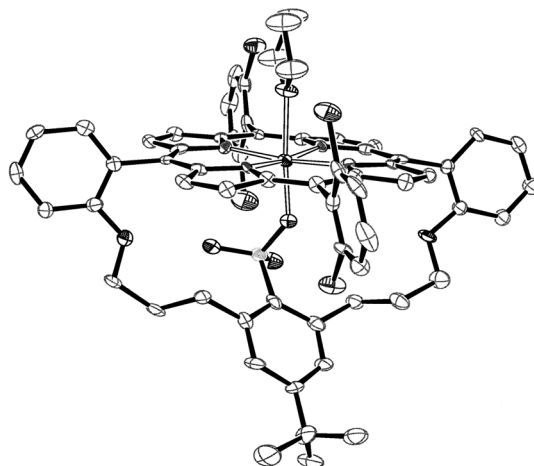
Figure 32. Cyclovoltammogram of porphyrin 55 (0.6 mM) in 0.1M LiClO₄ solution in DMF with ferrocene as internal standard.¹⁷³



R	1 st ox	1 st red	2 nd red	3 rd red
55b 	920 mV	-340 mV	-1480 mV	-1970 mV
55 	1010 mV	-280 mV	-1420 mV	-1900 mV

The X-ray structure of **55** (Figure 33) confirmed the accuracy of the synthetic design and more importantly reinforced the hypothesis that one of the oxygen atoms, and not the sulfur atom, of the SO_3^- group, was coordinated to the central iron.

Figure 33. ORTEP representation of model compound **55** (the solvent THF is coordinated to the Fe as sixth ligand).



The X-Ray also provided more information relating to the bond distances of the fifth ligand in the porphyrin resting state. A comparison can be made between the Fe-S bond distance of the P450cam (2.2\AA)¹⁷⁴ and the Fe-O bond distance (1.96\AA) of **55**. Unfortunately, at this present time, no DFT characterization of the resting state model is available which would have established the reliability of *Shaik's* calculations. It should be taken into consideration that a structural equivalence of the DFT model to the mimic is not always a prerequisite to the prediction of how the porphyrin behaves. Even if the mimic **55** has been synthesized in order to perform typical heme thiolate protein reactions it is interesting, from the structural point of view, to see that the Fe-O bond distance of **55** is similar to the Fe-OTyr (1.85\AA)¹⁷⁵ bond distance of human catalase, an enzyme which typically catalyses the disproportionation reaction of H_2O_2 into H_2O and O_2 in biological systems.

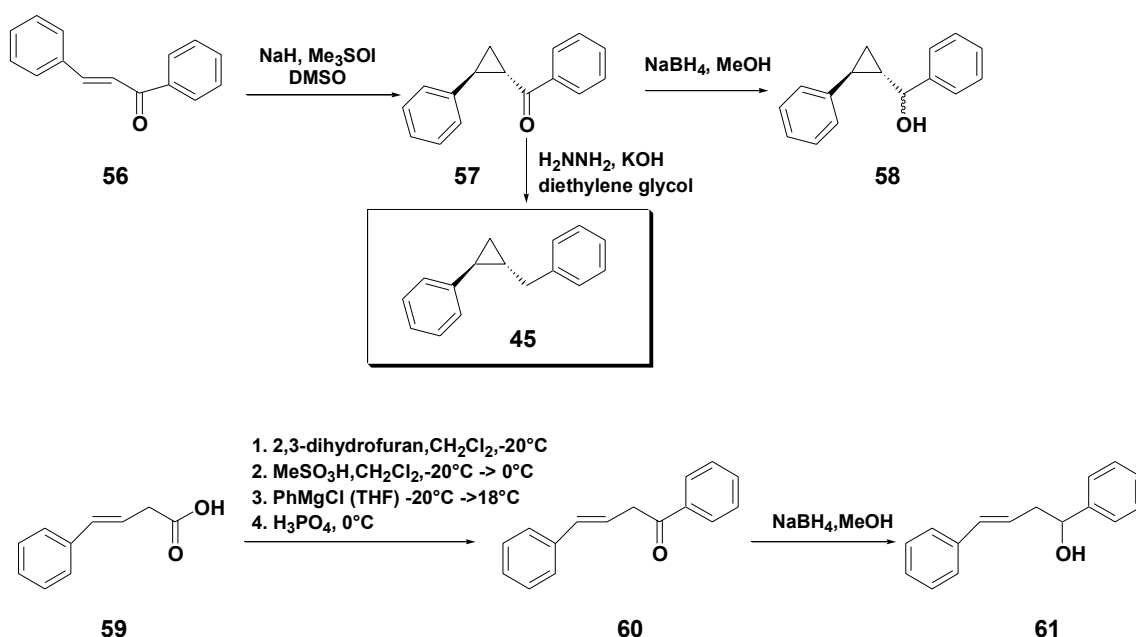
The coordination of one of the three oxygen atoms to the iron rather than the sulfur itself, seemed to undermine the hypothesis that the model **55** could, to some extent, mimic the Fe-SCys bond situation, within its hydrogen bond network. In spite of the structure of **55** not being true to the native enzyme system, the proximity of the redox potential of **55** and **55b** to the P450 redox potential, coupled with the reactivity predictions coming from the DFT calculations, led us to believe that this research was worth continuing with and had the potential to produce some interesting results.

3.5 Synthesis of the cyclopropyl derivatives – slow and fast radical clocks.

As already mentioned in the section 3.2., the molecules selected as substrates for the oxidation reactions catalyzed by the porphyrin model **55** were the 2-arylsubstituted cyclopropyl derivatives **10** and **45**. The analytical method chosen for the qualitative and quantitative analysis of the products generated during the oxidative reaction was gas chromatography analysis performed with a GC-FID instrument. Extensive analysis were initially undertaken using both normal and reverse phase HPLC but both proved inadequate due to the irreproducibility of the results and the lack of sensitivity. GC-MS analysis was also attempted to analyze the products formed but it again proved unsuitable due to a lack of sensitivity of the in-house machine. It should be noted that other research groups have successfully analyzed the products from these radical clock reactions with “finely tuned” GC-MS machines. Once the starting substrates were purified to a very high degree (typical purity >99.9%) GC-FID proved to be the only method suitable for quantitatively analyzing products with yields less than 1%. Before the radical clock experiments with subsequent GC analysis could be performed it was necessary to synthesize not only the substrates **10** and **45** but also standard compounds corresponding to the expected products of the oxidation.

The α -ketone-cyclopropane **57** was synthesized starting from the commercially available trans-chalcone **56** (Scheme 21).

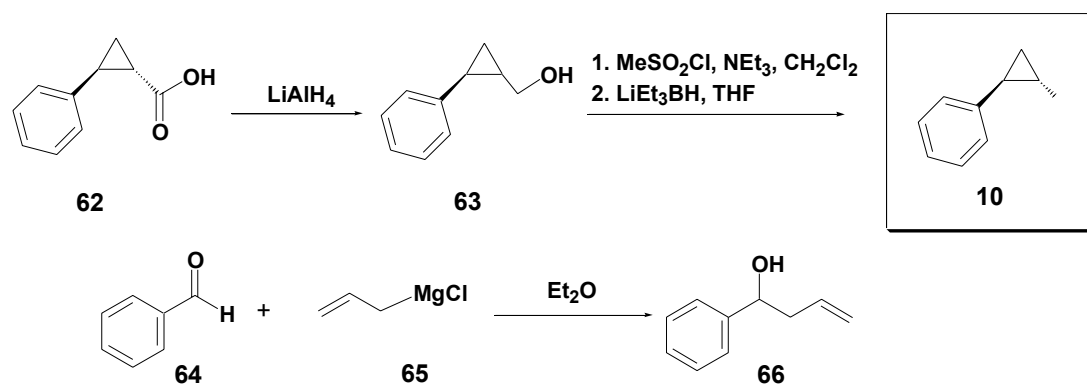
Scheme 20. Synthetic route of substrate 45 and its oxidation products.



The ketone intermediate **57** was formed by the reaction of chalcone **56** with oxosulfonium ylide whose reactivity was studied for the first time by Corey and Chaykovsky.¹⁷⁶ In this case, the ylide itself was formed by the reaction of trimethyloxosulfonium iodide with a strong hydride base. The ylide has a nucleophilic character and transfers the methylene to the C=C double bond in a stereoselective manner through a 1,4-Michael addition to the α,β -unsaturated ketone.^{177 178} The obtained 1,2-*trans*-di-substituted α -ketone-cyclopropane **57**, was then transformed into the corresponding alcohols by a simple reduction with NaBH₄. These two diastereoisomers were not only easily differentiated by TLC and 1H-NMR, but more importantly also by gas-chromatography. The substrate **45** was obtained by complete reduction of the carbonyl group of **57** using a Wolff-Kischner reduction. The synthetic strategy adopted for the synthesis of the (*E*)-1,4-diphenyl-3-buten-1-one **61** utilized the methodology of ketone synthesis from acid via acyl hemiacetal reported by Rapoport.¹⁷⁹ Thus, the protection of the acid as 2-tetrahydrofuranyl ester followed by the addition of the phenyl magnesium bromide and acid work-up afforded the desired unsaturated β,γ -unsaturated ketone. Simple reduction gave the compound **61**.

The synthesis of the second substrate, the *trans*-2-methylphenylcyclopropane **10**, started from the commercially available *trans*-2-phenylcyclopropanecarboxylic acid **62** (Scheme 21). The starting material was transformed into the correspondent alcohol **63** by simple reduction with LiAlH₄. The *trans*-(2-phenylcyclopropyl)methanol **63** was then converted to the mesylate. This was then subsequently reduced to the desired compound **10** using LiEt₃BH.

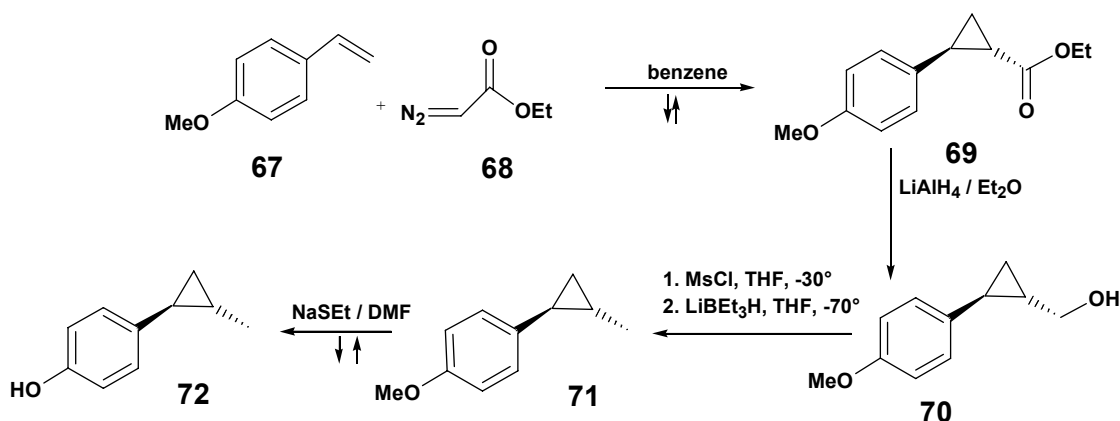
Scheme 21. Synthetic route for the substrate **10** and the standards for the predict products.



The allylic alcohol **66**, that is the expected oxidation product of the ring-opened radical, was obtained by simple Grignard reaction between benzaldehyde **64** and allylmagnesium chloride **65**. Another product detected during Newcomb's enzymatic

experiments with the substrate **10** was *trans*-2-(*p*-hydroxyphenyl)methylcyclopropane **72**.⁹⁵ Therefore it was also advisable to synthesize a standard for this phenolic derivative. This was required even if there was no proof that the porphyrin mimic system could perform an aromatic hydroxylation (Scheme 22).

Scheme 22. Synthetic route for the phenolic derivative **72**.



Reaction of *p*-vinylanisole **67** with ethyl diazoacetate¹⁸⁰ **68** gave a mixture of ethyl *cis*- and *trans*-2-(*p*-methoxyphenyl)cyclopropanecarboxylates **69**, which was separated by column chromatography and crystallization. The *trans* isomer, identified by NMR spectroscopy, was reduced with LiAlH_4 to the alcohol **70**. The product **70** was then converted to its mesylate that, without being isolated, was directly reduced in the same pot with LiEt_3BH at -78° . To prevent polymerization necessitated the need to work as such low temperatures. Finally the resulting *trans*-2-(*p*-methoxyphenyl)-methylcyclopropane was demethylated with NaSEt in DMF to give the desired product **72**.

4. Radical Clock Experiments and Discussion

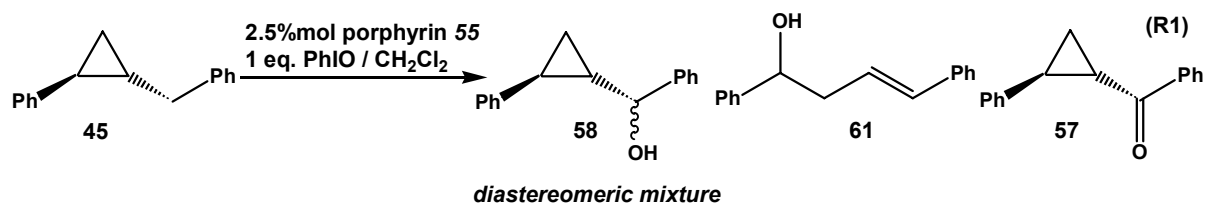
4.1. Radical Clock Experiments

The radical clock experiments were conducted in order to initially examine the suitability of the porphyrin mimic as a tool for substrate hydroxylation and, if successful, engage a debate about the exact nature of the catalytic pathway mechanism. Therefore it was proposed to use the porphyrin mimic **55** firstly in a systematic study of a “*slow*” radical clock **45** and subsequently in an examination of a “*fast*” radical clock **10**. As already mentioned in chapter 2 the value of this experiment was that, given the k_{rear} values, k_{OH} values can be deduced from the ratio of rearranged and unrearranged alcohols formed.

4.1.1 Slow Radical Clock Experiments

The first set of these experiments were performed with substrate **45**. Since this substrate has been categorized as a “*slow*” radical clock ($k_{\text{rear}} = 3.6 \times 10^8 \text{ sec}^{-1}$) it was not expected to give an insight into the kinetic mechanism of the hydroxylation.⁸⁸ What it could provide, on the other hand, was initial confirmation that the porphyrin mimic itself could perform the hydroxylation of substrates similar to those found in *Newcomb's* enzyme experiments. If the initial experiments were successful it was hoped to perform more detailed experiments with substrates defined as “*fast*” radical clocks.

The reaction was typically performed in anaerobic conditions at 20°C in CH₂Cl₂ using 2.5% of porphyrin mimic and 1 eq. of PhIO (*Scheme 23*). All substrates used during these experiments had an analytical purity of 99.9% by GC analysis. The purity of each substrate was examined prior to the start of each experiment to ensure no artifacts were present. Using analytical techniques described in the experimental chapter the crude reaction mixture was then analyzed with a GC-FID technique. The results of the oxidation R1 of substrate **45** are shown in Table 1. It is important to note that the distribution of products formed during this reaction was not as expected. As it is known that this substrate is a *slow* radical clock predisposed to a fast hydroxylation rate the presence of rearranged alcohol **61** and the ketone **57** in the GC analysis came as a surprise.

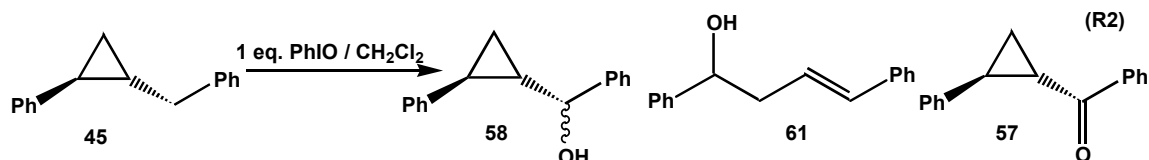
Scheme 23. Hydroxylation performed with porphyrin 55 in catalytic amount.**Table 1.**

Reaction	57*	58-dia-1*	58-dia-2*	61*
R1	226.7	505.0	242.6	11.7
R2	1.1	4.8	3.2	0.1
R3	186.5	488	238.9	12.4
R4	232.5	551.6	269	11.1
GC-retention time	20.7min.	22.7min.	22.9min.	23.6min.

* 1 unit corresponds to 0.013 $\mu\text{mol} / \text{mL}$ (CH_2Cl_2)

The overall yield was moderate but the products formed were easily distinguishable from each other using standard gradients (Table 1). The major products formed were the unrearranged diastereoisomer alcohols **58**. The minor product formed was the corresponding rearranged allylic alcohol **61** and the ketone **57**. In order to eliminate the possibility of other alternative routes to the products formed, subsequent blank reactions were performed. The logic behind these control experiments was the following.

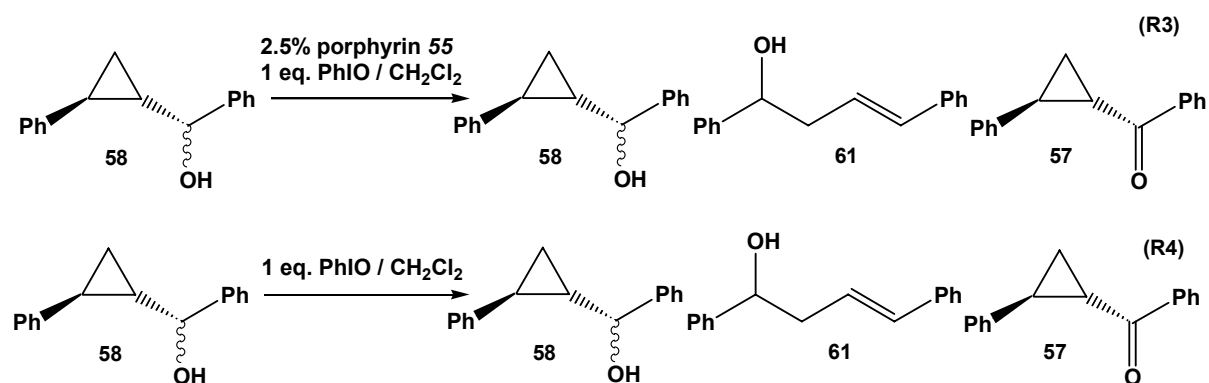
The blank reaction R2 was performed to control the effect of PhIO without the contribution of porphyrin catalyst. (Scheme 24)

Scheme 24. Blank reaction R2.

The control experiments R2, shown in Table 1, proved that PhIO, on its own, produces a background reaction which corresponds to $\approx 1\%$ of the overall yield seen in R1. The results from the R2 reaction prove how vital the porphyrin is in this oxidation process and demonstrates that this porphyrin mimic can act in a catalytic manner.

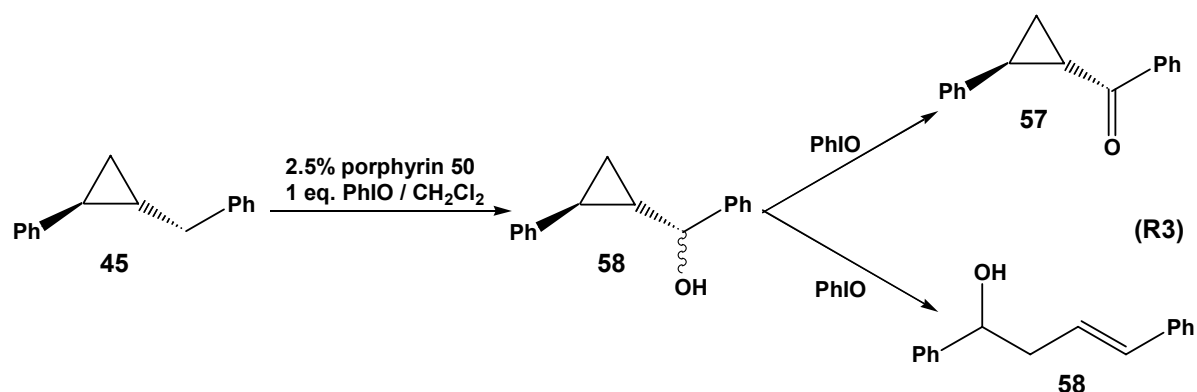
R3 and R4 blank experiments, conversely, were necessary to demonstrate whether it was possible to rearrange the alcohol **58**, formed from direct hydroxylation of **45** before the opening of the cyclopropyl ring, into the allylic alcohol **61**. (Scheme 25)

Scheme 25. Control reactions R3 and R4

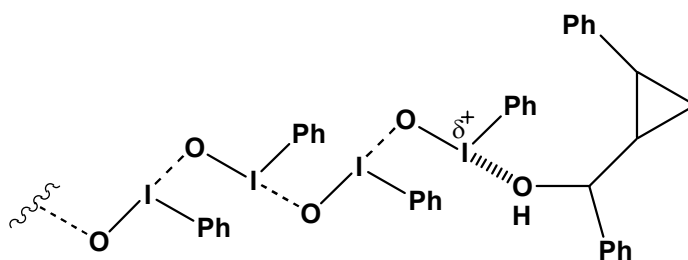


The reactions R3 and R4 were performed using the unrearranged alcohol **58** as the starting substrate. Here, the actual amount of starting substrate, **58**, used in R3 and R4 was equal to the quantity of unrearranged alcohol **58** that was produced during the R1 reaction. If both the rearranged alcohol **61** and ketone **57** are exclusively derived from the unrearranged starting alcohol **58**, then the yields of products formed in R3 and R4 should be consistent with those observed in R1. The results showed that the quantity of **61** and **57** observed in R1 were entirely derived from the action of PhIO on **58** (Scheme 26).

Scheme 26. Action of the PhIO on the alcohol **58**



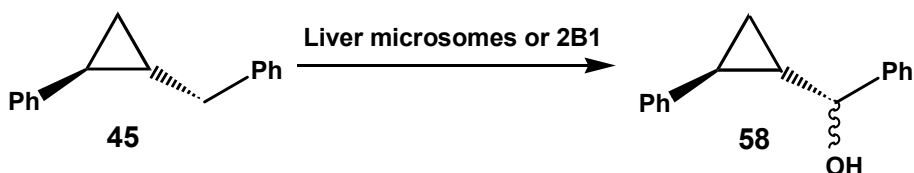
In summary, the formation of the ketone **57** is understandable as it is the product of a direct oxidation of alcohol **58**. The presence of the rearranged alcohol, on the other hand, is more difficult to rationalize. One plausible hypothesis about the mechanism of formation of the allylic alcohol **61** starting from the alcohol **58** is a probable action of the PhIO as an electrophile on the newly formed hydroxyl functional group of **61**.



In conclusion the proof that **61** and **57** are products of a side reaction makes it possible to state that the rebound rate for this specific substrate is greater than the rate of rearrangement $k_{rear} = 3.6 \times 10^8$.

After a detailed literature research it was discovered that **45** has not been used as a substrate in enzymatic oxidations. Therefore for completeness a decision was made to verify that the metabolites produced in such a process are actually the products obtained in R1. The enzymes that have been employed for this purpose are the liver microsomes, 2B1 and 2E1. The protocol used for this experiment is detailed in the experimental section. The 2E1 proved to be inactive but the liver microsomes and 2B1 enzyme gave only the unrearranged alcohol **58** as metabolites (*Scheme 27*).

Scheme 27. Enzymatic incubation with liver microsomes or 2B1



This is a further confirmation that the hydroxylation takes place before the substrate can undergo the ring opening rearrangement. It also demonstrates, for the first time, that a porphyrin model is a suitable mimic for P450 action on radical clocks.

4.1.2. Fast Radical Clock Experiments

It was logical at this time to continue the investigation by examining the hydroxylation of a substrate belonging to the class of fast radical clocks. For these new experiments it was practical to choose a substrate that, from previous DFT calculations and P450 experiments, had already triggered the debate on the existence of a second oxidative intermediate. For this purpose trans-methylphenyl cyclopropane **10** was the substrate of choice. This particular substrate was used extensively in *Newcomb's* enzymatic radical clock experiments to put

forward the proposal for a second oxidant. Here, the C-H hydroxylation was expected to be much more difficult. The energy required for the dissociation of a primary C-H bond is significantly higher than that required for the cleavage of a benzylic C-H seen with substrate **45**. Furthermore since the rearrangement rate constant for this substrate is up to three orders greater than that of the previous example ($k_{\text{rear}} = 1.8 \times 10^{11} \text{ sec}^{-1}$, 20°C) it was expected that the results from these experiments would contribute to a greater understanding of the hydroxylation rate and consequently of the nature of the oxidative intermediate(s).

Similar conditions to those shown previously were employed to perform the porphyrin mimic catalysis. Again all reactions were performed in CH_2Cl_2 under anaerobic conditions using PhIO as the oxygen source and 2.5% mol. of porphyrin **55** as a catalyst. The results of the catalysis were evaluated using GC-FID and are shown in the following Scheme 28.

Scheme 28. Hydroxylation of substrate 10 catalyzed by porphyrin 55

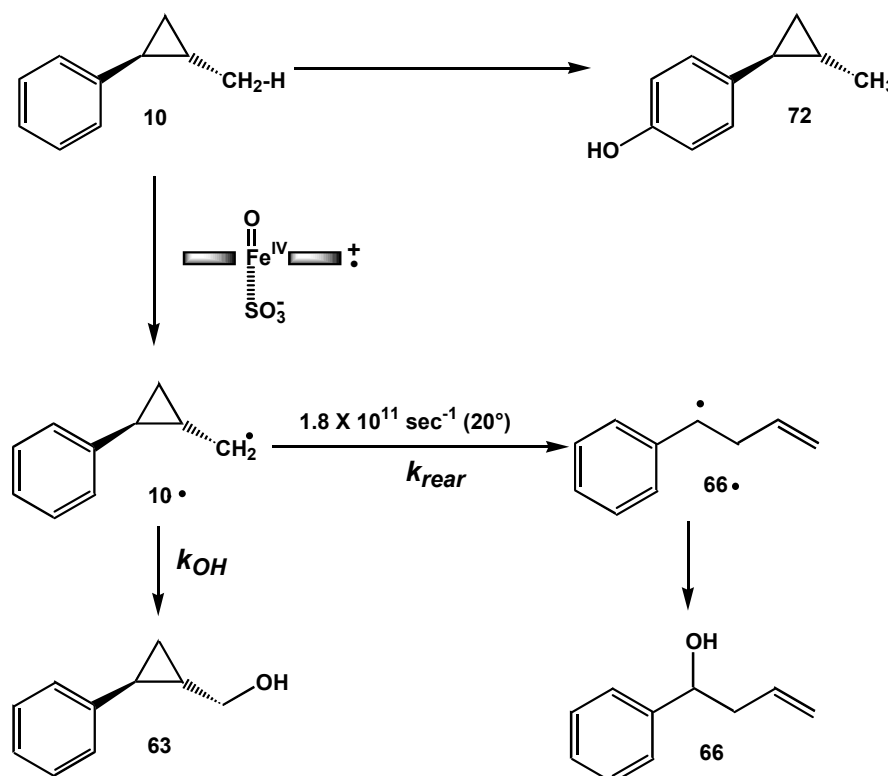


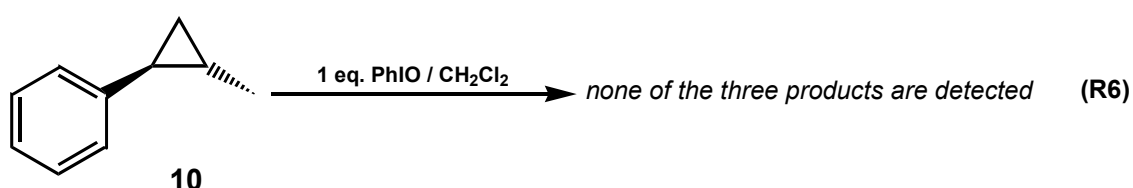
Table 2.

Reaction	66*	63*	72*
R5	1	9	22
Retention time	10.37 min.	13.02 min.	14.91 min.

* 1 unit corresponds to $0.003 \mu\text{mol} / \text{mL}$ (CH_2Cl_2)

This type of hydroxylation is very difficult to perform and in spite of the fact that it gave, as expected, a reduced yield, this experiment should be considered a success. More importantly the three distinctive products observed in the GC analysis correspond to the metabolites that *Newcomb* detected in his enzymatic experiments employing the same substrate.⁹⁵ It is first necessary to detail which exact reaction mechanism produces these products formed and therefore blank experiments were undertaken to eliminate any uncertainty about their formation. The first blank experiment R6 was performed to control the oxidative power of PhIO without the contribution of porphyrin catalyst.

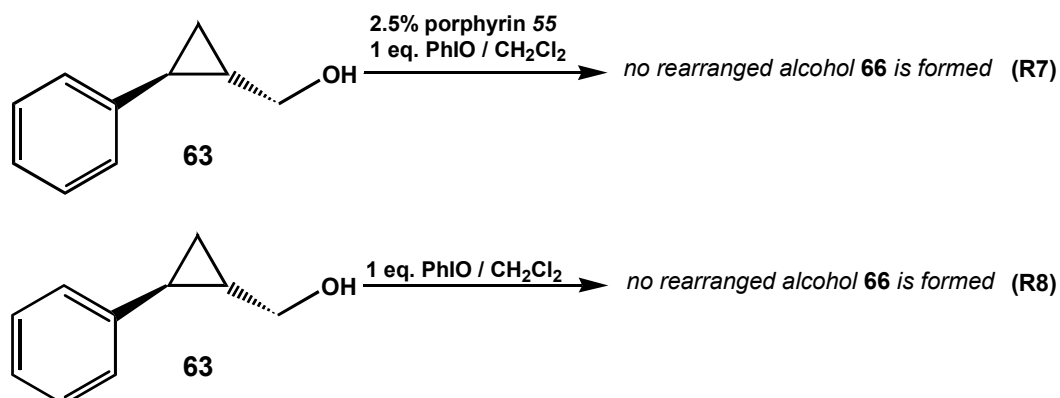
Scheme 29. Control reaction R6.



The substrate **10** was not subject to oxidation with PhIO and no products were observed. This demonstrated the essential role played by the porphyrin **55** in the hydroxylation reaction. Even in these more difficult oxidation reactions the porphyrin mimic possesses a reactivity similar to that of the parent enzyme.

The following blank experiments R7 and R8 were performed to investigate the possibility of the alcohol **63**, formed from direct hydroxylation of **10**, to rearrange into the alcohol **66** (Scheme 30).

Scheme 30. Control reactions R7 and R8.



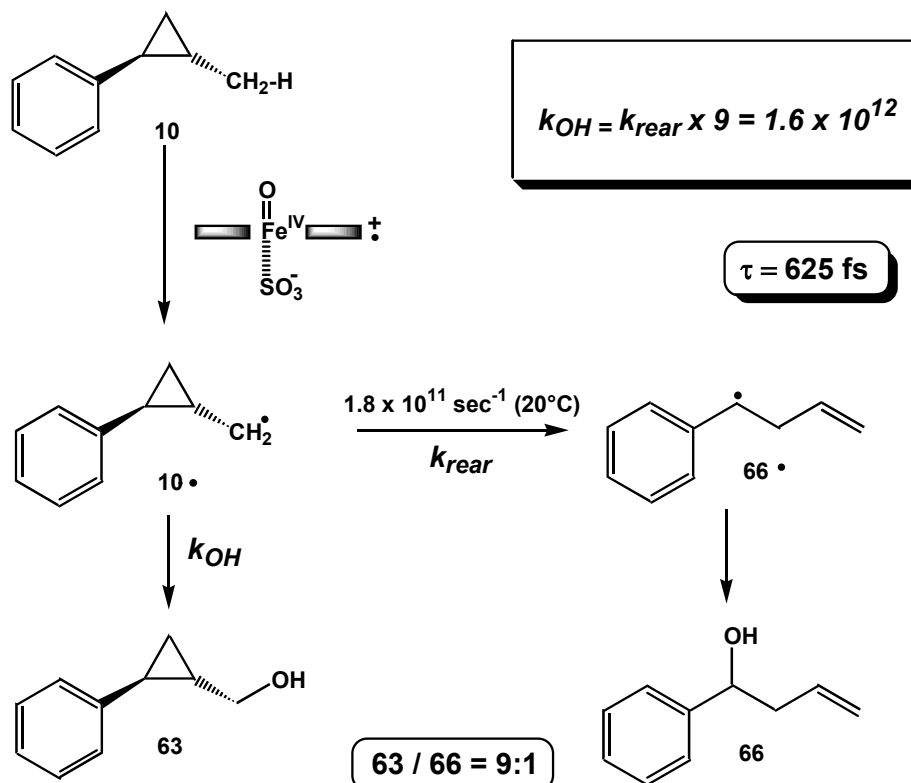
Although these blank experiments seem similar to the previous example with substrate **58** one important difference is noted. In the hydroxylation of substrate **10** the overall yield was extremely low with poor yields of the unrearranged alcohol **63**. This necessitated that the quantity of alcohol **63**, used as a starting material in the subsequent blank reactions R7 and R8, was not equivalent to the quantity of alcohol **63** produced in the

reaction R5. Because of this it was necessary to use a 25 fold excess of this alcohol **63** in experiments R7 and R8 in order to have product quantities above the detection limit of the GC machine. It consequently turned out that the results of R7 and R8 demonstrated that the iodosylbenzene was unable to transform the alcohol **63** into the corresponding rearranged allylic alcohol **66** on its own or in combination with the porphyrin.

Once the control experiments were completed it was then possible to unambiguously analyze the radical clock experiment R5 in detail. The relative amount of the three compounds was biased in favor of the phenol derivative **72**. The aromatic hydroxylation is an unexpected product from this catalysis. Using porphyrins as a catalytic source only a few examples of this type of aromatic oxidation have been published in the literature.¹⁸¹ The production of phenol competes with the oxidations at the cyclopropyl carbinyl position, but has no significance with respect to the mechanistic analysis.

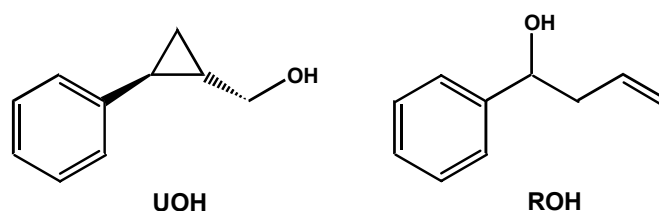
The GC analysis showed that the unrearranged and rearranged alcohols had an average ratio of 9:1 (Table 2). The formation of the rearranged alcohol (ROH) demonstrates that the reaction does not only proceed via a concerted oxygen atom insertion into the alkyl C-H bond.

Scheme 31. Hydroxylation of substrate 10 catalyzed by porphyrin 55



The ratio of alcohols formed was important in the estimation of the hydroxylation rate (k_{OH}) given that the rearrangement rate (k_{rear}) of the fast radical clock is already known. This ratio, when inserted into the equation *Eq.3* (see *Chapter 12*), produced a value for the rebound rate of $k_{\text{OH}} = 1.6 \times 10^{12} \text{sec}^{-1}$. This value translated in terms of the lifetime of the radical intermediate corresponding to **10**, is equal to **625 fs** (*Scheme 31*). Although this result on its own is very noteworthy it is interesting to see how this lifetime relates to lifetimes derived from other radical clock experiments using identical substrates, experimental conditions and appropriate rearrangement rate values. A comparison with the “lifetimes” obtained from *Ingold and Newcomb’s* enzymatic experiments with the *trans*-methylphenyl cyclopropane **10** is quite striking^{90, 93} (*Table 3*).

Table 3. Comparison of the UOH/ROH ratio obtained in our metalloporphyrin experiment and in the enzymatic experiment performed by Ingold and Newcomb.



Reaction	UOH/ROH	k_{rearr} , temp	Calculated Lifetimes (Eq 3)
*Metalloporphyrin	9:1	1.8×10^{11} , 20°C	625fs
**Enzyme	4:1	4.1×10^{11} , 37°C	~666fs

*Porphyrin **55**.

***Phenobarbital induced rat liver microsomal enzymes*

The table shows the values of the calculated lifetimes (derived from Eq 1) of the intermediates formed during the course of the reaction. It clearly illustrates that the metalloporphyrin yielded an intermediate with a lifetime identical, within experimental error, to the corresponding value calculated from the above product distribution (*Table 3*) in the P450 enzymatic hydroxylation of **10**. More importantly, for a detailed interpretation of these new results, the newly calculated lifetime greatly exceeds 170 fs, the generally accepted “lifetime” of a transition state.^{45, 126} Additionally, the anaerobic conditions and the use of the PhIO as an oxygen surrogate in the porphyrin catalyzed oxidation rule out the possibility that a peroxo- and/or hydroperoxo iron (III)-porphyrin complex could form. As it was already pointed out in

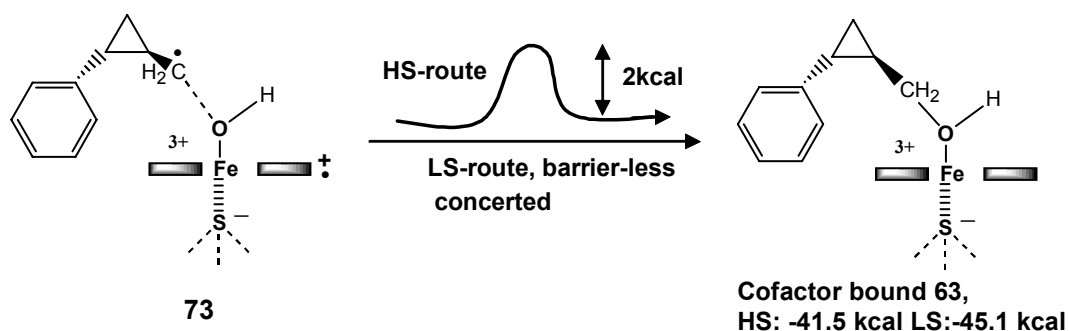
chapter one, the iodosyl benzene as a **mono**-oxygen donor can only generate the synthetic equivalent of Compound I and not a synthetic species corresponding to the Compound 0 or its protonated form. This automatically excludes any interpretation of these results in terms of a two oxidant theory, which has been the source of so much controversy.

4.1.3. Proposed Mechanism

This new synthetic porphyrin is clearly a good mimic of the parent enzyme due to the calculated lifetimes of the intermediates formed but since the overall legitimacy of these radical clock experiments have been questioned, perhaps it is necessary to interpret these new results in relation to new DFT calculations concerning trans-methylphenyl cyclopropane **10**.

In a recent paper^{120, 182} *Shaik* shows that the scenario of a two state (High Spin and Low Spin states: Chapter 1.3) rebound mechanism accommodates much of the experimental data. In this paper he outlines that there is little difference in the calculated high spin (HS) and low spin (LS) energy levels of the transition states and intermediates during the course of the oxidation. One exception to the rule is noted in the two divergent routes that key intermediate **73** (common to both HS and LS routes) can undergo during the reaction process. *Shaik* has computed that one transformation of **73** into the rebound product **63**, by concerted "O" insertion into the C-H bond, occurs in an LS route that has essentially no energetic barrier. Yet conversely by starting from **73** the alternative HS route, to give to the rebound product **63** via a H• abstraction, encounters a transition state (*Scheme 32*).

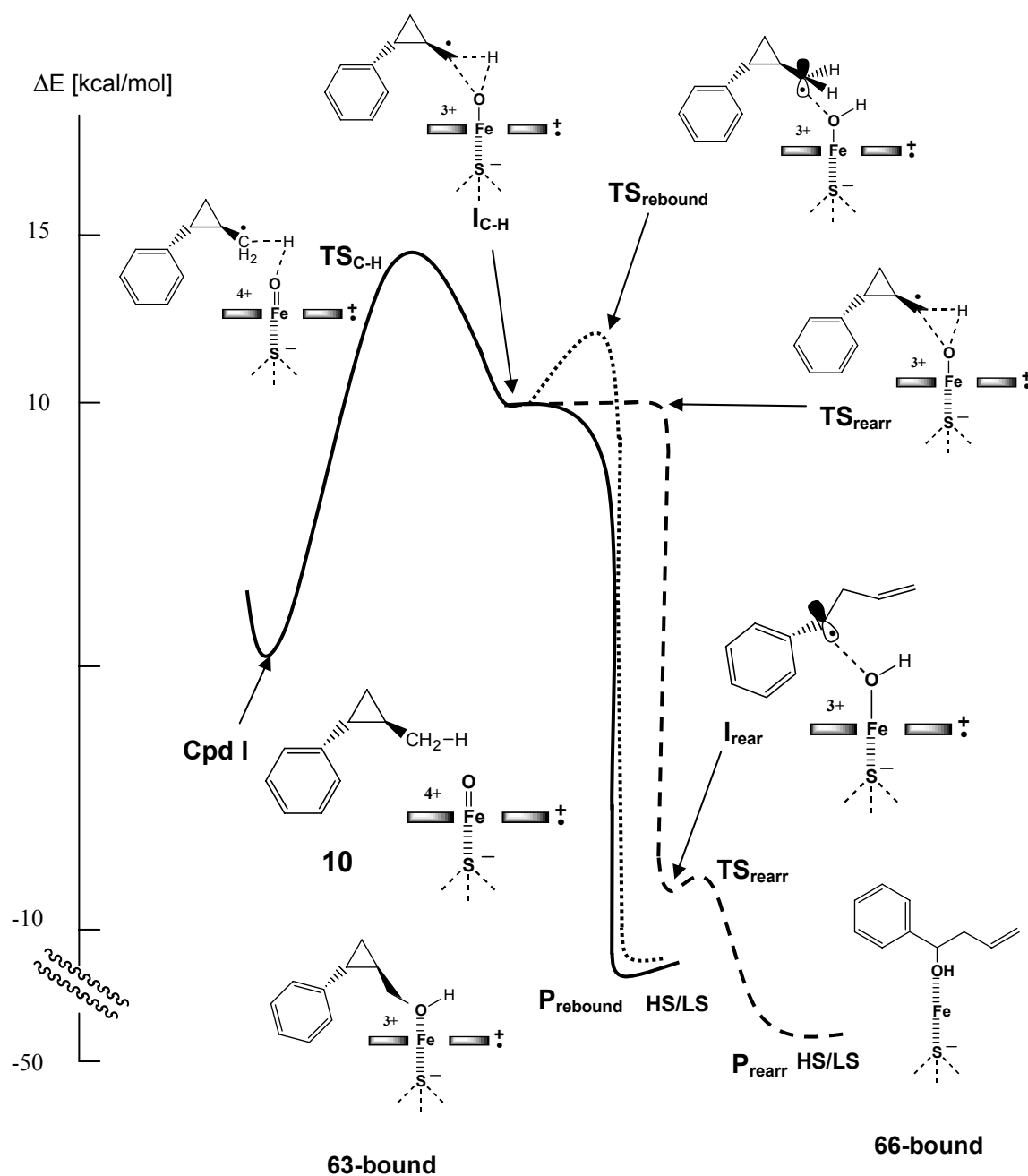
Scheme 32. Activation rebound energy on the HS route



This route is energetically unfavorable and lies 2 kcal above that of the intermediate **73**. From these calculated energy profiles it can be assumed that there is a preference in favor of one of the two possible routes for the formation of **63**.

Yet when the routes leading to the ROH product are examined a different scenario becomes apparent. The same communal intermediate **73** needs only to overcome a minute energy barrier of 0.2 kcal in order to transform itself into an open chain radical. This rearranged intermediate is later trapped in a “rebound” step to yield the cofactor bound product **66**. Although the overall picture seems complicated, the following *Figure 34* attempts to show graphically our interpretation of the reaction routes leading to both UOH and ROH products.¹⁸³

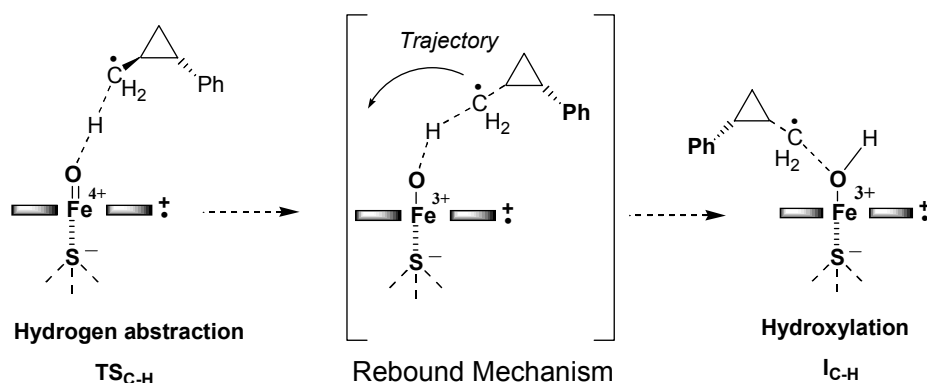
*Figure 34. Energetic profile of the proposed mechanism for this thesis work.*¹⁸³



This graphic is applicable to both the metalloporphyrin and enzyme model and uses the oxo-ferryl species (Cpd I) as a starting point for subsequent HS and LS routes. It uses Shaik's published relative energies of all the states and also takes into consideration that their HS and LS forms are not distinctly separated.¹²⁰

Thus the first transition state $\text{TS}_{\text{C-H}}$ is formed upon activation of the substrate complex **CpdI-10**. This transition state is itself changed into the already referred to key intermediate $\text{I}_{\text{C-H}}$. As the reaction progresses to this point it is impossible to distinguish between the energy levels of the HS and LS forms of both $\text{TS}_{\text{C-H}}$ and $\text{I}_{\text{C-H}}$ and therefore no distinction is made at this stage between the LS and HS routes. The way in which the oxygen atom approaches the primary C-H bond is a point of contention. Groves,^{86, 184} for example, proposes that the position of the incipient carbon radical, during the proton (H^\bullet) abstraction by the active oxygen is different from the position of the already formed carbon radical during the subsequent C-O bond formation (Scheme 33). The extent of the radical rearrangement could be greatly influenced by the "tightness" of the radical cage and the combination of steric and electronic factors experienced by the incipient radical with the cage.

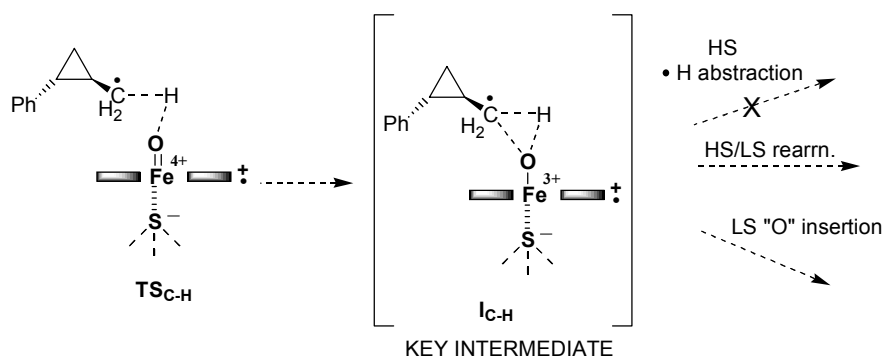
Scheme 33. Molecular trajectory of the radical carbon



Our view on how $\text{I}_{\text{C-H}}$ is formed is quite different.¹⁸³ We predict a "side-on" approach of the oxygen atom to the C-H bond rather than a linear H-abstraction as shown above since this would permit a mutually inclusive "O" insertion together with a $\cdot\text{H}$ abstraction (this HS route is improbable in this instance due to high activation energy) (Scheme 34).

A stretching is quite probable in the C-H of the methyl group which consequently creates a spin density at CH_2 with one of the cyclopropyl C-C bonds already compromised. The $\text{I}_{\text{C-H}}$ thus formed is predisposed to either a rearrangement or a direct hydroxylation.

Scheme 34. "Side-on" approach – mutually inclusive "O" insertion and H. abstraction



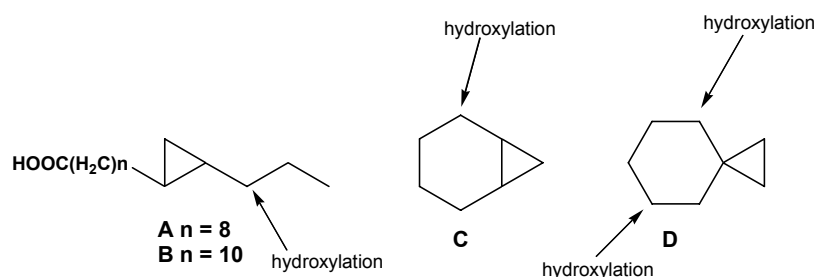
The activation energies needed by the HS and LS routes to complete their passage determines which contribution, if any, each separate route will have on the products formed. Since the HS rebound route has an activation energy of ~ 2 kcal in comparison to the rearrangement route ($\Delta H^\ddagger = 0.2$ kcal) the HS rebound route is thus excluded as a possible pathway in the formation of **63-bound**. The ratio of UOH and ROH products formed corroborates these calculated energies since, if in fact the **63-bound** includes a contribution from the HS pathway, then **66-bound** would also have a HS input up to 10 fold greater. Thus, for the HS pathway, a bias towards the formation of this rearranged species **66-bound** would be observed resulting in a different distribution of oxidized products. With a ratio of 9:1 observed in favor of **63-bound** this is clearly not the case. The opposite is observed in the LS route to form **63-bound**. This route is effectively barrierless and has to compete with the combined HS and LS rearrangement routes which travel a joint pathway of low activation energies via intermediate **I_{C-H}** and transition state **TS_{C-H}** to yield the rearranged species **66-bound**

The complex scenario above, with its dependence on the interplay of activation energies and type of intermediate (**I_{C-H}**) formed, is different to *Shaik's*¹²⁰ interpretation of how the TSR theory contributes to the formation of products. It is estimated that the observed product ratio may be due to a variation of $\Delta H^\ddagger = 1-2$ kcal in the two routes which form **63** and **66** respectively, bearing in mind that the rearrangement of a cyclopropyl methyl radical has an activation energy of about 1kcal in solution. In other words, since the high-spin and the low-spin form of the crucial intermediate **I_{C-H}** are equal in energy the observed product distribution **63/66** = 9:1 does not reflect the yield of HS-**I_{C-H}** over LS- **I_{C-H}** as stated by *Shaik* but is rather a matter of the respective activation energies of the forward reactions. For this theory to be workable it is crucial that the intermediate species **I_{C-H}** is not looked at in terms of a isolated radical but more in terms of a cluster containing a CH₂-group carrying spin density coupled to the spin system of the $\cdots\text{H}\cdots\text{O}\cdots\text{Fe}^{\text{III}}$ porphyrin radical cation. An exact determination of the true "nature" of the intermediate species **I_{C-H}** should eventually show how correct this theory is.

5. Future Directions

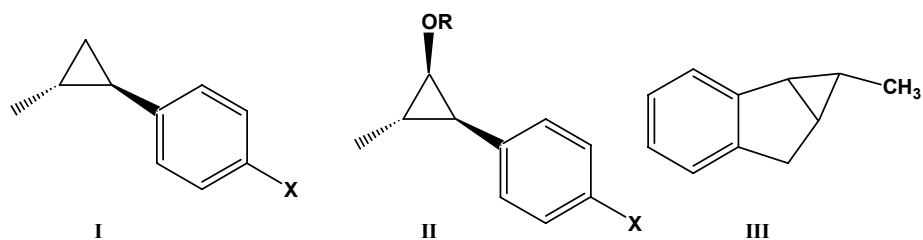
A logical continuation of this work is to examine how this applied theory relates to similar probes used in other radical clock experiments (*Scheme 35*).

Scheme 35. Radical probes used in the experiments by Ortiz de Montellano and Groves.



The life times observed for the alkyl radical intermediates of compounds A-D were in the range of 20-80 ps. Although, with our present understanding of molecular processes, it is not yet possible to rationalize the different physico-chemical parameters involved in the rebound mechanism some observations can still be put forward. Firstly all the carbon centers involved in the C-O bond formation are secondary carbons. Hence this will effect the environment of the radical cluster containing a CHR-group, its stability and ability to transform from an intermediate into a potential product. Secondly and specifically for the more rigid probes C and D, the effective C-H bond strength will depend on the stereoelectronics of the interaction of the C-H with the neighboring cyclopropyl groups. For the probe A and B the long fatty acid chain may interact with residues not necessarily surrounding the porphyrinic active site. This would then hinder the substrates approach to the active oxidative species. Certainly the strength of the C-H bond together with the activation energies needed to transform the intermediates I_{C-H} are crucial in determining the measured life time.

This is the first type of radical clock experiments using porphyrin mimics as a catalyst so it is evident more work is needed in this area to provide a more robust contribution to the rebound mechanism debate. It would be prudent to continue this research using other probes (*Scheme 36*).

Scheme 36. Radical clocks proposed for further experiments.

A similar experiment would be to use the analogue radical clock of **10**, **I**, with the *para*-position blocked by a substituent (i.e. CF₃). The second radical clock **II** could also be an interesting probe to verify if a metalloporphyrin system also gives the products that, in *Newcomb's* opinion, should be produced by a cationic pathway from P450 catalysis. Finally the third radical clock probe **III** would be an ideal substrate for working on the outer limit of what is generally accepted as transition states. In fact, it is this exact substrate, with its rebound constant estimated to be in the range 10¹³ that strongly provides evidence which undermines the existence of a radical intermediate.

More experimental and theoretical work needs to be conducted to define what extent the nature of the 5th ligand has in influencing the oxidative behavior of the porphyrin. Overall it is quite surprising that such a divergent (from nature) O-SO₂ ligand could indeed mimic the parent heme-thiolate enzyme to such a high degree. It is known that the oxidative character of the porphyrin can be affected by the nature of axial ligands harnessed by the heme iron, which can tune the electronic structure of the Cpd I species adequately for its own purpose in conjunction with amino acids surrounding the heme sites. In order to understand homologies and differences between the thiolate and sulfonate type porphyrins it could be interesting to conduct a more detailed systematic studies, with the aid of various spectroscopic techniques (EPR, UV-vis, NMR, Mössbauer, resonance Raman), of porphyrins which have the same 5th ligand (either SH or SO₃) but with diverse backbones. Furthermore, for porphyrins not prone to oxidation, it would also be appealing to test the ability of SO₃ porphyrins to catalyze the dismutation of hydrogen peroxide.

6. Summary

In summary, the porphyrin mimics designed and synthesized during the course of this thesis were successfully used as catalytic oxidants in radical clock experiments. Despite the contrasting nature of the SO₃ fifth ligand of the porphyrin mimic to the native cysteine ligand, found in the P450 enzyme, the results from subsequent catalytic oxidations showed a very good degree of similarity. These experiments, performed in organic solution, using a novel P450 Cpd-I model and specifically chosen probes, with the exclusion of any substrate protein interactions, have produced lifetimes (~625 fs) of the intermediate I_{C-H} which are analogous to the lifetimes observed in enzymatic hydroxylations. It was proposed that this intermediate is not a free radical but instead a cluster containing a CH₂ group carrying spin density joined to the spin system of the $\cdot\cdot\cdot\text{H}\cdot\cdot\cdot\text{O}-\text{Fe}(\text{III})$ porphyrin radical cation. The two routes to the final oxidized products, originating from this intermediate I_{C-H}, are divergent, the unrearranged alcohol is formed via a concerted route whereas the rearranged product is produced from either a high-spin or low spin pathway.

In conclusion the porphyrin mimic catalytic experiments performed and outlined above make a contribution towards understanding exactly how the P450 catalytic cycle works.

Experimental Part

7. Experimental Part

7. 1. General Remarks

7. 1. 1. Solvents and Reagents

Reagents were used as received from *Fluka AG* (Buchs, Switzerland), *Merck AG* (Darmstadt, Germany) and *Aldrich* (Buchs, Switzerland) unless otherwise stated. Chemicals of the quality *purum*, *purum p. a.* or >98% were used without further purification. 2,6-lutidine for iron insertions was purchased from *Aldrich*, dried over solid KOH, distilled from BaO and degassed in high-vacuum by four freeze-pump-thaw cycles.

Solvents for chromatography and extractions were distilled prior to use. Dry dichloromethane (CH₂Cl₂) was distilled from CaH₂, Et₂O and THF from Na/benzophenone, MeOH from Mg, DMF dried over solid KOH and distilled from BaO, dioxane and toluene distilled from Na. All freshly dried solvents were stored over activated molecular sieves. Further solvents used for reactions corresponded to the quality *puriss p. a.*, *abs.*, over *Molecular Sieves* from *Fluka AG*. HPLC-grade solvents were purchased and used for analytical RP-HPLC. Degassed solvents for reactions under oxygen-free condition (e.g. in the glove box) were obtained by at least four freeze-pump-thaw cycles.

For an inert atmosphere *Argon 56* (< 4 ppm other gases) from *Carbagas AG* (Lenzburg, Switzerland) was used.

7. 1. 2. Materials & Instruments

Solvents were removed with a *Büchi* (Switzerland) rotary evaporator (Waterbath 461, Rotavapor RE 111 and Vacuum Controller 168) and a MZ 2C membrane pump (*Vacuubrand*). For cooling a mixture of EtOH and water was kept at 4° with a UKW 300 thermostat (*Vacuubrand*).

For weighing compounds and reagents *Mettler* (Switzerland) balances P1200 (> 1 g) , AE163 (< 1 g), and AX205 (< 100 mg) were used.

A high-vacuum pump D5E from *Trivac* (Köln, Germany) was used for drying compounds and reagents.

Slow addition of reagents to a reaction mixture was achieved with a *Precidor 5003* syringe pump (*Inform HT*, Switzerland).

For all non-aqueous reactions glassware were flame dried either under vacuum or argon overpressure, and the atmosphere was exchanged by three cycles of evacuating and flushing with argon.

Iron insertions and all other reactions with iron porphyrins were carried out in a Labmaster 130 glove box (MBRAUN). The levels of dioxygen (< 2 ppm) and water (< 0.1 ppm) were measured with a combined H₂O/O₂-analyser (MBRAUN). All solvents and reagents used in the glove box were dried and degassed in high-vacuum.

melting points (mp) were determined on a Büchi 510 apparatus and are uncorrected. For the porphyrins, the melting points are > 250° and were not determined.

7. 1. 3. Chromatographic Methods

Analytical thin layer chromatography (TLC) was performed on 0.25 mm precoated glass plates (5×10 cm, silica gel 60 F₂₅₄, Merck AG, Darmstadt, Germany) or on 0.2 mm precoated plastic plates (5×10 cm, ALUGRAM® aluminum oxide N/UV₂₅₄, Macherey-Nagel, Germany). Compounds were detected at 254 nm (UV) or at 366 nm (fluorescence). Description: TLC (solvent): R_f.

Preparative thin layer chromatography was conducted on 0.25 mm precoated glass plates (20×20 cm, silica gel 60 F₂₅₄, Merck AG, Darmstadt, Germany).

For normal phase **column chromatography** silica gel 60 from Merck (0.043-0.06 mm, 230-400 mesh) or aluminum oxide 90 from Merck (standardized (activity II-III), 0.063-0.2 mm, 70-230 mesh) were used and for eluting the compounds pressure (0.3–0.5 bar N₂) was applied (flash chromatography).

Analytical **reversed phase HPLC (RP-HPLC)** was performed on LiChrospher® 100 RP-18 silica gel from Merck (5 µm particle size, 4×250 mm column) with nanopure water and HPLC-grade MeOH or acetonitrile. HPLC-System: Merck Hitachi LaChrom system with interface D-7000, pump L-7000, UV-detector L-7400, autosampler L-7200, column oven L-7300, column changer LabSource 6 Port Valve 7066 and on-line solvent degasser L-7612.

Gas chromatography (GC/MS) was performed on a Hewlett Packard 5890 series II using a 25 m dimethyl silane column coupled with a Hewlett Packard 5971 series mass selective detector

Gas Chromatography (GC-FID) was performed on *Finningan Focus* using a 15 m Supelcowax column.

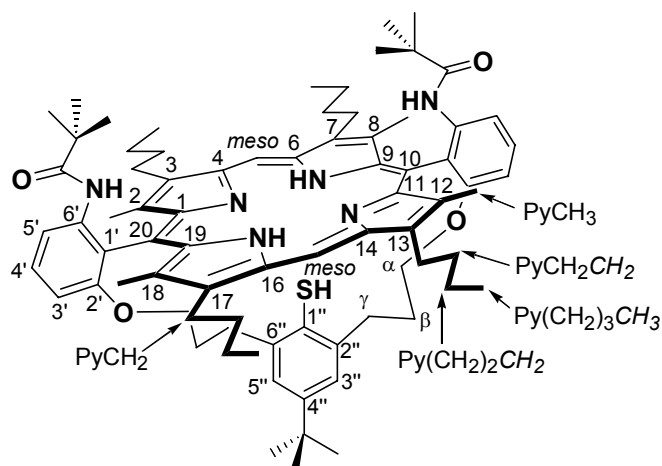
7. 1. 4. Spectroscopic Methods

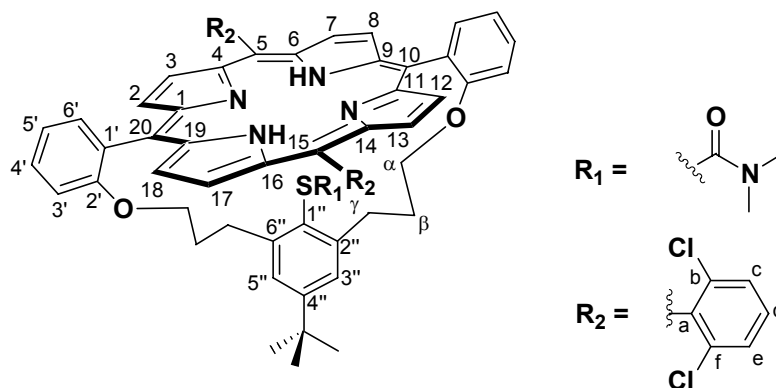
Ultra violet – visible absorption spectra (UV/Vis) were recorded on a *Hewlett-Packard* 8452A Diode Array spectrophotometer and a *Agilent* 8453 Diode Array spectrophotometer using optical 110-OS *Hellma* cuvettes (10 mm light path). Description: UV/Vis (solvent): wavelength of maxima (λ_{\max}) in nm (relative extinction coefficient in %). *sh* = shoulder.

^1H -Nuclear magnetic resonance spectroscopy ($^1\text{H-NMR}$) was performed using either a *Bruker* DPX-NMR (400 MHz), *Bruker* DRX-500 (500 MHz) or a *Bruker* DRX-600 (600 MHz) spectrometer. Solvents for NMR were obtained from *Dr. Glaser AG* (Basel, Switzerland) and *Cambridge Isotope Laboratories* (Andover, MA, USA). CDCl_3 was filtered through basic alumina prior to use. If not otherwise stated all spectra were recorded at room temperature. If necessary for the interpretation correlated spectra like COSY, TOCSY, NOESY and ROESY were recorded also. Description: $^1\text{H-NMR}$ (frequency, solvent): δ_{H} in ppm relative to residual solvent peaks (peak multiplicity: *s* = singlet, *d* = doublet, *t* = triplet, *q* = quartet, *quin* = quintet, *sext* = sextet, *m* = multiplet, *br* = broad; coupling constants *J* in Hertz).

^{13}C -Nuclear magnetic resonance spectra ($^{13}\text{C-NMR}$) were ^1H -decoupled and recorded on a *Bruker* DPX-NMR (100 MHz), *Bruker* DRX-500 (125 MHz) and *Varian* Gemini 300 (75 MHz) spectrometer. For the assignment of carbons APT, DEPT, HETCOR, HMQC and HMBC experiments were carried out if essential.

Porphyrin models atom numbering for NMR assignment:





Description: ^{13}C -NMR (frequency, solvent): δ_{C} in ppm relative to residual solvent peaks (multiplicity: *s* = singlet (C), *d* = doublet (CH), *t* = triplet (CH₂), *q* = quartet (CH₃)).

Electron impact mass spectra (EI-MS) and fast atom bombardment mass spectra (FAB-MS) were measured by *Dr. H. Nadig* on a *Varian* double focussing VG-70-250 spectrometer in the mass spectrometry laboratory of the institute. As matrix for FAB-MS nitrobenzyl alcohol was used and, if necessary KCl added. **Electron spray ionisation mass spectra (ESI-MS)** were recorded on a *Finnigan Mat* LCQ-700 or a Bruker Esquire 3000^{plus}. For **matrix-assisted laser desorption/ionisation mass spectra** in conjunction with **time of flight** mass analysis (**MALDI-TOF-MS**) a *Perseptive Biosystems Vestec Mass Spectrometry Products Voyager™ Elite Biospectrometry™* Research Station was used. Porphyrin samples were prepared as follows: either 1-2 μl of a diluted solution of porphyrin in dichloromethane was mixed with 1 μl of a 0.1M matrix solution of 2,5-dihydroxybenzoic acid in MeCN/H₂O/EtOH 50:45:5, placed on a 100-wells sample plate and left standing or the diluted porphyrin solution was placed directly on the sample plate and measured without matrix (**LDI-MS**). **Description:** MS (solvent): mass peaks in *m/z* (relative intensity in %). Peaks with an intensity of less than 5% were not considered.

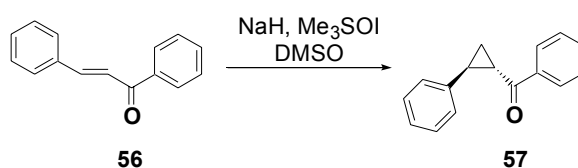
Continuous wave electron paramagnetic resonance spectroscopy (cw-EPR) was carried out using a *Bruker* ESP-300 X-band ($\nu_{\text{microwave}} = 9.485 \text{ GHz}$) spectrometer equipped with a T₁₀₂ cell and a ER4111VT liquid nitrogen cryostat to assure low temperature during measurement. Sample concentration was typically 5mM and spectra were measured with a microwave power of 20 mW, modulation frequency of 100 kHz, and a modulation amplitude of 5.2 G. Samples were measured in dry and degassed toluene and/or 2-methyl-tetrahydrofuran (2-MTHF) which was purchased from *Fluka (purum)* and distilled in high-vacuum over a small Vigreux column. *Caution ! 2-MTHF slowly decomposed upon heating and therefore distillation should be carried out under reduced pressure at room temperature. In addition 2-MTHF should not be dried by distilling from Na because this results in a solvent*

which is extremely basic ($\text{pH} \sim 10$). If this basic 2-MTHF is used for measuring iron porphyrin samples it can lead to low-spin signals (sometimes quantitatively) and accordingly to wrong interpretations! 2-MTHF mostly gave exactly the same spectra but sometimes with better resolution. Description: cw-EPR (solvent, temperature): g-values.

7. 2. Syntheses

7. 2. 1. Cyclopropyl Derivatives and Related Synthetic Studies

rac-Phenyl-(*trans*-2-phenylcyclopropyl-methanone (**57**).



Solid NaH (60% in oil, 231 mg, 5.77 mmol, 1.2 equiv.) was placed in a 3-necked flask, washed with n-hexane, and fully pumped to dryness. Trimethyloxosulfonium iodide (1270 mg, 5.77 mmol, 1.2 equiv.) was added, and DMSO (10 mL) was added dropwise to the solid mixture through an addition funnel. After hydrogen evolution, the milky solution turned clear and was stirred for 15 min. *trans*-Chalcone **56** (1 g, 4.81 mmol, 1 equiv.) was added. The mixture was stirred for 20 h, and the reaction was quenched with water. The mixture was extracted with ether, and the organic layers were dried, rotovapped, and chromatographed (silica gel hexane/diethylether 10:1) to give **57** (773 mg, 72%) as a white solid.

TLC (hexane/diethyl ether 8:1): $R_f = 0.30$.

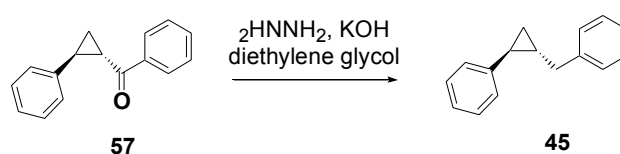
UV/Vis (CH_2Cl_2): 246 (100), 223(70).

¹H-NMR (400 MHz, CDCl_3): 8.01-7.98 (*m*, 2H, arylH); 7.59-7.56 (*m*, 1H, arylH); 7.49-7.43 (*m*, 2H, arylH); 7.35-7.29 (*m*, 2H, arylH); 7.25-7.22 (*m*, 1H, arylH); 7.21-7.17 (*m*, 2H, arylH); 2.91 (*ddd*, $J = 8.72, 5.32, 4.04$, 1H, cyclopropH), 2.70 (*ddd*, $J = 9.71, 6.56, 4.04$, 1H, cyclopropH); 1.95-1.91 (*m*, 1H, cyclopropH); 1.58-1.54 (*m*, 1H, cyclopropH).

¹³C-NMR (100 MHz, CDCl_3): 140.90 (C_{quat}); 138.13 (C_{quat}); 133.32 (arylCH); 128.97 (arylCH); 128.52 (arylCH); 127.01 (arylCH); 126.63 (arylCH); 30.43 (cyclopropCH); 29.71 (cyclopropCH); 19.66 (cyclopropCH₂).

EI-MS (70 eV, 50°): 222.0 (32, M^+), 297 (5), 105 (100), 77(33), 51(6).

EA calc. for $\text{C}_{16}\text{H}_{14}\text{O}$ (222.10).

rac-trans-1-benzyl-2-phenyl-cyclopropane (45)

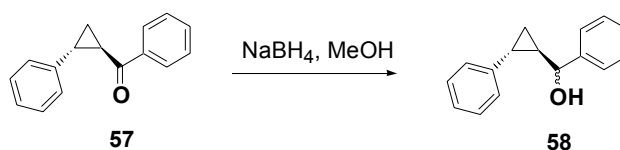
1.2 g of phenyl-(*trans*-2-phenylcyclopropyl)-methanone **57** (1 equiv., 5.40 mmol) was dissolved in 5.5 mL of diethylenglycol and 540 mg of 2HNNH_2 (525 μL , 12 equiv., 10.80 mmol) and 705 mg (2 equiv., 10.80 mmol) of KOH 86% were added. The yellowish solution was heated at 120°C (oil bath) for 1 hour. Then other 540 mg of 2HNNH_2 and 705 mg of KOH 86% were added and the reaction mixture was heated at 140°C for further 6 hours. After the orange solution was cooled at room temperature, treated with 5 ml of saturated aqueous NH_4Cl and extracted with three portions of hexane. The combined organic phases were washed with distilled water and dried over Na_2SO_4 . The crude was purified by a first flash chromatography (silica gel, hexane/diethyl ether 8:1) and a second one (alox, hexane + 5% diethyl ether). Each fraction was checked by GC-FID analysis. The final product obtained were 79 mg (60%) of a colourless viscous oil.

TLC (hexane/diethyl etehr 4:1): $R_f = 0.45$.

$^1\text{H-NMR}$ (400 MHz, CDCl_3): 7.31-7.18 (m, 7H, arylH); 7.15-7.10 (m, 1H, arylH); 7.06-7.03 (m, 2H, arylH); 2.84-2.66 (m, 2H, CH_2Ph); 1.82-1.75 (m, 1H, cyclopropH, PhCH_2CH); 1.41-1.30 (m, 1H, cyclopropH, PhCH); 1.02-0.90 (m, 2H, cycloprop CH_2).

EI-MS (70eV, RT): 208.1(7); 117.1 (100); 104.1 (25); 91.0 (20); 65.0 (5).

EA calc. for $\text{C}_{16}\text{H}_{16}$ (208.13).

α -[2-phenylcyclopropyl]- benzene methanol (58**)**

150 mg (1 equiv., 0.67 mmol) of Phenyl-(*trans*-2-phenylcyclopropyl)-methanone **57** was dissolved in 3.5 ml of MeOH and the solution as cooled at 0°C in an ice bath. 1.10 mmol) was added and the reaction mixture was stirred for 1.5 hours at 0°C and for further 1.5 hours at room temperature. Then, the solution was cooled in an ice bath and quenched with 2.0 ml of saturated aqueous NH₄Cl. The mixture was then extracted with diethyl ether. The combined organic layers were then washed twice with 5 mL of water, brine and finally dried over Na₂SO₄. The crude material was purified by two subsequent flash chromatographies (silica gel, hexane/ ethyl acetate 2:1). A white solid (130 mg, 86%) was obtained as a mixture of enantiomers of two diastereoisomers with a ratio of 1.4. The purity of each fraction was determined by GC-FID analysis.

TLC (hexane/ethyl acetate 1:1): $R_f = 0.41$ and $R_f = 0.50$

¹H-NMR (400 MHz, CDCl₃, less polar diastereoisomer): 7.46-7.24 (m, 7H, arylH); 7.17-7.13 (m, 1H, arylH); 7.10-7.08 (m, 2H, arylH); 4.32 (d, $J = 7.84$, 1H, PhCH₂OH); 2.11-2.07 (m, 1H, cyclopropH); 1.93 (br s, 1H, OH); 1.60-1.53 (m, 1H, cyclopropH); 1.11-1.05 (m, 1H, cyclopropH); 1.01-0.96 (m, 1H, cyclopropH).

¹H-NMR (400 MHz, CDCl₃, more polar diastereoisomer): 7.42-7.38 (m, 2H, arylH); 7.37-7.19 (m, 5H, arylH); 7.17-7.08 (m, 1H, arylH); 7.02-6.99 (m, 2H, arylH); 4.38 (d, $J = 7.32$, 1H, PhCH₂OH); 2.02-1.98 m, 1H, cyclopropH); 1.96 (br s, 1H, OH); 1.58-1.50 (m, 1H, cyclopropH); 1.21-1.17 (m, 1H, cyclopropH); 1.07-1.04 (m, 1H, cyclopropH).

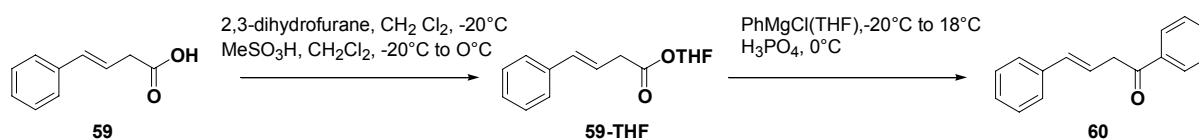
¹³C-NMR (100 MHz, CDCl₃, less polar diastereoisomer): 143.80 (C_{quat.}); 142.72 (C_{quat.}); 128.92 (arylCH); 128.79 (arylCH); 128.16 (arylCH); 126.48 (arylCH); 126.31(arylCH); 126.11 (arylCH); 77.95 (CHOH); 31.11 (cyclopropCH); 22.31 (cyclopropCH); 13.96 (cyclopropCH₂).

¹³C-NMR (100 MHz, CDCl₃, more polar diastereoisomer): 143.90 (C_{quat.}); 142.44(C_{quat.}); 128.91 (arylCH); 128.72 (arylCH); 128.11 (arylCH); 126.47 (arylCH); 126.42 (arylCH); 126.10 (arylCH); 77.24 (CHOH); 31.11 (cyclopropCH); 21.42 (cyclopropCH); 14.03 (cyclopropCH₂).

EI-MS (70eV, RT): 206.1 (3, [M⁺ -18]); 120 (100); 107.0 (17); 91.0 (24); 79.0 (17.84); 51.0 (4).

GC-MS: 224 (1, M⁺); 118(98); 107 (100); 79 (60); 51(6).

EA calc. for C₁₆H₁₆O (224.12).

(E)-1, 4-diphenyl-3-buten-1-one (60)

To a solution of trans-styryl acetic acid **59** (2.0 g, 12.33 mmol, 1 equiv.) in dichloromethane (48 mL) at -20°C was added 2,3-dihydrofuran (0.98 mL, 12.91 mmol, 1.05 equiv.) followed by methanesulfonic acid (1.6 mL, 24.80 mmol, 2 × 10⁻³ equiv.) dissolved in a solution of dichloromethane (0.16 mL). The mixture was allowed to warm to 0°C over 4 h and then recooled to -20°C. To this mixture was then added dropwise phenylmagnesium bromide (12.33 mL, 12.33 mmol, 1 M in THF, 1 equiv.) over 5 min. Stirring was continued for an additional 30 min, and then the solution was allowed to warm to ambient temperature over 18 h. The mixture was then cooled to 0°C and added dropwise to a solution of H₃PO₄ (16 mL, 1.0 M) at 0°C. The mixture was then allowed to warm to ambient temperature, diluted with water (12.3 mL) and dichloromethane (78 mL). The solution was then poured into a separatory funnel and the organic layer was removed. The aqueous phase was washed with dichloromethane (3 × 12 mL). The organic phases were combined and shaken with a solution of H₃PO₄ (14.7 mL, 0.25 M) for 5 minutes and separated again from the aqueous layer. Since the THF ester was still present (TLC control) in the dichloromethane solution, the latter was stirred overnight at room temperature together with methanesulfonic acid and methanol (few drops of Moshe in 1.2 mL of MeOH) in order to hydrolyze it. The reaction mixture was then washed with aqueous NaHCO₃ (3 × 20 mL, 1/1 H₂O/saturated aqueous NaHCO₃) and brine (25 mL). It was then dried over Na₂SO₄ and evaporated (up to 40°). Dilution and evaporation with hexanes (2 × 60 mL) yielded the crude ketone as an oil. The flash chromatography purification (silica gel, hexane / ethyl acetate 7:1) provided 1.10 mg (41%) of pure ketone **60** as a white soft solid.

TLC (hexane/AcOEt 5:1): *R_f* = 0.46.

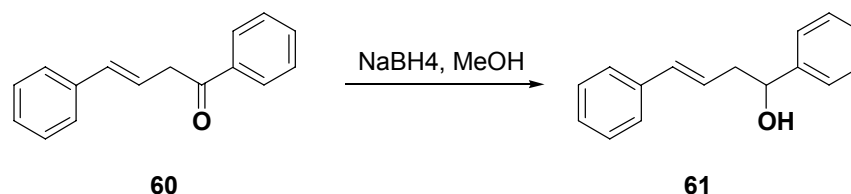
mp: 88-90 °C.

¹H-NMR (400 MHz, CDCl₃): 8.04-7.98 (*m*, 2H, arylH); 7.60-7.57 (*m*, 1H, arylH); 7.51-7.46 (*m*, 2H, arylH); 7.40-7.35 (*m*, 1H, arylH); 7.33-7.27 (*m*, 2H, arylH); 7.25-7.20 (*m*, 1H, arylH); 6.56 (*d*, *J* = 16.2, 1H, alkene-H, PhCH); 6.48 (*dt*, *J* = 16.0; 6.32, 1H, alkene-H, PhCHCH); 3.92 (*dd*, *J* = 6.32; 0.76, 2H, alkane-H, CH₂C(O)Ph).

ESI-MS (MeOH): 245.0 [M+Na⁺]; 223.0 [M+1]⁺.

EI-MS (70 eV, 50°): 222 (5, M⁺), 220(6), 105(100), 77 (27), 51 (5).

EA calc. for C₁₆H₁₄O (222.10).

rac- α -[(2E)-3-phenyl-2-propenyl]-benzenemethanol (61)

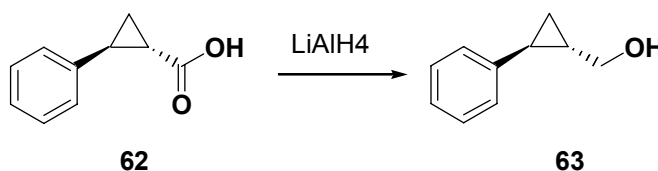
To a yellow solution of the ketone **60** (33.1 mg, 0.13 mmol, 1 equiv.) in MeOH (0.8 mL) at 0 °C the NaBH₄ (10.0 mg, 0.26 mmol, 1.95 equiv.) was added. After the addition of the reducing agent the solution became colourless. The solution was stirred at room temperature for 5 hours. The reaction mixture was then quenched with a saturated aqueous NH₄Cl (1 mL) and then extracted with diethyl ether (5 mL). The organic layer was then washed with water (2 X 2 mL) and brine (3 mL) and dried over Na₂SO₄. The crude was purified by flash chromatography (hexane/ethyl acetate 5:1) and 14.6 mg (48%) of a pure white solid **61** was obtained.

TLC (hexane/AcOEt 5:1): R_f = 0.08.

¹H-NMR (400 MHz, CDCl₃): 7.41-7.26 (m, 9H, arylH); 7.23-7.19 (m, 1H, arylH); 6.51(d, J = 15.8, 1H, PhCHCHCH₂); 6.21(dt, J = 15.8, 7.6, 1H, PhCHCHCH₂); 4.82(dd, J= 7.32, 7.32CHOH), 2.71-2.63(m, 2H, CH₂CHOH).

EI-MS (70eV, 50°): 316 (21, [M+1]⁺); 315 (100, M⁺); 313 (6); 255 (6); 254 (11); 125 (5); 77 (7); 58 (19).

EA calc. for C₁₆H₁₆O:(224.12).

trans-(2-phenylcyclopropyl)methanol (63)

To a solution of 2 g (12.33 mmol, 1 equiv.) of trans-2-phenyl cyclopropane carboxylic acid in diethyl ether (67 mL), 24.66 mL of a solution 1M of LiAlH₄ in Et₂O (24.66 mmol, 2 equiv.) was added and the reaction mixture was refluxed for 12 hours. Then it was treated sequentially with water (1.0 mL), 15% aqueous NaOH (1.0 mL) and water (6.0 mL). Then the ethereal solution was filtered off through a fritted funnel and dried over Na₂SO₄ and concentrated in vacuum. The obtained residue was distilled with the kugelröhr apparatus

(1.0E-1 mbar, 150°) providing 1.25 g of colorless viscous oil. The purity was tested by GC-FID and just the fractions 99.7% pure were collected together and used for the control experiments.

TLC (hexane/AcOEt 1:1): R_f = 0.60

bp: 152°, 30Torr

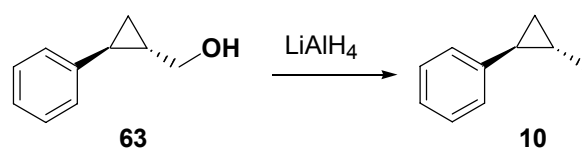
$^1\text{H-NMR}$ (400 MHz, CDCl_3): 7.28-7.23(m, 2H, arylH); 7.16 (tt, $J = 7.32, 1.24$, 1H, *para*-arylH); 7.08-7.04(m, 2H, arylH); 3.63 (d, $J = 6.8$, 1H, CH_2OH); 3.61 (d, $J = 6.8$, 1H, CH_2OH); 1.83 (dt, $J = 8.6, 4.8$, 1H, PhCH); 1.50-1.42 (m, 1H, cyclopropH); 0.99-0.91 (m, 2H, cyclopropH).

$^{13}\text{C-NMR}$ (100 MHz, CDCl_3): 143.07(C_{quat}); 128.81(arylCH); 126.29(arylCH); 126.08(arylCH); 66.71(arylCH); 25.68(cyclopropCH); 21.76(cyclopropCH); 14.39(cyclopropCH).

GC-MS: 148 (20, M^+); 117(100); 115(64); 104(35); 91(37).

EA calc. for $\text{C}_{10}\text{H}_{12}\text{O}$: (148.09).

***trans*-(2-phenylmethyl)cyclopropane (10)**



To a solution of 578 mg (3.90 mmol, 1 equiv.) of *trans*-(2-phenylcyclopropyl)-methanol **63** in dichloromethane (21 mL), 923 μL of triethylamine (6.63 mmol, 1.7 equiv.) and 364 μL of benzenesulfonyl chloride (4.68 mmol, 1.2 equiv.) were added at -10°C . The reaction mixture was stirred for 1 hour at -5°C and then transferred into a chilled separatory funnel and extracted with the following chilled solutions: water, 10% aqueous HCl, saturated aqueous NaHCO_3 and saturated aqueous NaCl. The solution was dried over Na_2SO_4 while standing at 0°C in an ice bath, filtered through a fritted funnel previously chilled up and then concentrated in vacuum at low temperature (around 5°C). Chilled THF (3.5 mL) was added and the solvent was again removed under reduce pressure at 5°C . The residue was dissolved in chilled THF (7 mL), treated with 8.5 mL of a solution 1M LiEt_3H in THF and stirred at 0°C for 5 hours and for further 12 hours at ambient temperature. The reaction mixture was quenched by drop wise addition of aqueous 3M NaOH (5 mL) and slow addition of 30% H_2O_2 (5 mL), refluxed for 1 hour, cooled down and then separated. The aqueous layer was extracted three times with hexane. The combined organic phases were washed with saturated aqueous NaCl, dried over Na_2SO_4 and concentrated under reduce pressure. The yellowish oil was distilled with the kugelröh apparatus ($4.5\text{E-}2$ mbar, 80°C) and a colourless oil was obtained. The

latter was further purified by flash chromatography (silica gel, hexane). The purity of the compound **10** was determined by GC-FID analysis and only the fraction 99.9% pure were used as substrate in the porphyrin catalyzed oxidation.

TLC (hexane): $R_f = 0.55$.

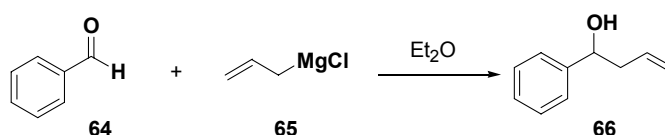
$^1\text{H-NMR}$ (400 MHz, CDCl_3): 7.30-7.25 (*m*, 2H, arylH); 7.19-7.15 (*m*, 1H, arylH); 7.09-7.06 (*m*, 2H, arylH); 1.64-1.59 (*m*, 1H, cyclopropH, PhCH); 1.23 (*d*, $J = 6.08$, 3h, CH_3); 1.14-1.06 (*m*, 1H, cyclopropH); 0.95-0.91 (*m*, 1H, cyclopropH); 0.81-0.76 (*m*, 1H, cyclopropH).

$^{13}\text{C-NMR}$ (100 MHz, CDCl_3): 144.48 (C_{quat}); 125.94 (arylCH); 125.86 (arylCH); 24.73 (arylCH); 19.51 (arylCH); 18.41 (arylCH); 18.03 (arylCH).

GS-MS: 132 (43, M^+); 131(15); 117 (100); 115 (42); 91 (30).

EA calc. for $\text{C}_{10}\text{H}_{12}$: (132.09).

1-phenyl-3-buten-1-ol (**66**)



1 g of benzaldehyde **64** (0.96 mL, 9.42 mmol, 1.0 equiv.) was dissolved in diethyl ether (2.5 mL) and the transparent solution was cooled at 0°C (ice bath). Then 7.1 mL of a solution 2M of allylmagnesium chloride in THF **65** (14.13 mmol, 1.5 equiv.) was added and the solution that turned orange was stirred for 2 hours. The reaction mixture was then quenched with aqueous saturated NH_4Cl (5 mL). The aqueous phase was extracted with Et_2O (2 X 8 mL) and the combined organic layers were then washed with water (10 mL) and dried over Na_2SO_4 . The solvent was removed under reduce pressure. The obtained 1.3 g of crude product **66** (92%) did not need any purification

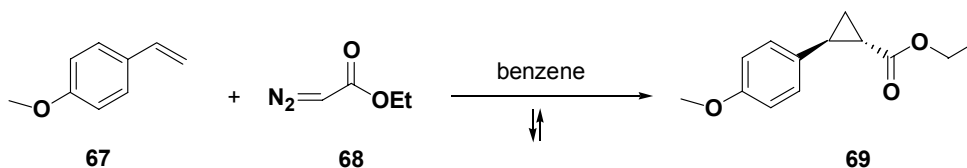
TLC (hexane/EtOAc 1:1): $R_f = 0.7$

$^1\text{H-NMR}$ (400 MHz, CDCl_3): 7.37-7.26(*m*, 5H, arylH); 5.87-5.76 (*m*, 1H, alkeneH, $\text{CH}_2=\text{CHCH}_2$); 5.20-5.13 (*m*, 2H, alkeneH, $\text{CH}_2=\text{CHCH}_2$); 4.76-4.72 (*m*, 1H, benzylicH PhCHOH); 2.58-2.46 (*m*, 2H, alkaneH, PhCH(OH)CH₂).

$^{13}\text{C-NMR}$ (100 MHz, CDCl_3): 144.41(C_{quat}); 134.99 (arylCH); 128.82 (arylCH); 128.82 (arylCH); 127.94 (arylCH); 126.35 ($\text{CH}=\text{CH}_2$); 118.60 ($\text{CH}_2=\text{CH}$); 73.82 (CHOH); 44.18 ($\text{CH}_2\text{CH}=\text{CH}_2$).

GC-MS: 148(5, M^+); 107(100), 91(5); 79(55); 77(30).

EA calc. for $\text{C}_{10}\text{H}_{12}\text{O}$: (148.09).

Ethyl *trans*-2-(4-methoxyphenyl)-cyclopropane-carboxylate (69)

To a mixture of 4.98 g of p-vinylanisole **67** (5 mL, 37.18 mmol, 1 equiv.) in benzene (15 mL) with 0.5 g of CuSO₄ (2.7 mmol, 7.5% mol equiv.) at 75°C was added dropwise over 2 hours 8.48 g of ethyl diazoacetate **68** (7.7 mL, 2 equiv.). After an additional 3 hours reflux (90°C), the mixture was allowed to stand for 12 hours at room temperature. Water (23 mL) was added, and benzene was removed by azeotropic distillation at normal pressure (68°C). Diethyl acetate (20 mL) was added to the orange residue, and the resulting solution was extracted with water, aqueous saturated NaCl and dried over Na₂SO₄. Concentration at reduced pressure gave a residue containing starting material and *cis*- and *trans*-cyclopropane carboxylic acid esters which was partially purified by flash chromatography (silica gel, hexane/ethyl acetate 10:1). A fraction enriched in the *trans* ester was obtained. Crystallization (ethyl acetate/hexane) gave 5.42g (33%) of ethyl *trans*-2-(p-methoxyphenyl)-cyclopropanecarboxylate **69**.

TLC (hexane/ ethyl acetate 10:1): R_f (*trans*) = 0.43; R_f (*cis*) = 0.38

mp (*trans*): 80-82 °C

¹H-NMR (400 MHz, CDCl₃) (*trans*-isomer): 7.03 (*d*, $J = 9$, 2H, arylH); 6.82 (*d*, $J = 9$, 2H, arylH); 4.16 (*q*, $J = 7.1$, 2H, OCH₂CH₃); 3.78 (*s*, 3H, OCH₃); 2.48 (*ddd*, $J = 9.2, 6.6, 4.2$, 1H, cyclopropH); 1.81 (*ddd*, $J = 8.7, 5.4, 4.2$, 1H, cyclopropH); 1.55 (*ddd*, $J = 9.6, 5.1, 4.2$, 1H, cyclopropH); 1.27 (*t*, $J = 7.1$, 3H, OCH₂CH₃), 1.26-1.22 (*m*, 1H, cyclopropH)

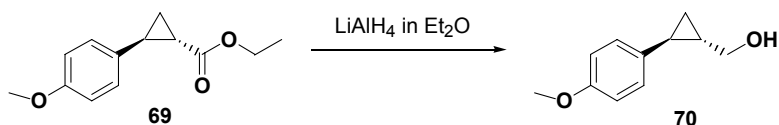
¹H-NMR (400 MHz, CDCl₃) (*cis*-isomer): 7.18 (*d*, $J = 8.1$, 2H, arylH); 6.80 (*d*, $J = 8.1$, 2H, arylH); 3.89 (*q*, $J = 7.2$, 2H, OCH₂CH₃); 3.78 (*s*, 3H, OCH₃); 2.52 (*m*, 1H, cyclopropH); 2.03 (*ddd*, $J = 9.3, 7.8, 5.7$, 1H, cyclopropH); 1.64 (*m*, 1H, cyclopropH), 1.29 (*ddd*, $J = 9.3, 8.1, 5.4$, 1H, cyclopropH), 1.01 (*t*, $J = 7.2$, 3H, OCH₂CH₃).

¹³C-NMR (100 MHz, CDCl₃) (*trans*-isomer): 173.9 (C=O), 158.7 (C=OCH₃), 132.4 (C_{quat}), 127.7 (arylCH), 114.2 (arylCH), 61.0 (CH₂CH₃), 55.7 (OCH₃), 26.1 (cyclopropCH), 24.2 (cyclopropCH), 17.1 (cyclopropCH), 14.6 (CH₂CH₃).

¹³C-NMR (100 MHz, CDCl₃) (*cis*-isomer): 171.4 (C=O), 158.6 (C=OCH₃), 130.6 (C_{quat}), 129.1 (arylCH), 113.6 (arylCH), 60.5 (CH₂CH₃), 55.5 (OCH₃), 25.2 (cyclopropCH), 22.0 (cyclopropCH), 14.4 (cyclopropCH), 11.6 (CH₂CH₃).

EI-MS (70eV, 50°): 220 (43, M⁺); 191(19); 175(19); 147(1000); 115(12); 91(13).

EA calc. for C₁₃H₁₆O₃ (220.11).

***trans*-2-(4-methoxyphenyl) - cyclopropanemethanol (70)**

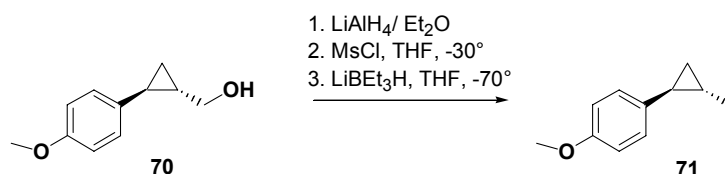
675.8 mg of the ester **69** (3.07 mmol, 1 equiv.) was dissolved in diethyl ether (12 mL) and refluxed with 5.9 mL of 1M LiAlH₄ in Et₂O (5.83 mmol, 1.9 equiv.) for 12 hours. Then the solution was cooled and treated sequentially with water (0.3 mL), 15% aqueous NaOH (0.3 mL) and water (1.0 mL). Then the ethereal solution was filtered off through a fritted funnel and dried over Na₂SO₄ and concentrated in vacuum. The obtained colourless oil (536.4 g, 80%) was used without further purification for the synthesis of the compound **70**.

TLC (hexane/ ethyl acetate 1.1): *R_f* = 0.21

¹H-NMR (400 MHz, CDCl₃): 7.01-6.98 (*m*, 2H, arylH); 6.82-6.79 (*m*, 2H, arylH); 3.77 (*s*, 3H, OCH₃); 3.65-3.61 (*m*, 2H, CH₂OH); 1.81-1.76 (*m*, 1H, cyclopropH, *p*-OMePhCH); 1.46 (*br s*, 1H, OH); 1.43-1.34 (*m*, 1H, cyclopropH); 0.91-0.84 (*m*, 2H, cyclopropH, CH₂).

¹³C-NMR (100 MHz, CDCl₃): 158.17 (Cquat); 134.73 (Cquat); 127.40 (arylCH₂); 114.23 (arylCH₂); 67.10 (CH₂OH); 55.73 (OCH₃); 25.17 (cyclopropH); 20.98 (cyclopropH); 13.68 (cyclopropCH₂).

EA calc. for C₁₁H₁₄O₂: (172.10)

***trans*-1-methyl-2-(4-methoxyphenyl)-cyclopropane (71)**

A solution of 105 mg *trans*-2-(4-methoxyphenyl)-cyclopropanemethanol **70** (0.59 mmol, 1 equiv.) in THF (5.5 mL) under Argon atmosphere was cooled to -30°C. To this was added sequentially via syringe 164 μL of triethylamine (1.18 mmol, 2 equiv.) and 55 μL of methanesulfonyl chloride (0.71 mmol, 1.2 equiv.). The mixture was stirred at -30°C for 30 minutes and then cooled to -78°C. Then 2.4 mL of a solution of LiBEt₃H (2.36 mmol, 1M in THF, 4 equiv.) was added via syringe. The reaction mixture was allowed to warm slowly to room temperature, it was stirred for 13 hours and finally quenched by the addition of 30% H₂O₂ (1 mL) and 15% aqueous NaOH (1 mL). The resulting mixture was heated at reflux for

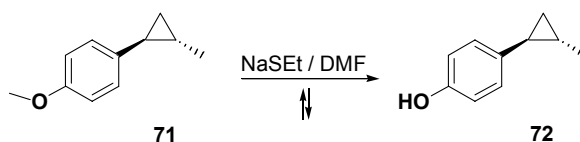
1 hour and then cooled to room temperature. The organic layer was separated, and the aqueous layer was extracted with ether (3 X 10 mL). The combined organic phase was washed with brine (20 mL), dried over Na₂SO₄, filtered and concentrated in vacuum at 0°C. The crude product was opalescent oil that was purified by flash chromatography (silica gel, hexane) to give 83.15 mg (87%) of transparent oil **71**.

TLC (hexane/ ethyl acetate 10:1): $R_f = 0.3$

¹H-NMR (400 MHz, CDCl₃): 6.95-6.91 (*m*, 2H, arylH); 6.78-6.74 (*m*, 2H, arylH); 3.74 (*s*, 3H, OCH₃); 1.51-1.46 (*dt*, $J = 8.3, 4.8$, 1H, cyclopropH); 1.13 (*d*, $J = 6.1$, 3H, CH₃); 0.95-0.90 (*m*, 1H, cyclopropH); 0.76 (*dt*, $J = 8.6, 4.8$, 1H, cyclopropH); 0.64 (*dt*, $J = 8.6, 4.8$, 1H, cyclopropH).

EA calc. for C₁₁H₁₄O: (162.10)

***trans*-2-(4-hydroxyphenyl)-methylcyclopropane (72)**



To a solution of 52.5 mg of NaSEt (0.62 mmol, 2.5 equiv.) in 1.5 mL of freshly distilled dimethylformamide 40 mg of *trans*-1-methyl-2-(4-methoxyphenyl)-cyclopropane **71** (0.25 mmol, 1 equiv.) dissolved in 1 mL of DMF was added. The mixture was heated at reflux (150°C) for 3 hours and then allowed to stand at room temperature for 12 hours. The yellow mixture was extracted with diethyl ether and the combined ethereal extract was washed with a 3M aqueous HCl solution, brine and dried over Na₂SO₄. Distillation of the solvent at reduce pressure gave 31.5 mg (85%) of crude **72**.

TLC (hexane/ACOEt 3:1): $R_f = 0.1$

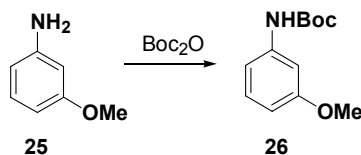
¹H-NMR (400 MHz, CDCl₃): 6.93-6.90 (*m*, 2H, arylH); 6.73-6.70 (*m*, 2H, arylH); 1.59 (*br s*, 1H, OH); 1.53-1.48 (*m*, 1H, cyclopropH, *p*-(OH)PhCH); 1.16 (*d*, $J = 5.8$, 3H, CH₃); 1.00-0.92 (*m*, 1H, cyclopropH); 0.80-0.76 (*m*, 1H, cyclopropH); 0.68-0.63 (*m*, 1H, cyclopropH).

GC-MS : 148 (53, M⁺); 133(100); 105(33), 91(10).

EA calc. for C₁₀H₁₂O : (148.09).

7. 2.2. Pivaloyl Porphyrins

tert- Butyl- *N*-(3-methoxyphenyl)carbamate (**26**)

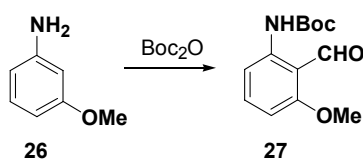


To a solution of 2.5 ml of *m*-anisidine **25** (1 equiv., 22.3 mmol) in 50 ml of THF was added 7.8 g (1.6 equiv., 35.6 mmol) of di-*tert* butyl carbonate and the resulting solution was stirred overnight at room temperature. The solvent was removed by evaporation under reduced pressure and the obtained crude brown oil was distilled bulb-to-bulb (150° at 0.08 mbar) to yield 6.0 g (*quant.*) of the desired product **26** as yellowish oil.

¹H-NMR (400 MHz, CDCl₃): 7.19 (*t*, *J* = 9.4, 1H, arylH-5); 7.10 (*s*, 1H, arylH-2); 7.09 (*d*, *J* = 10.5, 1H, arylH-6); 6.65 (*br, s*, 1H, NH); 6.52 (*d*, *J* = 9.8, 1H, arylH-4); 3.80 (*s*, 3H, OCH₃); 1.53 (*s*, 9H, *t*-Bu).

EI-MS (70eV): 223 (16, *M*⁺); 167 (83); 150 (17); 149 (27); 123 (54); 106 (8); 94 (13); 93 (11); 59 (39); 57 (100); 41 (33).

tert- Butyl- *N*-(2-formyl-3-methoxyphenyl)carbamate (**27**)



4 g (1 equiv., 17.9 mmol) of *tert*-Butyl *N*-(3-methoxyphenyl)-carbamate **26** was dissolved in 20 ml of dry Et₂O and cooled to -30°C (dry ice/*i*-PrOH). To this solution 26.72 ml (2.2 equiv., 39.4 mmol) of a 1.5M solution of *t*-BuLi (in hexane) was added dropwise and the temperature was kept below -15°C. When the addition was terminated the solution was stirred for 3.5 h at -10°C. Then the reaction mixture was cooled to -76°C and 2.86 ml (2 equiv., 37.1 mmol) of DMF in 5 ml of dry Et₂O was added dropwise. Afterwards it was warmed to room temperature and stirring was continued overnight. The reaction was then quenched with brine and extracted three times with Et₂O. The organic layers were separated, washed with water, dried over Na₂SO₄ and concentrated *in vacuo*. The viscous yellow oil was distilled bulb-to-bulb

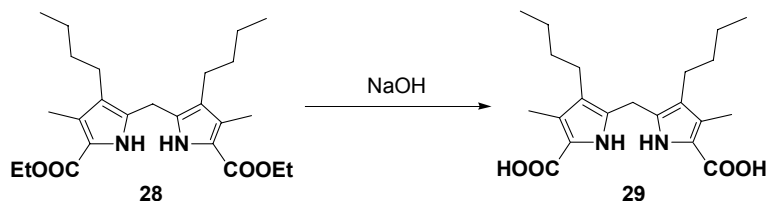
(180°C, 0.1 mbar) which gave 4.0 g (88%) of the title compound **27** as light yellow oil which solidified on storing at 4°C.

TLC (hexane/ethyl acetate 5:1): $R_f = 0.41$

$^1\text{H-NMR}$ (300 MHz, CDCl_3): 10.96 (*br, s*, 1H, NH); 10.45 (*s*, 1H, CHO); 8.10 (*d*, $J = 10.1$, 1H, arylH-5); 7.40 (*t*, $J = 9.8$, 1H, arylH-4); 6.53 (*d*, $J = 9.8$, 1H, arylH-3); 3.90 (*s*, 3H, OCH_3); 1.45 (*s*, 9H, *t*-Bu).

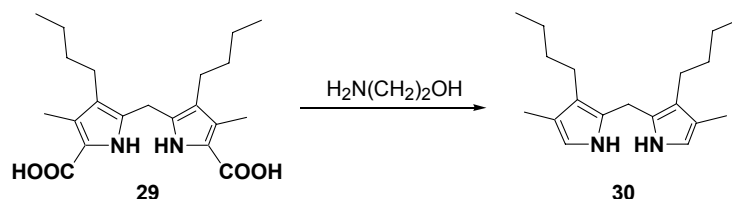
EI-MS (70eV): 251 (15, M^+); 195 (24); 178 (29); 167 (16); 151 (47); 123 (15); 122 (43); 93 (16); 57 (100); 41 (26).

3,3'-Dibutyl-4,4'-dimethyl-2,2'-dipyrrylmethane-5,5'-dicarboxylic acid (**29**)



In 155 mL of EtOH were suspended 10.0 g (1 equiv., 23.2 mmol) of diethyl 3,3'-dibutyl-4,4'-dimethyl-2,2'-dipyrrylmethane-5,5'-dicarboxylate **28** and after heating a clear solution was obtained. Then 4.6 g (5 equiv., 116 mmol) of NaOH dissolved in 50 ml of water was added and the reaction mixture was stirred at reflux for 4 h. After cooling down unreacted starting material was removed from the mixture by two consecutive extractions with CH_2Cl_2 . The aqueous phase was acidified with 1M HCl until pH \sim 5. The acid **29** precipitated as colourless, soft solid which was take out from the aqueous phase performing for three times an extraction with Et_2O . The organic layers were dried over Na_2SO_4 and concentrated *in vacuo*. In this way 8.5 g (97%) of crude acid **29** as a pale pink powder was obtained and was used without further purification in the following step.

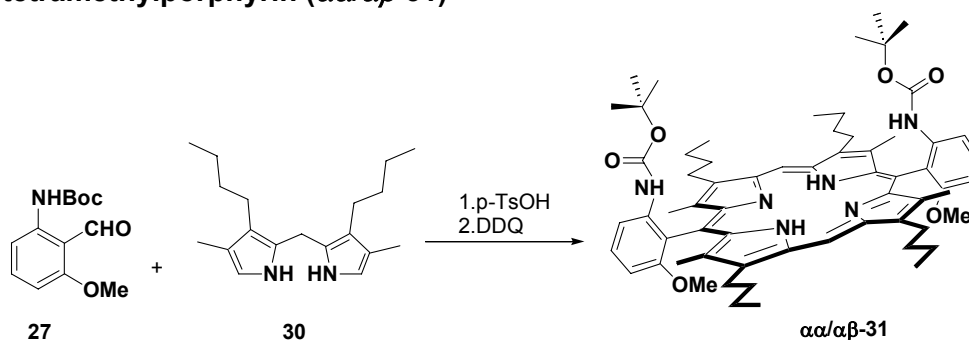
$^1\text{H-NMR}$ (400 MHz, CDCl_3): 11.62 (*br, s*, 2H, COOH); 11.07 (*br, s*, 2H, NH); 3.77 (*s*, 2H, PyCH_2Py); 2.27 (*t*, $J = 7.1$, 4H, PyCH_2); 2.14 (*s*, 6H, PyCH_3); 1.15-1.33 (*m*, 8H, PyCH_2CH_2 and $\text{Py}(\text{CH}_2)_2\text{CH}_2$); 0.88 (*t*, $J = 7.1$, $\text{Py}(\text{CH}_2)_3\text{CH}_3$).

3,3'-Dibutyl-4,4'-dimethyl-2,2'-dipyrromethane (30)

A solution of 8 g (1 equiv., 21.3 mmol) of crude diacid **29** in 100 ml of freshly distilled ethanolamine was stirred in the dark at 120°C for 50 min. After CO_2 formation was over the hot reaction mixture was poured into ice-water and the crude product precipitated immediately as pink solid. The crude product was extracted three times with Et_2O , the organic layers were dried over Na_2SO_4 and all volatiles were removed under reduced pressure. The crude product was purified by column chromatography (silica gel, CH_2Cl_2 , argon, in the dark) followed by recrystallisation from degassed hexane which yielded 3.87 g (63%) of dipyrromethane **30** as pale pink needles. This compound is extremely sensitive to light and air, especially if in solution, and should be used immediately for the next step.

TLC (CH_2Cl_2): $R_f = 0.78$.

$^1\text{H-NMR}$ (400 MHz, CDCl_3): 7.38 (*br, s*, 2H, NH); 6.73 (*s*, 2H, pyrrolyH-5, pyrrolyH-5'); 3.81 (*s*, 2H, PyCH_2Py); 2.41 (*t*, $J = 7.1$, 4H, PyCH_2); 2.04 (*s*, 6H, PyCH_3); 1.28-1.50 (*m*, 8H, PyCH_2CH_2 and $\text{Py}(\text{CH}_2)_2\text{CH}_2$); 0.94 (*t*, $J = 7.1$, 6H, $\text{Py}(\text{CH}_2)_3\text{CH}_3$).

 $\alpha\alpha\beta\beta$ -10,20-Bis[6-(*tert*-butoxycarbonyl)-amino-2-methoxyphenyl]-3,7,13,17-tetrabutyl-2,8,12,18-tetramethylporphyrin ($\alpha\alpha\beta\beta$ -31)

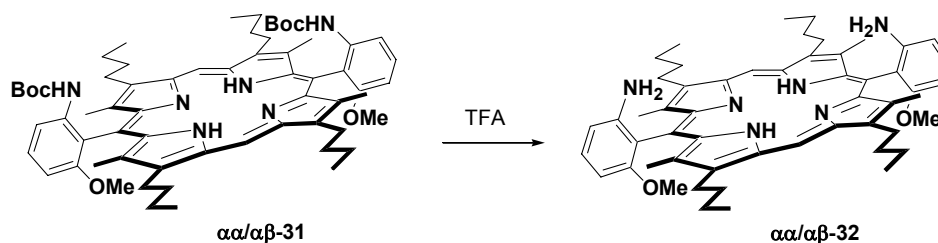
In 300 ml of MeCN 3.5 g (13.9 mmol, 1 equiv.) of *tert*-butyl *N*-(2-formyl-3-methoxyphenyl) carbamate **27** was dissolved and the solution so obtained was degassed by bubbling with argon for 20 min. Then 4.0 g (13.9 mmol, 1 equiv.) of 3,3'-dibutyl-4,4'-dimethyl-2,2'-dipyrromethane **30** was added with a spatula in the dark under argon atmosphere. The reaction mixture was bubbled again with argon for another 20 min. Subsequently 264 mg (1.4 mmol, 0.1 equiv.) of *p*-toluenesulfonic acid was added and the solution turned immediately

dark-brown. The reaction mixture was left stirring in the dark overnight at room temperature. In order to oxidize the formed greenish porphyrinogens, formed during the Mac Donald condensation, 6.31 g (27.8mmol, 2 equiv.) of DDQ dissolved in THF (0.4M) was added. The black mixture was stirred at room temperature and completion of the oxidation was followed with UV/Vis (in CH₂Cl₂ + 1% Et₃N) by the disappearance of the porphyrinogen absorption at 486 nm and the appearance of the porphyrin *Soret* absorption at 410 nm. After 1.5 h all the volatiles were removed *in vacuo* which gave 16 g of crude product which was dissolved in CH₂Cl₂ and filtered through aluminum oxide, using. Fractions were controlled by TLC (silica gel, hexane/ethyl acetate 2:1 + 1% Et₃N) and MALDI-TOF-MS and those displaying mass peaks at *m/z* 1033 (*M*⁺), 933 ([*M*-Boc]⁺) and 833 ([*M*-2Boc]⁺) were combined. The 5.10 g of crude porphyrin mixture $\alpha\alpha/\alpha\beta$ -**31** obtained after removal of the solvent *in vacuo* was used without further purification for the next step.

TLC (hexane/ EtOAc + 1% NEt₃): *R_f*=0.59 *R_f*=0.64

MALDI-TOF-MS :1033 (*M*⁺), 933 ([*M*-Boc]⁺) and 833 ([*M*-2Boc]⁺)

$\alpha\alpha/\alpha\beta$ -10,20-Bis(6-amino-2-methoxyphenyl)-3,7,13,17-tetrabutyl-2,8,12,18-tetramethylporphyrin ($\alpha\alpha/\alpha\beta$ -32**)**



To a solution of 2.0 g (1 equiv., 1.93 mmol) of the atropisomeric mixture $\alpha\alpha/\alpha\beta$ -**31** dissolved in 180 ml of CH₂Cl₂ 13 ml (82 equiv., 160 mmol) of trifluoroacetic acid in 30 ml of CH₂Cl₂ was added slowly by the use of dropping funnel at room temperature under vigorous stirring. The color of the solution turned from red-purple to greenish purple. This reaction mixture was then stirred for 6 h at room temperature and subsequently it was cooled in an ice bath and quenched with 180 ml of saturated aqueous NaHCO₃. After phase separation the organic layer was washed again with 120 ml of saturated aqueous NaHCO₃. The combined aqueous phases were extracted twice with CH₂Cl₂ until colourless. The combined organic phases were finally washed with water (180 ml) and brine (120 ml), dried over Na₂SO₄ and the volatiles were removed under reduced pressure. The crude product was purified by flash chromatography (silica gel, hexane/ethyl acetate 5:1 + 1% Et₃N) which yielded 1.42 g (88%) of a 6:4-mixture of $\alpha\alpha$ -**32** and $\alpha\beta$ -**32**, respectively (estimated from ¹H-NMR) as purple, metallic solid.

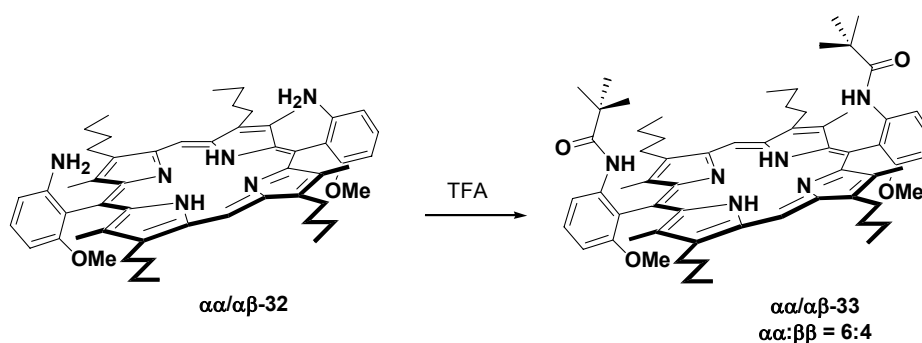
TLC (hexane/ethyl acetate 3:1 + 1% Et₃N): $R_f = 0.40$ $R_f = 0.44$.

UV/Vis (CH₂Cl₂ + 1% Et₃N): 410 (100, *Soret*); 508 (12); 576 (9); 583 (5).

¹H-NMR (400 MHz, CDCl₃): 10.16 (s, 2H, *meso*-H); 7.55 (t, $J = 8.2$, 2H, arylH-4'); 6.76 (m, 4H, arylH-3', arylH-5'); 4.00 (m, 8H, PyCH₂); 3.63 (s, 6H, $\alpha\alpha$ -OCH₃); 3.55 (s, 6H, $\alpha\beta$ -OCH₃); 3.36 (br, s, 2H, $\alpha\beta$ -NH₂); 3.23 (br, s, 2H, $\alpha\alpha$ -NH₂); 2.74 (s, 12H, PyCH₃); 2.17 (m, 8H, PyCH₂CH₂); 1.75 (m, 8H, Py(CH₂)₂CH₂); 1.09 (t, $J = 7.3$, 12H, Py(CH₂)₃CH₃); -2.32 (br, s, 2H, NH pyrrole).

MALDI-TOF-MS: 834 (100, [M+1]⁺).

$\alpha\alpha$ -10,20-Bis(6-pivaloylamino-2-methoxyphenyl)-3,7,13,17-tetrabutyl-2,8,12,18-tetramethylporphyrin($\alpha\alpha$ -33) and $\alpha\beta$ -10,20-Bis(2-pivaloylamino-6-methoxyphenyl)-3,7,13,17-tetrabutyl-2,8,12,18-tetramethylporphyrin($\alpha\beta$ -33)



1.65 g (1 equiv., 1.98 mmol) of the atropisomeric mixture of porphyrin $\alpha\alpha/\alpha\beta$ -32 was dissolved in 130 ml of dry CH₂Cl₂ and then 0.35 ml (3.3 equiv., 6.68 mmol) of dry pyridine and 52 mg (0.2 equiv., 0.42 mmol) of DMAP were added. At this point the drop wise addition of 1.46 ml (6 equiv., 11.88 mmol) of PivCl mixed with 60 ml of dry CH₂Cl₂ was performed within 30 min at room temperature. The reaction mixture was stirred at room temperature for 18 h and quenched with ice. Subsequently, at the temperature of an ice bath, 130 ml of saturated aqueous NaHCO₃ (till pH ~8) were poured into the reaction mixture. The layers were separated and the aqueous phase was extracted two times with 60 ml of CH₂Cl₂. The combined organic layers were washed with water (160 ml) and brine (120 ml), dried over Na₂SO₄ and the solvents were removed under reduced pressure. Purification of the crude product and separation of the two atropisomers was accomplished by repetitive flash chromatography (silica gel, hexane/ethyl acetate 4:1 + 1% Et₃N). 872.4 g (44%) of $\alpha\alpha$ -33 and 575.0 mg (29%) of $\alpha\beta$ -33 as purple solids were obtained

Physical data of $\alpha\alpha$ -33:

TLC (hexane/ethyl acetate/ 5:1 + 01% Et₃N): $R_f = 0.16$.

UV/Vis (CH₂Cl₂ + 1% Et₃N): 412 (100, *Soret*); 510(6); 539 (8); 577 (5)

¹H-NMR (400 MHz, CDCl₃): 10.18 (s, 2H, *meso*-H); 8.45 (d, *J* = 8.3, 2H, arylH-5'); 7.78 (t, *J* = 8.5, 2H, arylH-4'); 7.09 (d, *J* = 8.3, 2H, arylH-3'); 7.05 (*br, s*, 2H, NHPiv); 3.90 (*m*, 8H, PyCH₂); 3.55 (s, 6H, OCH₃); 2.59 (s, 12H, PyCH₃); 2.20 (*m*, 8H, PyCH₂CH₂); 1.74 (*m*, 8H, Py(CH₂)₂CH₂); 1.09 (t, *J* = 7.3, 12H, Py(CH₂)₃CH₃); -0.05 (s, 18H, COC(CH₃)₃); -2.19 (*br, s*, 2H, NHpyrrole).

MALDI-TOF-MS: 1002 (100, [M+1]⁺); 916 (5, [M-Piv]⁺).

RP-HPLC (90-100% MeOH/H₂O in 30 min, then 100% MeOH for 10 min, flow 1.5 ml/min, λ_{det} = 412 nm, T = 40°): R_t = 19.8 min.

Physical data of αβ-33:

TLC (hexane/ethyl acetate 5:1 + 1% Et₃N): R_f = 0.23.

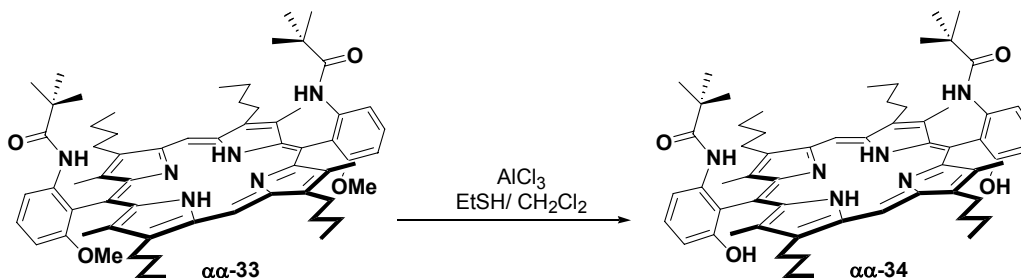
UV/Vis (CH₂Cl₂ + 1% Et₃N): 412 (100, *Soret*); 510(5); 539 (8); 579 (3)

¹H-NMR (400 MHz, CDCl₃): 10.21 (s, 2H, *meso*-H); 8.46 (d, *J* = 8.6, 2H, arylH-5'); 7.79 (t, *J* = 8.5, 2H, arylH-4'); 7.13 (d, *J* = 8.3, 2H, arylH-3'); 6.99 (*br, s*, 2H, NHPiv); 3.91 (*m*, 8H, PyCH₂); 3.64 (s, 6H, OCH₃); 2.59 (s, 12H, PyCH₃); 2.15 (*m*, 8H, PyCH₂CH₂); 1.71 (*m*, 8H, Py(CH₂)₂CH₂); 1.07 (t, *J* = 7.4, 12H, Py(CH₂)₃CH₃); -0.11(s, 18H, COC(CH₃)₃); -2.21 (*br, s*, 2H, NHpyrrole).

MALDI-TOF-MS: 1002 (100, [M+1]⁺); 916 (5, [M-Piv]⁺).

RP-HPLC (90-100% MeOH/H₂O in 30 min, then 100% MeOH for 10 min, flow 1.5 ml/min, λ_{det} = 412 nm, T = 40°): R_t = 24.0 min.

$\alpha\alpha$ -10,20-Bis(6-pivaloylamino-2-hydroxyphenyl)-3,7,13,17-tetrabutyl-2,8,12,18-tetramethylporphyrin ($\alpha\alpha$ -34)



To a solution of 513.5 mg (1 equiv., 0.51 mmol) of $\alpha\alpha$ -**33** in 70 ml of dry CH_2Cl_2 , 100 ml of ethanethiol was added. 2.6 g (38 equiv., 19.45 mmol) of dry AlCl_3 was then added in portion. The solution turned grass-green and it was stirred at room temperature for 48 h. The course of the reaction was followed by taking aliquots from the reaction mixture that were analyzed after a mini-work up by MALDI TOF MS (1002 ($[\text{M}+\text{H}]^+$, educt); 988 ($[\text{M}+\text{H}-\text{CH}_3+\text{H}]^+$); 974 ($[\text{M}+\text{H}-2\text{CH}_3+2\text{H}]^+$). The reaction was stopped by cooling the mixture in an ice bath and adding first some pieces of ice to destroy unreacted AlCl_3 and finally 100 ml of saturated aqueous NaHCO_3 . The two organic phases were then separated and washed with two portions of 80 ml of saturated aqueous NaHCO_3 , while the aqueous phases were extracted twice with CH_2Cl_2 (2 \times 200 ml). Finally the combined organic phases were washed with water (200 ml) and brine (150 ml), dried over Na_2SO_4 followed by removal of volatiles *in vacuo*. The crude purple solid was purified by flash chromatography (silica gel, hexane/ethyl acetate 4:2 + 1% Et_3N) which yielded 471 mg (95%) of pure purple solid $\alpha\alpha$ -**34**.

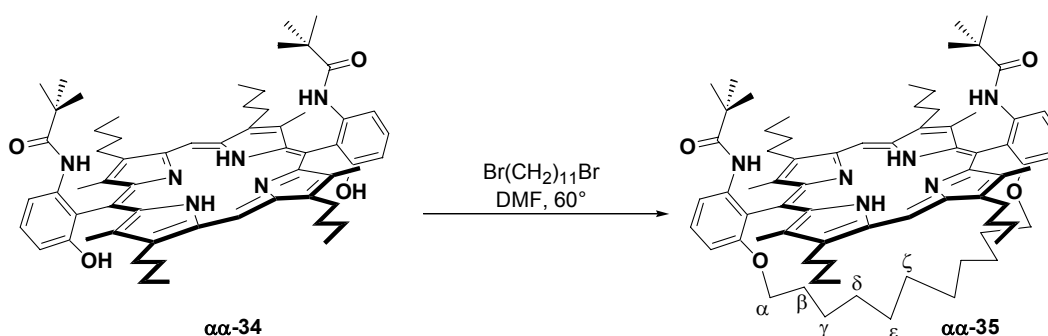
TLC (hexane/ethyl acetate 3:1 + 1% Et_3N): R_f = 0.25.

UV/Vis (CH_2Cl_2 + 1% Et_3N): 408 (100, *Soret*); 510(7); 542(10); 577 (3)

$^1\text{H-NMR}$ (400 MHz, CDCl_3): 10.30 (s, 2H, *meso*-H); 8.43 (d, J = 8.1, 2H, arylH-5'); 7.74 (t, J = 8.3, 2H, arylH-4'); 7.17 (s, 2H, NHPiv); 7.12 (dd, J = 8.3, J = 0.8, 2H, arylH-3'); 3.99 (m, 8H, PyCH_2); 2.69 (s, 12H, PyCH_3); 2.20 (m, 8H, PyCH_2CH_2); 1.76 (m, 8H, $\text{Py}(\text{CH}_2)_2\text{CH}_2$); 1.12 (t, J = 7.5, 12H, $\text{Py}(\text{CH}_2)_3\text{CH}_3$); 0.12 (s, 18H, $\text{COC}(\text{CH}_3)_3$); -2.31 (br, s, 2H, NHPyrrole).

MALDI-TOF-MS: 974 (100, $[\text{M}+1]^+$); 996 (15, $[\text{M}+\text{Na}]^+$).

10,20-[Di-(6-pivaloylamino)-undecamethylenedioxydi-2,1-phenylene]-3,7,13,17-tetrabutyl-2,8,12,18-tetramethylporphyrin (35)



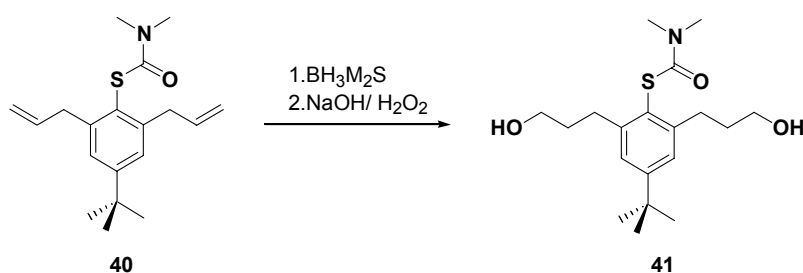
A solution of 8.0 mg (1 equiv., 8.2 μmol) of bisphenol porphyrin $\alpha\alpha\text{-33}$ in 5 ml of dry DMF and 85.5 mg (32 equiv., 262.4 μmol) of Cs_2CO_3 (previously dried overnight at 100°C in high-vacuum) was added. This suspension was heated to 60°C and stirred for 30 min. Then a solution of 3.1 μl (1.5 equiv., 12.3 μmol) of 1, 11 -dibromoundecane in 1 ml of dry DMF was added *via* syringe pump within 3 h at 60°C . Stirring was continued at 60°C for 1 h after which the reaction mixture was poured into a ice-cooled mixture of 2 ml of 1M HCl and 5 ml of CH_2Cl_2 . The aqueous phase was separated from the organic layer and then extracted twice with CH_2Cl_2 (2X 5 ml). The combined organic phases were washed with saturated aqueous NaHCO_3 (2x15 ml), water (10 ml) and brine (10 ml), dried over Na_2SO_4 and all volatiles were removed under reduced pressure. Purification by flash chromatography (silica gel, hexane/ethyl acetate 2:1 + 1% Et_3N) yielded 9.6 mg (70%) of the "bridged" porphyrin $\alpha\alpha\text{-35}$ as purple solid.

TLC (hexane/ethyl acetate 1:1 + 1% Et_3N): $R_f = 0.53$.

UV/Vis (CH_2Cl_2 + 1% Et_3N): 412 (100, *Soret*); 510(7); 542(10); 577 (3).

$^1\text{H-NMR}$ (400 MHz, CDCl_3): 10.18 (s, 2H, *meso*-H); 8.51 (d, $J = 8.3$, 2H, arylH-5'); 7.75 (t, $J = 8.3$, 2H, arylH-4'); 7.65 (s, 2H, NHPiv); 7.03 (dd, $J = 8.3$, $J = 0.8$, 2H, arylH-3'); 3.90 (m, 8H, PyCH_2); 3.79 (m, 4H, $\alpha\text{-CH}_2$); 2.61 (s, 12H, PyCH_3); 2.23 (m, 8H, PyCH_2CH_2); 1.79 (m, 8H, $\text{Py}(\text{CH}_2)_2\text{CH}_2$); 1.13 (t, $J = 7.3$, 12H, $\text{Py}(\text{CH}_2)_3\text{CH}_3$); 0.68 (m, 4H, $\beta\text{-CH}_2$); 0.23 (s, 18H, $\text{COC}(\text{CH}_3)_3$); -0.25 (m, 4H, $\gamma\text{-CH}_2$); -0.52 (m, 4H, $\delta\text{-CH}_2$); -1.40 (br, s, 6H, $\varepsilon\text{-CH}_2$, $\zeta\text{-CH}_2$); -2.20br, s, 2H, NHPyrrole).

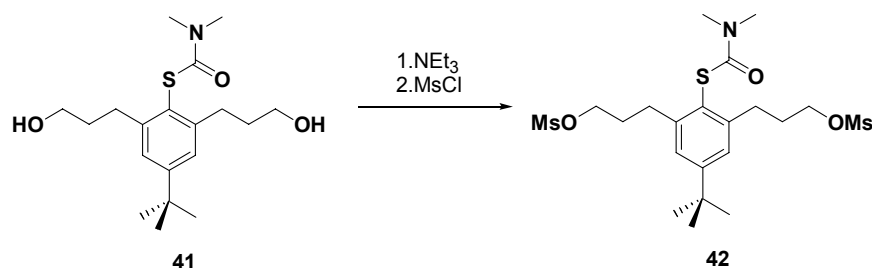
ESI-MS (MeOH): *Positive* ion mode: 1126.2 (100, $[M+\text{H}]^+$); 1148 (30, $[M+\text{Na}]^+$).

S-[4-(*tert*-Butyl)-2,6-bis(3-hydroxypropyl)-1-phenyl]*N,N*-dimethylthiocarbamate (41)

A solution of 4.0 g (1 equiv., 12.6 mmol) of S-[2,6-Diallyl-4-(*tert*-butyl)-1-phenyl] *N,N*-dimethylthiocarbamate (**40**) in 100 ml of dry THF was cooled to 5°C (ice bath) and then 4.5 ml (3.6 equiv., 45.3 mmol) of $\text{BH}_3 \cdot \text{SMe}_2$ was added dropwise *via* syringe within 5 min. The solution was then stirred at room temperature for three hours. After one hour the reaction became cloudy and the addition of 20 mL more of THF was necessary. The reaction mixture was cooled in an ice bath and 13 ml of 3M NaOH was added drop by drop carefully followed by 13 ml of 10% aqueous H_2O_2 . The reaction mixture so obtained was then refluxed for 1 h and subsequently cooled to room temperature and poured onto ice-water 1:1. The resulting biphasic mixture was extracted with three portions of 330 ml of CH_2Cl_2 , the combined organic phases were washed with water (250 ml) and brine (200 ml), dried over Na_2SO_4 and concentrated *in vacuo*. The obtained pale yellow oil was purified by flash chromatography (silica gel, $\text{CH}_2\text{Cl}_2/\text{MeOH}$ 95:5) and gave 3.47 g (78%) of pure **41** as colourless oil.

TLC ($\text{CH}_2\text{Cl}_2/\text{MeOH}$ 95:5): $R_f = 0.25$.

$^1\text{H-NMR}$ (400 MHz, CDCl_3): 7.19 (s, 2H, arylH-3, arylH-5); 3.64 (t, $J = 6.2$, 4H, CH_2OH); 3.16, 3.01 (br, s, 6H, NCH_3); 2.88 (t, $J = 7.6$, 4H, $\text{CH}_2(\text{CH}_2)_2\text{OH}$); 1.88 (m, 4H, $\text{CH}_2\text{CH}_2\text{CH}_2\text{OH}$); 1.79 (s, 2H, OH); 1.30 (s, 9H, *t*-Bu).

S-[4-(*tert*-Butyl)-2,6-bis(3-methanesulfonylpropyl)-1-phenyl]-*N,N*-dimethylthiocarbamate (42)

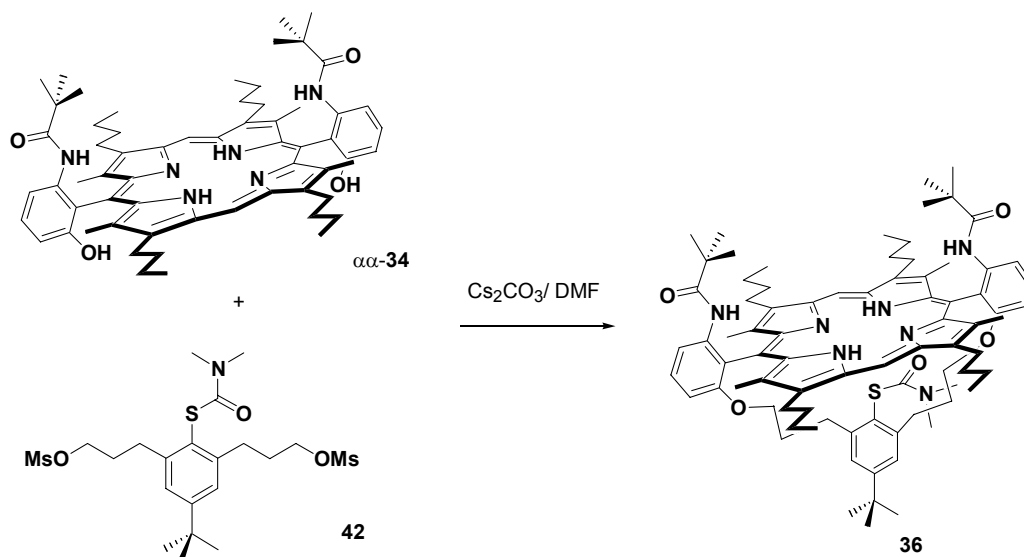
To a solution of 1.0 g (1 equiv, 2.82 mmol) of diol **41** in 100 ml of dry CH_2Cl_2 3.25 ml (8 equiv., 22.5 mmol) of Et_3N was added. This solution was cooled to 0°C (ice bath) and then a solution of 1.95 ml (4.7 equiv., 13.5 mmol) of methanesulfonyl chloride in 63 ml of dry CH_2Cl_2

was added dropwise within 1 h, keeping the temperature constantly around 0°. The reaction mixture became torpid due to the formation of Et₃N•HCl. Subsequently the stirring of the reaction mixture was continued for 2h at room temperature. The reaction mixture was cooled in an ice bath and quenched with 60 ml of 1M HCl. The layers were separated and the aqueous phase was extracted with two portions of 100 ml of CH₂Cl₂. The organic phases were washed with saturated aqueous NaHCO₃ (200 ml), water (100 ml) and brine (60 ml), dried over Na₂SO₄ and the solvent was removed *in vacuo*. The crude was then purified by flash chromatography (silica gel, hexane/ethyl acetate 1:2) and 1.34 g (95%) of titled compound was obtained. The product **42** was a viscous oil that solidified on storing at 4°C.

TLC (CH₂Cl₂/MeOH 95:5): *R_f* = 0.70.

¹H-NMR (400 MHz, CDCl₃): 7.19 (s, 2H, arylH-3, arylH-5); 4.24 (t, *J* = 6.4, 4H, CH₂OMs); 3.18, 3.01 (*br, s*, 6H, NCH₃); 3.00 (s, 6H, CH₃SO₃); 2.90 (t, *J* = 7.7, 4H, CH₂(CH₂)₂OMs); 2.05 (*m*, 4H, CH₂CH₂CH₂OMs); 1.31 (s, 9H, *t*-Bu).

10,20-[[4-(*tert*-Butyl)-2-(*N,N*-dimethylcarbamoyl)thio-1,3-phenylene]bis(trimethyleneoxy)]-di-(6-pivaloylamino)-di-2,1-phenylene]-3,7,13,17-tetrabutyl-2,8,12,18-tetramethylporphyrin (36**)**



To a solution of 200 mg (1 equiv., 205 μ mol) of bisphenol porphyrin $\alpha\alpha$ -**34** in 90 ml of dry DMF was added 2.0 g (30 equiv., 6.15 mmol) of Cs₂CO₃ which was previously dried at 100°C in high-vacuum overnight. The resulting suspension was heated to 60°C and stirred for 30 min. Then a previously prepared solution of 156 mg (1.5 equiv., 307 μ mol) of dimesylate **42** in 30 ml of dry DMF was added *via* syringe pump within 4 h at 60°C. Stirring was continued for 40 min at 60°C. The reaction mixture was then cooled with an ice bath and the reaction was quenched with 60 ml of 1M HCl. The two layer were then separated the aqueous phase

was extracted with two portions of 100 ml of CH_2Cl_2 . The combined organic layers were washed with twice with 200 ml of saturated aqueous NaHCO_3 , water (170 ml) and brine (100ml), dried over Na_2SO_4 and concentrated *in vacuo*. The DMF was removed at 60°C under reduced pressure. The crude product was purified by flash chromatography (silica gel, hexane/ethyl acetate 2:1 + 0.5% Et_3N) which gave 210 mg (79%) of the bridged porphyrin as purple solid.

TLC (hexane/ethyl acetate 2:1 + 0.5% Et_3N): $R_f = 0.42$

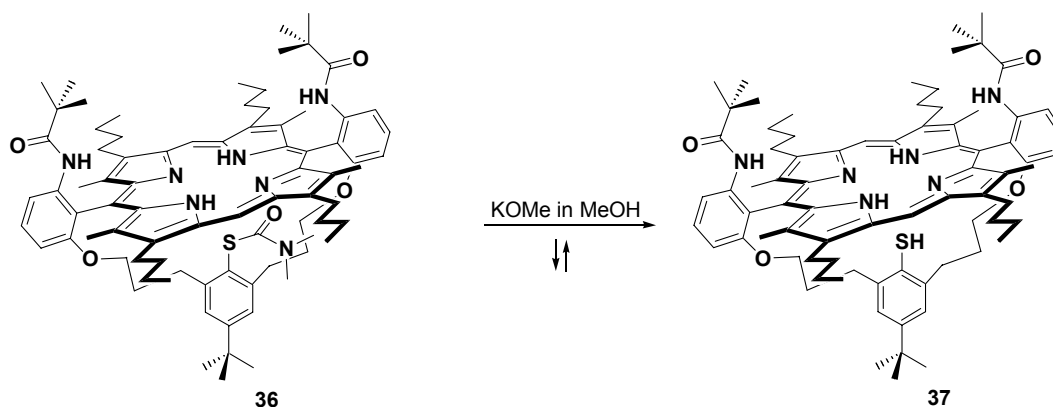
UV/Vis (CH_2Cl_2 + 1% Et_3N): 413(100, *Soret*); 510 (9); 579 (3); 658 (2).

$^1\text{H-NMR}$ (400 MHz, CDCl_3): 10.10 (s, 1H, *meso*-H); 9.71 (s, 1H, *meso*-H); 8.60 (d, $J = 8.3$, 2H, arylH-5'); 8.41 (s, 2H, *NHPiv*); 7.77 (t, $J = 8.3$, 2H, arylH-4'); 6.94(d, $J = 8.3$, 2H, arylH-3'); 6.36 (s, 2H, arylH-3'', arylH-5''); 4.06 (m, 2H, PyCH_2); 3.93 (m, 2H, PyCH_2); 3.84 (m, 4H, PyCH_2 and $\alpha\text{-CH}_2$); 3.58 (m, 4H, PyCH_2 and $\alpha\text{-CH}_2$); 2.71 (s, 6H, PyCH_3); 2.54 (s, 6H, PyCH_3); 2.23(m, 4H, PyCH_2CH_2); 1.98 (m, 2H, PyCH_2CH_2); 1.76 (m, 2H, PyCH_2CH_2); 1.79 (m, 4H, $\text{Py}(\text{CH}_2)_2\text{CH}_2$); 1.53(br, s, NCH_3); 1.71 (m, 4H, $\text{Py}(\text{CH}_2)_2\text{CH}_2$); 1.54 (s, 6H, COCH_3); 1.13 (t, $J = 7.3$, 6H, $\text{Py}(\text{CH}_2)_3\text{CH}_3$); 1.10 (t, $J = 7.3$, 6H, $\text{Py}(\text{CH}_2)_3\text{CH}_3$); 1.07(s, 9H, *t*-Bu); 0.65 (m, 6H, $\beta\text{-CH}_2$ and $\gamma\text{-CH}_2$); 0.50 (s, 18H, $\text{COC}(\text{CH}_3)_3$); 0.05 (m, 2H, $\gamma\text{-CH}_2$); -1.10(br, s, 3H, NCH_3); -2.06 (br, s, 2H, NHpyrrole).

MALDI-TOF-MS: 1219 (20, $[\text{M-CONMe}_2]^+$); 1291(100, $[\text{M}+1]^+$), 1348 (10, $[\text{M}+\text{Cs}]^+$);

RP-HPLC (90-100% $\text{MeOH}/\text{H}_2\text{O}$ in 10 min, then 100% MeOH for 20 min, flow 1.5 ml/min, $\lambda_{\text{det}} = 413 \text{ nm}$, $T = 40^\circ$): $R_t = 15.8 \text{ min}$.

10,20-[[[4-(*tert*-Butyl)-2-mercapto-1,3-phenylene]bis(trimethylene-oxy)]-di-(6-pivaloylamino)-di-2,1-phenylene]-3,7,13,17-tetrabutyl-2,8,12,18-tetramethyl-porphyrin (37)



In an oxygen-free atmosphere a solution of 132 mg (1 equiv., 102.2 μmol) of porphyrin **36** in 80 ml of dry and degassed dioxane was heated to 80°C . To this hot solution was added 460 μl (10 equiv., 1.02 mmol) of freshly prepared and degassed KOMe solution (2.18M in

MeOH) and the resulting grass-green solution was heated at reflux for 10 min. [This solution was prepared following a procedure described in M. Lochner Dissertation Basel 2003]. The reaction mixture was cooled in an ice bath and the reaction was quenched with 50 ml of saturated aqueous NH_4Cl . [All of the used solvents and solutions for the aqueous work up were quickly degassed by bubbling with argon for 15-20 min to use]. 20 ml of CH_2Cl_2 were then added, the two layers were separated and the aqueous phase was extracted with two portions of 2 ml of CH_2Cl_2 (40 X2 ml). The combined organic layers were washed with water (40 ml), dried over Na_2SO_4 and concentrated *in vacuo*. The obtained crude residue was purified by flash chromatography (silica gel, hexane/AcOEt 2:1 + 1% Et_3N , under argon, solvents were quickly degassed by bubbling with argon for 5-10 min prior to use) which yielded 81 mg (65%) of pure thiophenyl porphyrin.

TLC (hexane/ AcOEt 3:1 + 0.05% Et_3N): $R_f = 0.31$.

UV/Vis (CH_2Cl_2 + 1% Et_3N): 413 (100, *Soret*); 510 (9); 542 (4); 578 (5); 630 (2); 658 (1).

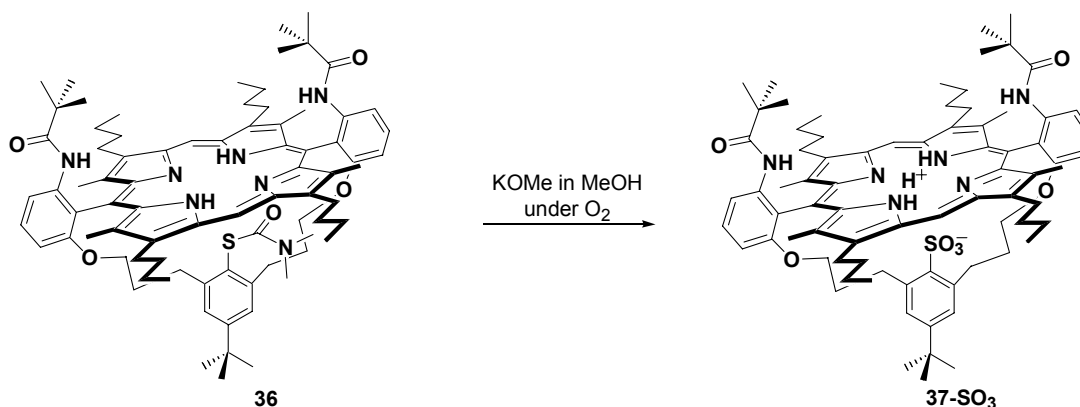
$^1\text{H-NMR}$ (400 MHz, CDCl_3): 10.11(s, 2H, *meso*-H); 8.61 (*d*, $J = 8.0$, 2H, arylH-5'); 8.43 (*s*, 2H, *NHPiv*); 7.76 (*t*, $J = 8.4$, 2H, arylH-4'); 6.92 (*d*, $J = 7.5$, 2H, arylH-3'); 6.17 (*s*, 2H, arylH-3'', arylH-5''); 4.02 (*m*, 4H, PyCH_2); 3.88 (*m*, 4H, PyCH_2); 3.61 (*m*, 4H, $\alpha\text{-CH}_2$); 2.61 (*s*, 12H, PyCH_3); 2.10 (*m*, 8H, PyCH_2CH_2); 1.66 (*m*, 8H, $\text{Py}(\text{CH}_2)_2\text{CH}_2$); 1.02 (*t*, $J = 7.3$, 12H, $\text{Py}(\text{CH}_2)_3\text{CH}_3$); 0.85(*s*, 9H, *t*-Bu); 0.65 (*m*, 4H, $\beta\text{-CH}_2$, $\gamma\text{-CH}_2$); 0.53 (*s*, 18H, $\text{COC}(\text{CH}_3)_3$); 0.46 (*m*, 4H, $\beta\text{-CH}_2$, $\gamma\text{-CH}_2$); -2.12(*s*, 2H, *NHpyrrole*); -3.01 (*s*, 1H, SH).

MALDI-TOF-MS: 1220 (100, $[M+1]^+$).

ESI-MS (MeOH): *Positive ion mode*: 1219.7 (100, $[M+H]^+$); 1241 (30, $[M+\text{Na}]^+$); 1257 (17, $[M+\text{K}]^+$). *Negative ion mode*: 1218 (100, M^-).

RP-HPLC (90-100% MeOH/ H_2O in 10 min, then 100% MeOH for 20 min, flow 1.5 ml/min, $\lambda_{\text{det}} = 413$ nm, $T = 40^\circ$): $R_t = 23.9$ min.

10,20-[[4-(*tert*-Butyl)-2-sulfonate-1,3-phenylene]bis(trimethylene-oxy)]-di-(6-pivaloylamino)-di-2,1-phenylene]-3,7,13,17-tetrabutyl-2,8,12,18-tetramethyl-porphyrin (37-SO₃)



In an oxygen-enriched atmosphere a solution of 20 mg (1 equiv., 16.4 μmol) of porphyrin **36** in 10 ml of dry dioxane [previously enriched in O₂ by oxygen-bubbling] was heated to 80°. To this hot solution 57.5 mg (50 equiv., 0.82 mmol) of solid dry KOMe was added and the resulting grass-green solution was heated at reflux for 24 h. The completion of the deprotection and subsequent thiolate oxidation were followed by TLC and ESI-MS. [The oxidation reaction did not reach more than 40% of conversion of the thiolate into the sulfonate]. The reaction mixture was cooled in an ice bath and the reaction was quenched with 10 ml of saturated aqueous NH₄Cl. 20 ml of CH₂Cl₂ were then added, the two layers were separated and the aqueous phase was extracted with two portions of 2 ml of CH₂Cl₂ (10 X2 ml). The combined organic layers were washed with water (10 ml), dried over Na₂SO₄ and concentrated *in vacuo*. The obtained crude residue was purified by flash chromatography (silica gel, hexane/AcOEt 3:1) which yielded 7.28 mg (35%) of pure **37-SO₃**.

TLC (Hexane/AcOEt 5:1): $R_f = 0.25$

UV/Vis (CH₂Cl₂): 418 (100, *Soret*); 510 (12); 540 (3); 643 (2).

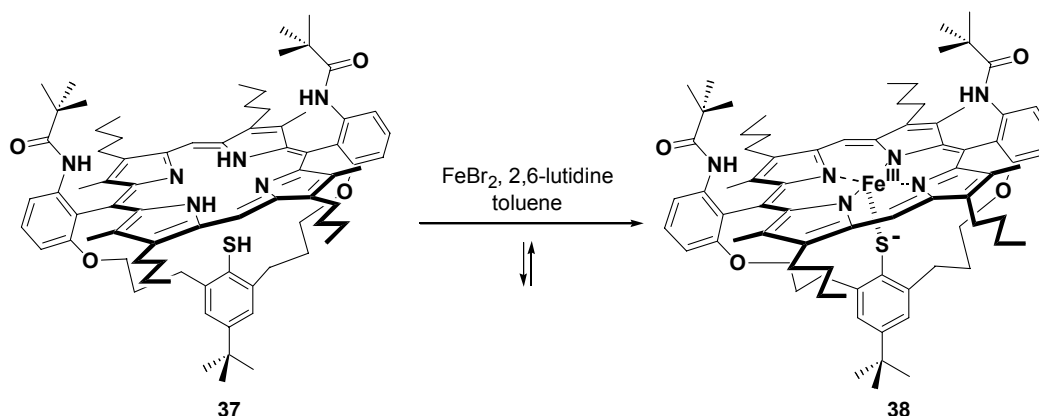
¹H-NMR (500 MHz, CDCl₃): 10.34 (s, 2H, *meso*-H); 8.59 (d, $J = 8.2$, 2H, arylH-5'); 8.12 (s, 1H, *NHPiv*); 7.81 (t, $J = 8.4$, 2H, arylH-4'); 7.05 (d, $J = 8.1$, 2H, arylH-3'); 6.06 (s, 2H, arylH-3'', arylH-5''); 4.07 (m, 4H, PyCH₂); 3.83 (m, 4H, PyCH₂); 3.56 (m, 4H, α -CH₂); 2.64 (s, 12H, PyCH₃); 2.50 (m, 8H, PyCH₂CH₂); 1.65 (m, 8H, Py(CH₂)₂CH₂); 1.04 (t, $J = 7.4$, 12H, Py(CH₂)₃CH₃); 0.82 (s, 9H, *t*-Bu); 0.65 (m, 4H, β -CH₂); 0.57 (m, 4H, γ -CH₂); 0.52 (s, 18H, COC(CH₃)₃).

MALDI-TOF-MS: 1268(100, [M+1]⁺); 1290 (10, [M+1+Na]⁺);

ESI-MS (MeOH): *Positive ion mode*: 1267 (1100, M⁺); 1286(60, [M+Na]⁺). *Negative ion mode*: 1266 (100, M⁻).

RP-HPLC (90-100% MeOH/H₂O in 10 min, then 100% MeOH for 20 min, flow 1.5 ml/min, $\lambda_{\text{det}} = 414 \text{ nm}$, $T = 40^\circ$): $R_t = 9.1 \text{ min}$.

10,20-[[4-(*tert*-Butyl)-2-mercapto-1,3-phenylene]bis(trimethylene-oxy)]-di-(6-pivaloylamino)-di-2,1-phenylene]-3,7,13,17-tetrabutyl-2,8,12,18-tetramethyl-porphyrinato iron(III) (38**)**



Inside the glove box, to a solution of 20.8 mg (1 equiv., 17.13 μmol) of thiophenol porphyrin **37** in 14 ml of dry and degassed toluene was added 100 μl (50 equiv., 856.5 μmol) of dry and degassed 2,6-lutidine. Subsequently the resulting solution was heated to reflux for 5 min. Then a suspension of 53.0 mg (20 equiv., 247 μmol) of FeBr_2 in 4 ml of dry and degassed toluene was added. The resulting brown reaction mixture was stirred at reflux for 30 min, cooled to room temperature and filtered through a small pad of celite. [The completion of the iron insertion was checked by TLC (silica gel, hexane/ AcOEt 5:1) directly inside the glove box. The residue on the pad was washed with toluene portions until the filtrate was colourless. The combined brown filtrates were evaporated under reduced pressure and the crude iron porphyrin was purified by column chromatography (silica gel, hexane/ AcOEt 5:1) which yielded 20.7mg (95%) of iron porphyrin **38** as brown solid.

TLC (hexane/AcOEt 5:1): $R_f = 0.28$.

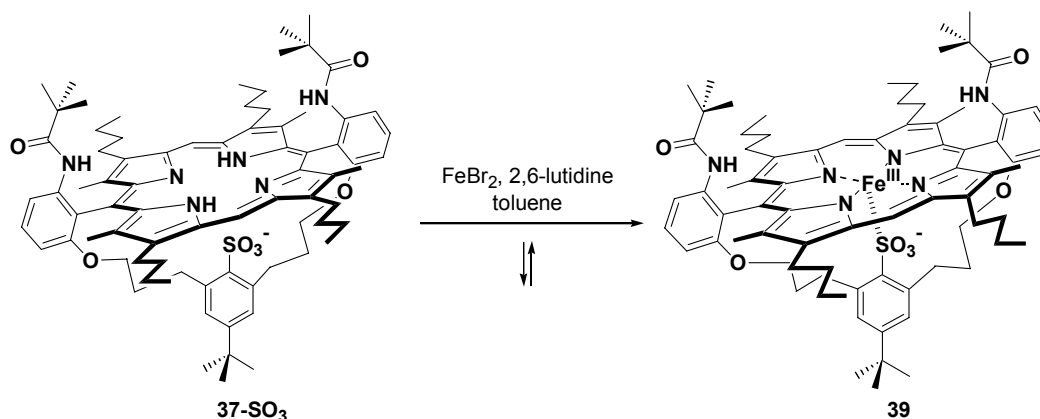
UV/Vis (toluene): 404 (100, *Soret*); 488 (12); 510 (25); 583 (5); 658 (3); 767 (2).

MALDI-TOF-MS: 1272 (100, $[M^+]$).

ESI-MS (MeOH): *Positive ion mode*: 1272 (30, $[M+H]^+$); 1295 (100, $[M+Na]^+$); 1310 (20, $[M+K]^+$). *Negative ion mode*: 1271 (100, M^-); 1303 (15, $[M+CH_3O]^-$).

cw-EPR (toluene, 100 K): 8.53, 5.43, 3.34, 2.67 (rhombohedral, high-spin).

10,20-{{[4-(*tert*-Butyl)-2-sulfonate-1,3-phenylene]bis(trimethylene-oxy)}}-di-(6-pivaloylamino)-di-2,1-phenylene}-3,7,13,17-tetrabutyl-2,8,12,18-tetramethyl-porphyrinato iron(III) (39**)**



To a solution of 15 mg (1 equiv., 11.8 μmol) of sulfonate porphyrin **37-SO₃** in 10 ml of dry toluene was added 68 μl (50 equiv., 590 μmol) of dry 2,6-lutidine. Subsequently the resulting solution was heated to reflux for 5 min. Then a suspension of 50.6 mg (20 equiv., 236 μmol) of FeBr₂ in 4 ml of dry toluene was added. The resulting brown reaction mixture was stirred at reflux for 30 min, cooled to room temperature and filtered through a small pad of celite. [The completion of the iron insertion was checked by TLC (silica gel, hexane/ AcOEt 5:1) directly inside the glove box. The residue on the pad was washed with toluene portions until the filtrate was colourless. The combined brown filtrates were evaporated under reduced pressure and the crude iron porphyrin was purified by column chromatography (silica gel, hexane/ AcOEt 5:1) which yielded 14.0 mg (90%) of iron porphyrin **38** as brown solid

TLC (hexane/AcOEt 4:1): R_f = 0.32.

UV/Vis (toluene): 389-416 (100, *Soret*); 483 (9); 510 (25); 587 (2); 670 (2).

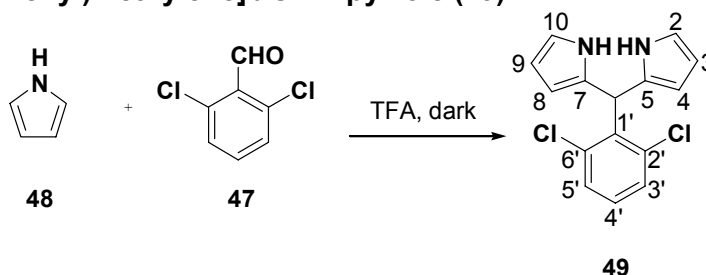
MALDI-TOF-MS: 1321 (100, $[M+1]^+$).

ESI-MS (MeOH): *Positive ion mode*: 1321 (20, $[M+H]^+$); 1343 (100, $[M+Na]^+$). *Negative ion mode*: 1319 (100, M^-); 1350 (15, $[M+CH_3O]^-$).

cw-EPR (toluene, 102 K): $g_{\perp} = 5.57$, $g_{\parallel} = 2.10$ (axial, high-spin).

7.2.3. Dichloroporphyrin

2, 2'-[(2,6-dichlorophenyl)methylene]bis-1H-pyrrole (49)



In the dark, under argon atmosphere, at -15°C , 5 g of 2, 6-dichloro-benzaldehyde (1 equiv, 28.57 mmol) was dissolved in 158 mL of pyrrol (80 equiv., 2.28 mol). The solution was then bubbled with argon for 20 minutes and finally 88 μL of TFA (0.08 equiv., 2.28 mmol) was added. After 5 minutes the reaction was quenched with aqueous saturated NaHCO_3 (250 mL) and extracted twice with ethyl acetate (2 X 200mL). The combined organic phase was washed with water (2 X 100 mL) and dried over Na_2SO_4 (always under argon atmosphere). The crude product (mixture of six different compounds) was purified by flash chromatography (silica gel, hexane/ethyl acetate 3:1). The collected fractions of the desired compound were then concentrated in vacuum and subjected to a crystallization process using hexane/ ethyl acetate and dried at the high vacuum pump for 24 hours. 8.32 g (26%) of white solid was obtained. This compound should be used immediately for the following step or stored at -20°C , under argon and in the dark just for few days.

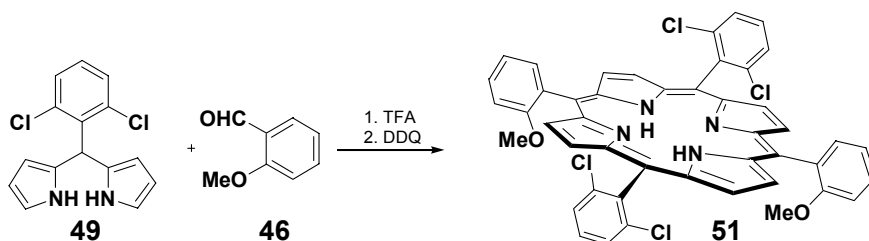
TLC (hexane/ AcOEt 3:1): $R_f = 0.50$.

mp : 102-103 $^{\circ}\text{C}$

$^1\text{H-NMR}$ (400 MHz, CDCl_3) : 8.28 (*br s*, 2H, NH); 7.33 (*d*, $J = 8$ Hz, 2H, H-3', H-5'); 7.13 (*t*, $J = 8$ Hz, 1H, H-4'); 6.73-6.71 (*m*, 2 H, H-2, H-10); 6.48 (*s*, 1H, H-6); 6.19 (*q*, $J = 2.8$, 2H, H-3, H-9); 6.06 (*m*, 2H, H-4, H-8).

$^{13}\text{C-NMR}$ (100 MHz, CDCl_3): 137.1(2C, C-2',C-6'); 135.8 (1C, C-1'); 129.75 (1C, C-4'); 129.02 (2C,C-3', C-5'); 128.5 (2C, C-5, C-7); 117.3 (2C, C-2, C-10); 109.07 (2C, C-4, C-8); 107.8 (2C, C-3, C-9); 40.4 (1C, C-6).

EI-MS (70eV) : 290 (68, M^+); 188 (29) ;145 (100).

5,15-bis(2,6-dichlorophenyl)-10,20-bis(2-methoxyphenyl)-porphyrin (51)

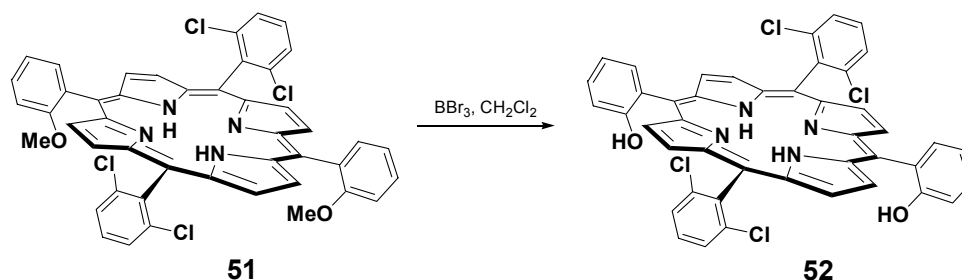
1.2 g of 2,2' -[(2,6-dichlorophenyl)methylene]bis-1H-pyrrole **49** (1 equiv, 4.12 mmol) and 561mg of 2-methoxy-benzaldehyde **46** (1 equiv., 4.12 mmol) were dissolved in 415 ml of dichloromethane and bubbled with a light flow of argon for 15 minutes in the dark. Afterwards 561 mL of TFA (1.8 equiv., 7.42 mmol,) were added and the reaction mixture was stirred for 15 hours at room temperature in light exclusion. For the subsequent oxidation of the formed porphyrinogens 1.87 g of 1, 2-dichloro-4, 5-dicyano-p-benzoquinone (DDQ) (2 equiv., 8.24 mmol) was added and the solution was refluxed for 1 hour. As for the synthesis of the other porphyrin the completion of the oxidation was followed by the disappearance of the porphyrinogen absorption at 485 nm and the appearance of the porphyrin Soret absorption at 418 nm. All the volatiles were removed in vacuum, after a previous addition of 4.15 mL of triethylamine (1% in volume) to the cooled reaction mixture. The residue was re-dissolved in $\text{CH}_2\text{Cl}_2 + 1\% \text{NEt}_3$, filtrated trough a silica gel pad and finally purified by flash chromatography (silica gel,). 784 mg (23%) of purple porphyrin **51** (mixture of two atropisomers) were obtained.

TLC (CH_2Cl_2 / hexane 3:1): $R_f = 0.35$, $R_f = 0.40$

UV/Vis ($\text{CH}_2\text{Cl}_2 + 1\% \text{Et}_3\text{N}$): 418 (100, *Soret*); 512 (8); 548(3); 637 (1).

$^1\text{H-NMR}$ (400 MHz, CDCl_3): 8.78 (*d*, $J = 4.8$, 4H, H-2, H-8, H-12, H-18); 8.61 (*d*, $J = 4.8$, 4H, H-3, H-7, H-13, H-17); 8.02-7.99 (*m*, 2H, H-6'); 7.79-7.77(*m*, 4H, H-c,H-e); 7.76-7.73 (*m*, 2H, H-4'); 7.71-7.66 (*m*, 2H, H-d); 7.35-7.33 (*m*, 2H, H-5'); 7.32-7.30 (*m*, 2H, H-3'); 3.60 (*s*, 6H, OCH_3); -2.56 (*br s*, 2H, NH).

ESI-MS (MeOH): *Positive* ion mode: 811.0(100, $[\text{M}+\text{H}]^+$); 945 (56); 1097 (40). *Negative* ion mode: 809.3 (100, $[\text{M}-\text{H}]^-$).

5,15-bis(2,6-dichlorophenyl)-10,20-bis(2-hydroxyphenyl)-porphyrin (52)

100 mg of porphyrin **51** (123 μmol , 1 equiv.) were dissolved in 40 mL of CH_2Cl_2 (~ 3.1 M) and the solution was cooled down to -78°C (dry ice and acetone). Then 380 μL of BBr_3 (3.94 mmol, 32 equiv.) were added slowly via syringe and the reaction mixture was stirred for 12 hours at room temperature. The completion of the double demethylation reaction was controlled by ESI-MS. The reaction was quenched with 30 mL of aqueous saturated NaHCO_3 and the organic layer was washed with water (2 X 20 mL). The combined organic phases were then dried over Na_2SO_4 and concentrated under reduced pressure. The residue was then re-dissolved in CH_2Cl_2 and filtered through a silica gel pad. The purification at this stage was quite complex and so the 93.6 mg (97%) of crude **52** was just filtered (silica gel, CH_2Cl_2) and used for the following step without further purification.

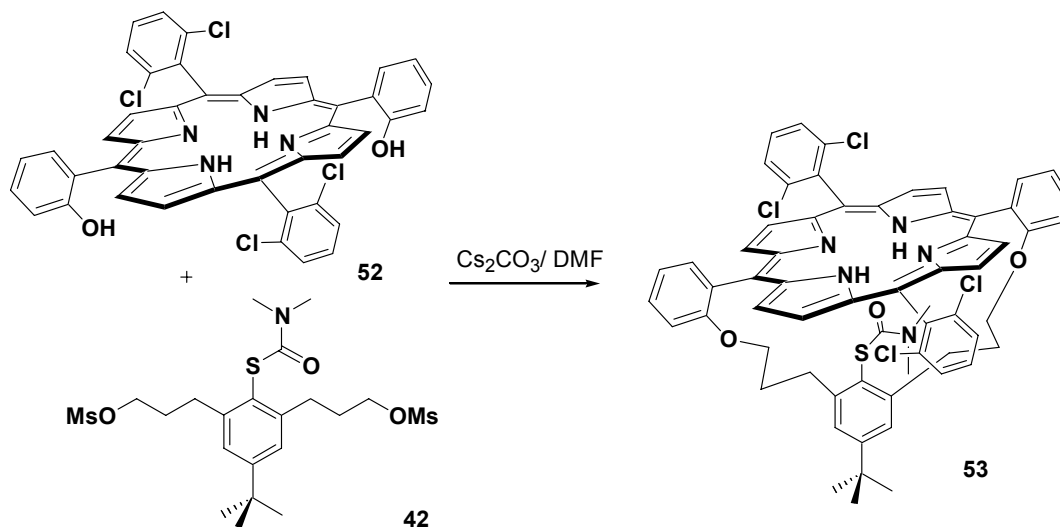
TLC (CH_2Cl_2): $R_f = 0.13$ $R_f = 0.65$

UV/Vis ($\text{CH}_2\text{Cl}_2 + 1\% \text{Et}_3\text{N}$): 418 (100, *Soret*); 512 (7).

$^1\text{H-NMR}$ (400 MHz, CDCl_3): 8.88 (*d*, $J = 4.8$, 4H, H-2, H-8, H-12, H-18); 8.69 (*d*, $J = 4.8$, 4H, H-3, H-7, H-13, H-17); 8.01-7.98 (*m*, 2H, H-6'); 7.82-7.79 (*m*, 4H, H-c, H-e); 7.74-7.68 (*m*, 4H, H-4', H-d); 7.35-7.31 (*m*, 4H, H-5', H-3'); -2.64 (*br s*, 2H, NH).

ESI-MS (CH_2Cl_2): *Positive ion mode*: 783.1 (100, $[\text{M}+\text{H}]^+$); *Negative ion mode*: 781.3 ($[\text{M}-\text{H}]^-$).

5,15-[[4-(t-butyl)-2-(N,N-dimethylcarbamoyl)thio-1,3-phenylene]-bis(tri-methyleneoxy)]-di-2,1-phenylene]-10,20-di-(2,6-dichlorophenyl)-porphyrin (53)



To a solution of 93.6 mg (119.3 μmol , 1 equiv.) of crude of bisphenol porphyrin **52**, in 75 ml of dry DMF was added 1.17 g (3.81 mmol, 32 equiv.) of Cs_2CO_3 which was previously dried at 100°C in high-vacuum overnight. The resulting suspension was heated to 60°C and stirred for 30 min. Then a solution of 86.7 mg (178 μmol , 1.5 equiv.) of dimesylate **42** in 20 ml of dry DMF was added *via* syringe pump within 4 h (velocity 0.3 mm/min) at 80°C . Stirring was continued for 30 min at 80°C after which the reaction mixture was cooled with an ice bath and the reaction was quenched with 40 ml of 1M HCl. For better phase separation 90 ml of CH_2Cl_2 was added. After phase separation the aqueous phase was extracted with two portions of 80 ml of CH_2Cl_2 . The combined organic layers were washed with two portions of 150 ml of saturated aqueous NaHCO_3 , water (100 ml) and brine (100ml), dried over Na_2SO_4 and concentrated under reduced pressure (silica gel, CH_2Cl_2 . The crude product was purified by flash chromatography + 1% NEt_3) which gave 202 mg (0.43 mmol, 45% in the last two step) of the bridged porphyrin **53** as purple solid.

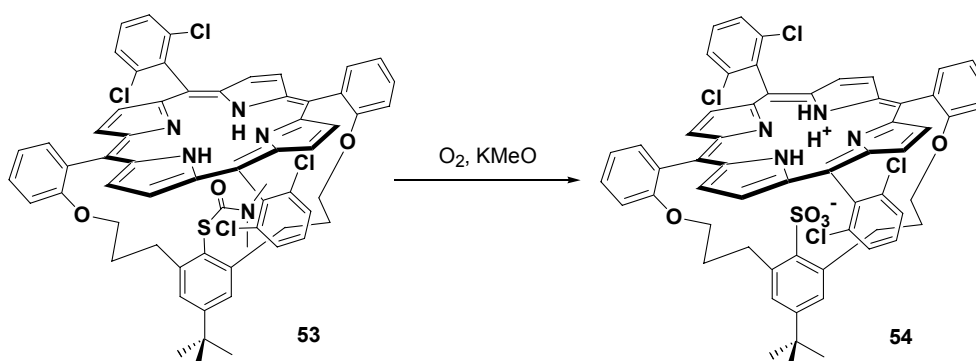
TLC (CH_2Cl_2 + 1% NEt_3): R_f = 0.34.

UV/Vis (CH_2Cl_2): 423 (100, *Soret*); 517 (9); 543 (2); 580 (4).

$^1\text{H-NMR}$ (400 MHz, CDCl_3): 9.07 (*d*, J = 4.73, 2H, pyrrylH); 8.70 (*d*, J = 3.98, 2H, pyrrylH); 8.68 (*d*, J = 4.02, 2H, pyrrylH); 8.64 (*dd*, J = 7.33, 1.72, 2H, H-6'); 8.40 (*d*, J = 4.69, 2H, PyH); 7.91 (*m*, 1H, H-d); 7.74 (*td*, J = 7.80, 1.75, 2H, H-4'); 7.69 (*m*, 1H, H-c); 7.60 (*m*, 1H, H-d); 7.55 (*m*, 1H, H-c); 7.51 (*td*, J = 7.5, 0.90, 2H, H-5'); 6.55 (*s*, 2H, H-3'', H-5''); 3.85 (*m*, 2H, H- α); 3.74 (*m*, 2H, H- α); 1.31 (*m*, 2H, H- γ); 1.13 (*s*, 9H, $\text{C}(\text{CH}_3)_3$); 0.96 (*m*, 2H, H- γ); 0.89 (*m*, 2H, H- β); 0.66 (*m*, 2H, H- β); 1.66 (*br s*, 3H, NCH_3); -1.45 (*br s*, 3H, NCH_3); -1.97 (*s*, 2H, *NH*).

ESI-MS (MeOH): *Positive ion mode*: 1139.2 ($[\text{M}+\text{K}]^+$); 1122.1 ($[\text{M}+\text{Na}]^+$); 1101.2 ($[\text{M}+\text{H}]^+$); *Negative ion mode* : 1098.0 ($[\text{M}-\text{H}]^-$)

[5,15-{[4-(*t*-butyl)-2-sulfate-1,3-phenylen]-bis(tri-methylenoxy)-diphenylen}-10,20-di-(2,6-dichlorophenyl)-porphyrin (54**)**



In a oxygen-enriched atmosphere 60 mg (1 equiv., 54.45 μmol) of porphyrin **53** was dissolved in 20 ml of dry dioxane. Then 228 mg of KOMe (60 equiv., 3.26 mmol) were added. The KOMe had been previously dried at 100°C overnight at the high vacuum pump. The dioxane solution was then bubbled with O₂ for 15 minutes and heated at 110-115°C. After half an hour its color turned dark green. The reaction mixture was left to reflux for 35 hours. Then it was cooled in an ice bath and quenched with 20 ml of saturated aqueous NH₄Cl. The obtained suspension was diluted with 15 ml of water and 20 ml of CH₂Cl₂. The layers were separated and the aqueous phase was extracted with two portions of 25 ml of CH₂Cl₂. The combined organic phases were washed with water (2×10 ml), dried over Na₂SO₄ and evaporated under reduced pressure. The crude product was filtered through a silica gel pad (CH₂Cl₂ + MeOH 2%) and it was afterwards purified by flash chromatography (silica gel, hexane/ethyl acetate: from 2:1 to 1:5). 18.3 mg of pure porphyrin **54** were obtained (31%).

TLC (hexane/ethyl acetate 1:5): R_f = 0.20

UV/Vis (MeOH): 420 (100, *Soret*); 516 (5).

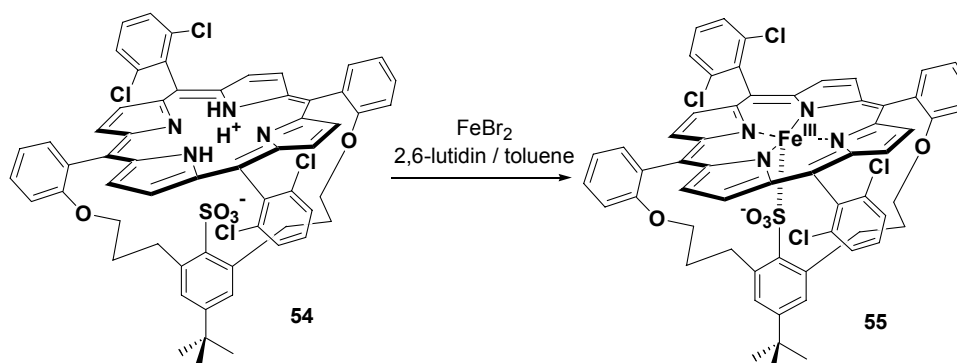
(CH₂Cl₂): 424 (100, *Soret*); 581 (6).

¹H-NMR (400 MHz, CDCl₃): 9.07 (*d*, J = 4.8, 4H, pyrrolyH); 8.72 (*d*, J = 4.8, 4H, pyrrolyH); 8.44 (*dd*, J = 7.32, 1.51, 2H, H-6'); 7.82-7.69 (*m*, 9H, arylH); 7.53-7.49 (*m*, 3H, arylH); 6.10 (*s*, 2H, H-3'', H-5''); 3.69 (*m*, 4H, H- α); 0.90-0.83 (*m*, 8H, H- β , H- γ); 0.93 (*s*, 9H, *tert*-Bu).

¹³C-NMR (125 MHz, CDCl₃): 230.8; 186.9; 160.5; 149.1; 144.8; 140.3; 138.9; 138.4; 137.4; 133.1; 132.3; 132.1; 131.1; 131.0; 129.9; 129.25; 128.32; 127.6; 123.5; 119.9; 113.7; 77.27; 77.22; 77.02; 76.76; 76.30; 68.99; 38.72; 31.93; 30.86; 29.71; 29.37; 28.93; 28.55; 23.14; 22.70; 14.13; 10.97; 2.03; 1.03; 0.01; -13.21.

ESI-MS (MeOH): *Positive ion mode*: 1101.1 ([*M*+Na]⁺); 1123.1([*M*-H+2Na]⁺). *Negative ion mode*: 1077.3 ([*M*-H]⁻).

[5,15-[[4-(*t*-butyl)-2-sulfate-1,3-phenylen]-bis(tri-methylenoxy)]-diphenylen}-10,20-di-(2,6-dichlorophenyl)-porphyrinate]iron(III) (55)



50 mg of porphyrin **54** (46.3 μmol , 1 equiv.) was dried for 24 hours at the Schlenk-line. Once three cycles of vacuum/argon were then completed under argon atmosphere, 25 mL of degassed, dry toluene were added. Subsequently an addition of 269 μL of 2,6-lutidine (2.315 mmol, 50 equiv., 291 mg) dissolved in 10 mL of toluene was done. The reaction mixture was refluxed for 10 minutes at 130°C and soon after ca 200 mg of FeBr₂ (926 μmol , 20 equiv.) were introduced into the flask and the solution was refluxed for another hour. After cooling down to room temperature the reaction mixture was poured over a celite pad and filtrated through it. The crude was purified by flash chromatography (silica gel, hexane/CH₂Cl₂/ethyl acetate 5:5:1). The porphyrin **55** was obtained in 90% yield.

TLC (hexane/CH₂Cl₂/ethyl acetate 5:5:1) $R_f = 0.35$

UV/Vis (CH₃Cl): 416 (100, Soret) and 467(6), 509 (10), 582 (2), 687 (2)

cw-EPR (toluene, 95 K): $g_{\perp} = 5.51$, $g_{\parallel} = 2.00$ (axial, high-spin).

ESI-MS (MeOH): *Positive ion mode*: 1130.1 ($[M+H]^+$); *Negative ion mode*: 1029.3 ($[M-H]^-$).

7.3. Porphyrin catalyzed oxidations

7.3.1. General procedure for catalytic oxidation of probe 45

In a 1.5 mL glass vial *trans*-1-benzyl-2-phenyl-cyclopropane **45** (5.0 mg, 24.0 μmol >99.5% GC-pure, 1 equiv.) was dissolved under argon in 250 μL of previously degassed and dried dichloromethane. The iron (III)-porphyrin **55** (0.70 mg, 0.60 μmol , 2.5mol %) and subsequently PhIO (5.3 mg, 24.0 μmol , 1 equiv.) were added under Argon. The reaction mixture was then stirred vigorously for 10 min at room temperature. After this time an aliquot was taken and centrifuged in order to precipitate the undissolved PhIO. The supernatant was directly by GC-FID. [Column Supelcowax; inlet temp. (230°C); detector temp. (265°C); constant pressure (50 kPa); temperature gradient : 100°(2 min); 100°-200° (10°/min); 200°C (5 min); 200°C - 260°C(10°C/ min); 260°C (5 min)]. Compounds were identified by distinct retention times: 13.3 min (**45**), 20.7 min (**57**), 22.7 min (**58-dia-1**), 22.9 min (**58-dia-2**), 23.6 (**61**) and by coinjection with the authentic material >99% GC-pure that were prepared according to slightly modified published procedure. The product distribution is shown in table 4

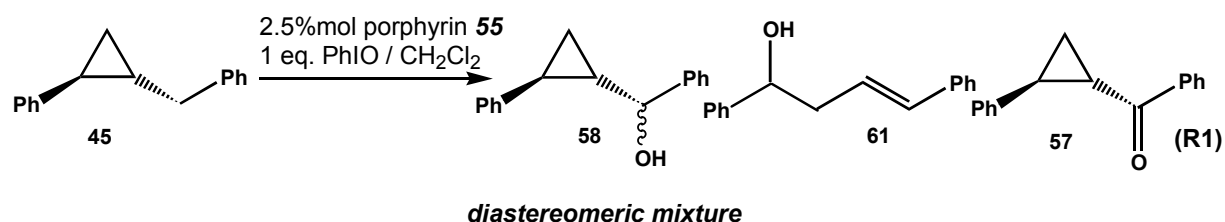


Table 4.

Reaction	57*	58-dia-1*	58-dia-2*	61*
R1	226.7	505.0	242.6	11.7
Chemical yield %	3.12	7.56	3.64	0.15
GC-retention time	20.7min.	22.7min.	22.9min.	23.6min.

* 1 unit corresponds to 0.013 μmol / mL (CH_2Cl_2)

Control Reaction R2 (without porphyrin 55)

The reaction of **45** with the oxidant was performed in exactly the same manner as shown above except that the synthetic porphyrin **55** was not used. In a 1.5 mL glass vial *trans*-1-benzyl-2-phenyl-cyclopropane **45** (5.0 mg, 24.0 μmol >99.5% GC-pure, 1 equiv.) was dissolved under argon in 250 μL of previously degassed and dried dichloromethane. Subsequently PhIO (5.3 mg, 24.0 μmol , 1 equiv.) was added under Argon. The reaction

mixture was then stirred vigorously for 10 min at room temperature. After this time an aliquot was taken and centrifuged in order to precipitate the undissolved PhIO. The supernatant was directly by GC-FID. The product distribution is shown below

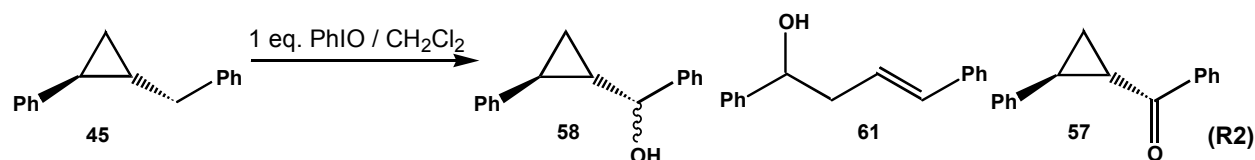


Table 5.

Reaction	57*	58-dia-1*	58-dia-2*	61*
R2	1.1	4.8	3.2	1
GC-retention time	20.7min.	22.7min.	22.9min.	23.6min.

* 1 unit corresponds to 0.013 $\mu\text{mol} / \text{mL}$ (CH_2Cl_2)

Control Reaction R3

In a 1.5 mL glass *vial* a degassed dichloromethane 9.72 mM solution of **58** (> 99.5% Gc-pure), the concentration equal to the amount of **58** produced in the reaction R1, was treated with iron (III)-porphyrin **55** (0.70 mg, 0.60 μmol , 2.5mol % with respect to **45** in R1) and subsequently PhIO (5.3 mg, 24.0 μmol , 1 equiv. with respect to **45** in R1) were added under Argon. The reaction mixture was then stirred vigorously for 10 min at room temperature. After this time an aliquot was taken and centrifuged in order to precipitate the undissolved PhIO. The supernatant was directly by GC-FID. The product distribution is shown in table 6:

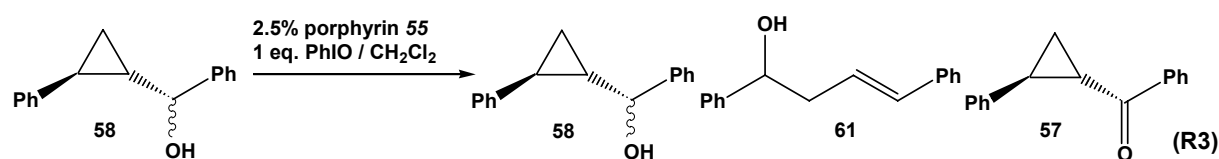


Table 6.

Reaction	57*	58-dia-1*	58-dia-2*	61*
R3	186.5	488	238.9	12.4
GC-retention time	20.7min.	22.7min.	22.9min.	23.6min.

* 1 unit corresponds to 0.013 $\mu\text{mol} / \text{mL}$ (CH_2Cl_2)

Control Reaction R4 (without porphyrin 55)

In a 1.5 mL glass *vial* a degassed dichloromethane 9.72 mM solution of **58**, the concentration equal to the amount of **58** produced in the reaction R1, was simply treated with PhIO (5.3 mg, 24.0 μmol , 1 equiv. with respect to **45** in R1) were added under Argon. The reaction mixture was then stirred vigorously for 10 min at room temperature. After this time an aliquot was taken and centrifuged in order to precipitate the undissolved PhIO. The supernatant was directly by GC-FID. The product distribution is shown in table 7:

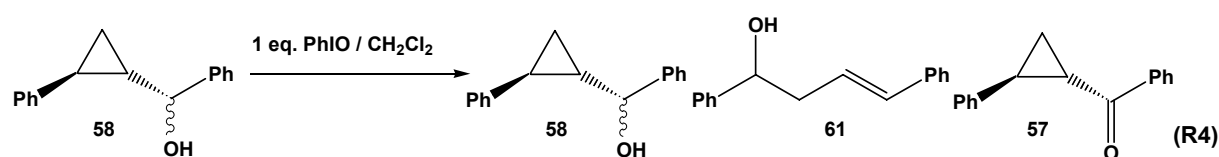
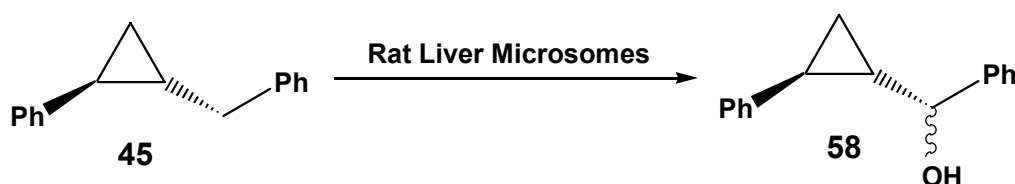


Table 7.

Reaction	57*	58-dia-1*	58-dia-2*	61*
R4	232.5	551.6	269	11.1
<i>GC-retention time</i>	<i>20.7min.</i>	<i>22.7min.</i>	<i>22.9min.</i>	<i>23.6min.</i>

* 1 unit corresponds to 0.013 $\mu\text{mol} / \text{mL}$ (CH_2Cl_2)

7.3.2 Qualitative Enzymatic Experiments with Rat Liver Microsomes, CYP 2B1 and CYP 2E1.**General Incubation Conditions****Rat Liver Microsome**

10 μL of MeCN 1 mM solution of substrate **45** inside an eppendorf tube was pre-heated at 37°C for 3 min in shaking water bath. Then the following reagents (see list 1) were added, mixed and incubated at 37°C for 1 h.

List 1:

25 μL of Rat Liver Microsome (1mg/mL of protein)

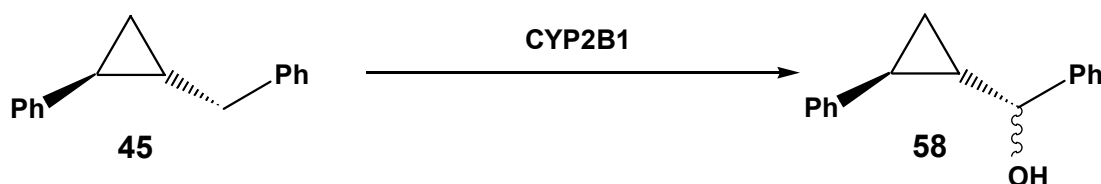
50 μL of solution R (1.3 mM NADP; 3.3 mM Glu-6-ph; 3.3 mM $\text{MgCl}_2 \cdot 6\text{H}_2\text{O}$)

50 μL of Glu-6-ph dehydrogenase (0.4 U/mL)

365 μL of potassium phosphate buffer (pH = 7.4).

The reaction was then quenched with 100 μL of dichloromethane, mixed using the vortex and finally was centrifugated. 80 μL of this organic phase was extracted and injected directly into the GC-FID. The Rat Liver Microsome resulted to be able to transform the substrate **45** into the alcohol **58**. No rearranged alcohol **61** and ketone **57** were detected.

CYP2B1



10 μL of MeCN 1 mM solution of substrate **45** inside an eppendorf tube was pre-heated at 37°C for 3 min in shaking water bath. Then the following reagents (see list 2) were added, mixed and incubated at 37° for 1 h.

List 2:

50 μL of CYP2B1 (50 pmol in 0.5 mL)

50 μL of solution R (1.3 mM NADP; 3.3 mM Glu-6-ph; 3.3 mM $\text{MgCl}_2 \cdot 6\text{H}_2\text{O}$)

50 μL of Glu-6-ph dehydrogenase (0.4 U/mL)

365 μL of potassium phosphate buffer (pH = 7.4).

The reaction was then quenched with 100 μL of dichloromethane, mixed using the vortex and finally was centrifugated. 80 μL of this organic phase was extracted and injected directly into the GC-FID. The CYP2B1 resulted to be able to transform the substrate **45** into the alcohol **58**. No rearranged alcohol **61** and ketone **57** were detected.

CYP2E1



10 μL of MeCN 1 mM solution of substrate **45** inside an eppendorf tube was pre-heated at 37°C for 3 min in shaking water bath. Then the following reagents (see list 3) were added, mixed and incubated at 37°C for 1 h.

List 3:

50 μL of CYP 2E1 (100 pmol in 0.5 mL) + 50 μL buffer solution.

50 μL of solution R (1.3 mM NADP; 3.3 mM Glu-6-ph; 3.3 mM $\text{MgCl}_2 \cdot 6\text{H}_2\text{O}$)

50 μL of Glu-6-ph dehydrogenase (0.4 U/mL)

365 μL of potassium phosphate buffer (pH = 7.4).

The reaction was then quenched with 100 μL of dichloromethane, mixed using the vortex and finally was centrifugated. 80 μL of this organic phase was extracted and injected directly into the GC-FID. CYP2E1 could not metabolize the substrate **45**.

7.3.3. General procedure for catalytic oxidation of probe **10**

In a 1.5 mL glass vial *trans*-2-phenyl-methylcyclopropane **10** (3.3 mg, 25.0 μmol >99.5% GC-pure, 1 equiv.) was dissolved under argon in 250 μL of previously degassed and dried dichloromethane. The iron (III)-porphyrin **55** (0.75 mg, 0.650 μmol , 2.5mol %) and subsequently PhIO (5.5 mg, 25.0 μmol , 1 equiv.) were added under Argon. The reaction mixture was then stirred vigorously for 10 min at room temperature. After this time an aliquot was taken and centrifuged in order to precipitate the undissolved PhIO. The supernatant was directly by GC-FID. [Column Supelcowax; inlet temp. (230°C); detector temp. (265°C); constant pressure (50 kPa); temperature gradient : 70°C (2 min); 70°C -200°C (10°C/ min) ; 200°C (10 min); 200°C -250°C (10°C /min); 250°C (5 min)]. Compounds were identified by distinct retention times: 3.9 min (**10**), 10.3 min (**66**), 13.0 min (**63**), 14.9 (**70**) and by coinjection with the authentic material >99% GC-pure that were prepared according to slightly modified published procedure. Oxidation experiments were repeated four times and standard deviation of +/- 5% was determined for product ratios. The product distribution is shown in table 8:

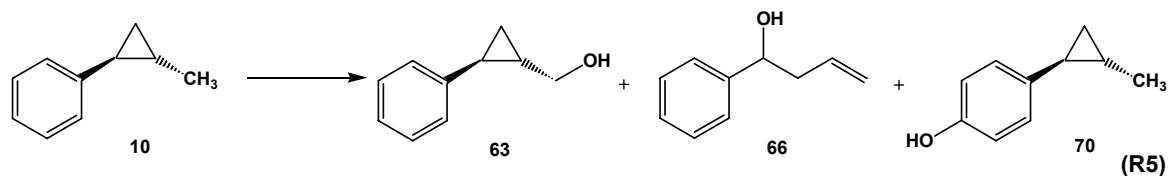


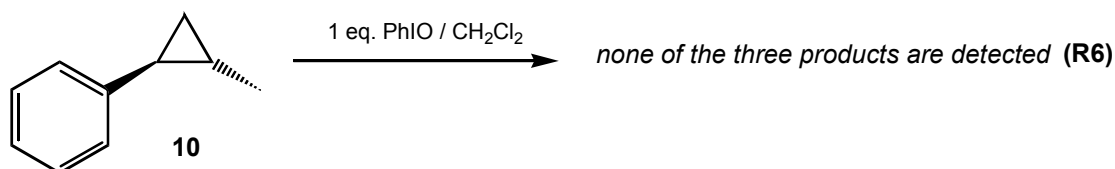
Table 8.

Reaction	66*	63*	70*
R5	1	9	22
Chemical yield %	0.003	0.027	0.066
Retention time	10.37 min.	13.02 min.	14.91 min.

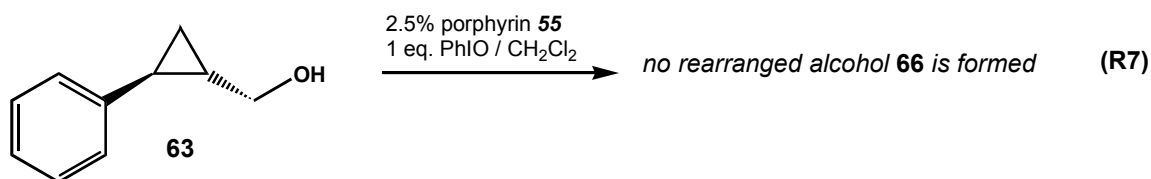
* 1 unit corresponds to 0.003 $\mu\text{mol} / \text{mL}$ (CH_2Cl_2)

Ratio $[\text{70} / (\text{66} + \text{63})] = 2.2$ and Ratio $(\text{63} / \text{66}) = 9$

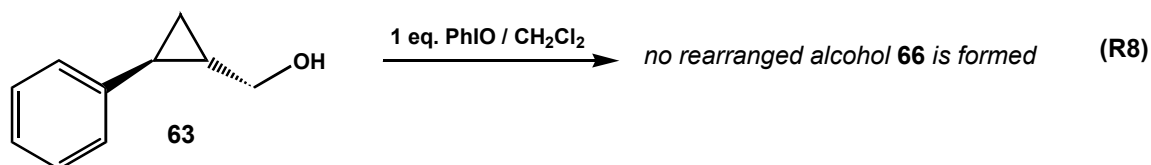
Control Reaction R6 (without porphyrin 55)



The reaction of **10** with the oxidant was performed in exactly the same manner as shown above except that the synthetic porphyrin **55** was not used. In a 1.5 mL glass vial *trans*-2-phenyl-methylcyclopropane **10** (3.3 mg, 25.0 μmol >99.5% GC-pure, 1 equiv.) was dissolved under argon in 250 μL of previously degassed and dried dichloromethane. PhIO (5.5 mg, 25.0 μmol , 1 equiv.) was added under Argon. The reaction mixture was then stirred vigorously for 10 min at room temperature. After this time an aliquot was taken and centrifuged in order to precipitate the undissolved PhIO. The supernatant was directly by GC-FID. No products were detected.

Control Reaction R7

In a 1.5 mL glass *vial* a degassed dichloromethane 0.67 mM solution of **63**, the concentration equal to 25-fold the amount of **63** produced in the reaction R5, was treated with the iron (III)-porphyrin **55** (0.75 mg, 0.650 μ mol, 2.5mol % respect to **10** in R5) and subsequently with PhIO (5.5 mg, 25.0 μ mol, 1 equiv. respect to **10** in R5) under Argon. The reaction mixture was then stirred vigorously for 10 min at room temperature. After this time an aliquot was taken and centrifuged in order to precipitate the undissolved PhIO. The supernatant was directly by GC-FID. The alcohol **63** does not rearrange to **66** in the presence of the porphyrin %5 together with PhIO.

Control Reaction R8 (without porphyrin 55).

In a 1.5 mL glass *vial* a degassed dichloromethane 0.67 mM solution of **63**, the concentration equal to 25-fold the amount of **63** produced in the reaction R5, was simply treated with PhIO (5.5 mg, 25.0 μ mol, 1 equiv. respect to **10** in R5) under Argon. The reaction mixture was then stirred vigorously for 10 min at room temperature. After this time an aliquot was taken and centrifuged in order to precipitate the undissolved PhIO. The supernatant was directly by GC-FID. The alcohol **63** does not rearrange to **66** in the presence of the only PhIO.

APPENDIX

8. References

- [1] Rietjens, I. M. C. M.; Osman, A. M.; Veeger, C.; Zakharieva, O.; Antony, J.; Grodzicki, M.; Trautwein, A. X., *JBIC, Journal of Biological Inorganic Chemistry* **1996**, 1, (4), 372-376.
- [2] Mansuy, D.; Battioni, P., *Porphyrin Handbook* **2000**, 4, 1-15.
- [3] Otey Christopher, R., *Methods in molecular biology (Clifton, N.J.)* **2003**, 230, 137-9.
- [4] Chothia, C.; Lesk, A. M., *EMBO journal* **1986**, 5, (4), 823-6.
- [5] Lewis, D. F. V.; Wiseman, A., *Enzyme and Microbial Technology* **2005**, 36, (4), 377-384.
- [6] Williams, P. A.; Cosme, J.; Sridhar, V.; Johnson, E. F.; McRee, D. E., *Journal of Inorganic Biochemistry* **2000**, 81, (3), 183-190.
- [7] Kirton Stewart, B.; Kemp Carol, A.; Tomkinson Nicholas, P.; St-Gallay, S.; Sutcliffe Michael, J., *Proteins* **2002**, 49, (2), 216-31.
- [8] Williams, P. A.; Cosme, J.; Ward, A.; Angove, H. C.; Vinkovic, D. M.; Jhoti, H., *Nature (London, United Kingdom)* **2003**, 424, (6947), 464-468.
- [9] Wester Michael, R.; Yano Jason, K.; Schoch Guillaume, A.; Yang, C.; Griffin Keith, J.; Stout, C. D.; Johnson Eric, F., *Journal of biological chemistry* **2004**, 279, (34), 35630-7.
- [10] Schoch, G. A.; Yano, J. K.; Wester, M. R.; Griffin, K. J.; Stout, C. D.; Johnson, E. F., *Journal of Biological Chemistry* **2004**, 279, (10), 9497-9503.
- [11] Yano, J. K.; Wester, M. R.; Schoch, G. A.; Griffin, K. J.; Stout, C. D.; Johnson, E. F., *Journal of Biological Chemistry* **2004**, 279, (37), 38091-38094.
- [12] Williams, P. A.; Cosme, J.; Vinkovic, D. M.; Ward, A.; Angove, H. C.; Day, P. J.; Vonnrhein, C.; Tickle, I. J.; Jhoti, H., *Science (Washington, DC, United States)* **2004**, 305, (5684), 683-686.
- [13] Scott Emily, E.; Halpert James, R., *Trends in biochemical sciences* **2005**, 30, (1), 5-7.
- [14] Sundaramoorthy, M.; Ternier, J.; Poulos, T. L., *Chemistry & biology* **1998**, 5, (9), 461-73.
- [15] Sundaramoorthy, M.; Ternier, J.; Poulos, T. L., *Structure (London)* **1995**, 3, (12), 1367-77.
- [16] Crane, B. R.; Arvai, A. S.; Gachhui, R.; Wu, C.; Ghosh, D. K.; Getzoff, E. D.; Steuhr, D. J.; Tainer, J. A., *Science (Washington, D. C.)* **1997**, 278, (5337), 425-431.
- [17] Ortiz de Montellano, P. R.; Editor, *Cytochrome P450: Structure, Mechanism, and Biochemistry, Second Edition*. ed.; 1995; 'Vol.' p 630 pp (approx).
- [18] Kupfer, R.; Liu, S. Y.; Allentoff, A. J.; Thompson, J. A., *Biochemistry* **2001**, 40, (38), 11490-501.
- [19] He, K.; Bornheim, L. M.; Falick, A. M.; Maltby, D.; Yin, H.; Correia, M. A., *Biochemistry* **1998**, 37, (50), 17448-57.
- [20] Li, S.; Wackett, L. P., *Biochemistry* **1993**, 32, (36), 9355-61.
- [21] Castro, C. E.; Wade, R. S.; Belsler, N. O., *Biochemistry* **1985**, 24, (1), 204-10.
- [22] Nakahara, K.; Tanimoto, T.; Hatano, K.; Usuda, K.; Shoun, H., *Journal of Biological Chemistry* **1993**, 268, (11), 8350-5.
- [23] Ioannides, C.; Lewis, D. F. V., *Current Topics in Medicinal Chemistry (Sharjah, United Arab Emirates)* **2004**, 4, (16), 1767-1788.
- [24] Kemp, C. A.; Marechal, J.-D.; Sutcliffe, M. J., *Archives of Biochemistry and Biophysics* **2005**, 433, (2), 361-368

- [25] De Mot, R.; Parret, A. H. A., *Trends in Microbiology* **2002**, 10, (11), 502-508.
- [26] Williams, P. A.; Cosme, J.; Sridhar, V.; Johnson, E. F.; McRee, D. E., *Molecular Cell* **2000**, 5, (1), 121-131.
- [27] Gutierrez, A.; Grunau, A.; Paine, M.; Munro, A. W.; Wolf, C. R.; Roberts, G. C. K.; Scrutton, N. S., *Biochemical Society transactions* **2003**, 31, (Pt 3), 497-501.
- [28] Porter, T. D., *Journal of Biochemical and Molecular Toxicology* **2002**, 16, (6), 311-316.
- [29] Koljak, R.; Boutaud, O.; Shieh, B. H.; Samel, N.; Brash, A. R., *Science* **1997**, 277, (5334), 1994-6.
- [30] Kobori, T.; Sasaki, H.; Lee, W. C.; Zenno, S.; Saigo, K.; Murphy, M. E. P.; Tanokura, M., *Journal of Biological Chemistry* **2001**, 276, (4), 2816-2823.
- [31] Gonzalez, F. J., *Handbook of Experimental Pharmacology* **1993**, 105, (Cytochrome P450), 211-19.
- [32] Oscarson, M.; Ingelman-Sundberg, M., *Drug Metabolism and Pharmacokinetics* **2002**, 17, (6), 491-495.
- [33] Nelson, D. R., *Archives of Biochemistry and Biophysics* **1999**, 369, (1), 1-10.
- [34] Domanski, T. L.; Halpert, J. R., *Current Drug Metabolism* **2001**, 2, (2), 117-137.
- [35] Dai, R.; Pincus, M. R.; Friedman, F. K., *Journal of Protein Chemistry* **1998**, 17, (2), 121-129.
- [36] Kent, U. M.; Jushchyshyn, M. I.; Hollenberg, P. F., *Current Drug Metabolism* **2001**, 2, (3), 215-243.
- [37] Spatzenegger, M.; Wang, Q.; He, Y. Q.; Wester, M. R.; Johnson, E. F.; Halpert, J. R., *Molecular Pharmacology* **2001**, 59, (3), 475-485.
- [38] Wang, Q.; Halpert James, R., *Drug metabolism and disposition: biological fate of chemicals* **2002**, 30, (1), 86-95.
- [39] Morgan, E. T.; Koop, D. R.; Coon, M. J., *Biochemical and Biophysical Research Communications* **1983**, 112, (1), 8-13.
- [40] Koop, D. R.; Morgan, E. T.; Tarr, G. E.; Coon, M. J., *Journal of biological chemistry* **1982**, 257, (14), 8472-80.
- [41] Morgan, E. T.; Koop, D. R.; Coon, M. J., *Journal of biological chemistry* **1982**, 257, (23), 13951-7.
- [42] Lieber, C. S.; DeCarli, L. M., *Science (Washington, DC, United States)* **1968**, 162, (3856), 917-18.
- [43] Koop, D. R.; Coon, M. J., *Alcoholism, clinical and experimental research* **1986**, 10, (6 Suppl), 44S-49S.
- [44] Groves, J. T., *Journal of Chemical Education* **1985**, 62, (11), 928-31.
- [45] Ortiz de Montellano Paul, R.; De Voss James, J., *Natural product reports* **2002**, 19, (4), 477-93.
- [46] Gonzalez, F. J.; Gelboin, H. V., *Drug Metabolism Reviews* **1994**, 26, (1-2), 165-83.
- [47] Sharrock, M.; Munck, E.; Debrunner, P. G.; Marshall, V.; Lipscomb, J. D.; Gunsalus, I. C., *Biochemistry* **1973**, 12, (2), 258-65.
- [48] Bangcharoenpaupong, O.; Rizos, A. K.; Champion, P. M.; Jollie, D.; Sligar, S. G., *Journal of Biological Chemistry* **1986**, 261, (18), 8089-92.
- [49] Schlichting, I.; Berendzen, J.; Chu, K.; Stock, A. M.; Maves, S. A.; Benson, D. E.; Sweet, R. M.; Ringe, D.; Petsko, G. A.; Sligar, S. G., *Science (Washington, D. C.)* **2000**, 287, (5458), 1615-1622.
- [50] Brewer, C. B.; Peterson, J. A., *Journal of biological chemistry* **1988**, 263, (2), 791-8.

- [51] Hiner, A. N. P.; Raven, E. L.; Thorneley, R. N. F.; Garcia-Canovas, F.; Rodriguez-Lopez, J. N., *Journal of Inorganic Biochemistry* **2002**, 91, (1), 27-34.
- [52] Sono, M.; Roach, M. P.; Coulter, E. D.; Dawson, J. H., *Chemical Reviews (Washington, D. C.)* **1996**, 96, (7), 2841-2887.
- [53] Poulos, T. L., *JBIC, Journal of Biological Inorganic Chemistry* **1996**, 1, (4), 356-359.
- [54] Ogliaro, F.; de Visser, S. P.; Shaik, S., *Journal of Inorganic Biochemistry* **2002**, 91, (4), 554-567.
- [55] Vidakovic, M.; Sligar, S. G.; Li, H.; Poulos, T. L., *Biochemistry* **1998**, 37, (26), 9211-9.
- [56] Benson, D. E.; Suslick, K. S.; Sligar, S. G., *Biochemistry* **1997**, 36, (17), 5104-5107.
- [57] Dawson, J. H., *Science (Washington, DC, United States)* **1988**, 240, (4851), 433-9.
- [58] Davydov, R.; Makris, T. M.; Kofman, V.; Werst, D. E.; Sligar, S. G.; Hoffman, B. M., *Journal of the American Chemical Society* **2001**, 123, (7), 1403-1415.
- [59] Denisov, I. G.; Makris, T. M.; Sligar, S. G., *Journal of Biological Chemistry* **2001**, 276, (15), 11648-11652.
- [60] Kellner David, G.; Hung, S.-C.; Weiss Kara, E.; Sligar Stephen, G., *Journal of biological chemistry* **2002**, 277, (12), 9641-4.
- [61] Davydov, R.; Kappl, R.; Huttermann, J.; Peterson, J. A., *FEBS letters* **1991**, 295, (1-3), 113-5.
- [62] Denisov, I. G.; Hung, S. C.; Weiss, K. E.; McLean, M. A.; Shiro, Y.; Park, S. Y.; Champion, P. M.; Sligar, S. G., *Journal of inorganic biochemistry* **2001**, 87, (4), 215-26.
- [63] Denisov, I. G.; Makris, T. M.; Sligar, S. G., *Journal of Biological Chemistry* **2002**, 277, (45), 42706-42710.
- [64] Jin, S.; Makris, T. M.; Bryson, T. A.; Sligar, S. G.; Dawson, J. H., *Journal of the American Chemical Society* **2003**, 125, (12), 3406-3407.
- [65] Hishiki, T.; Shimada, H.; Nagano, S.; Egawa, T.; Kanamori, Y.; Makino, R.; Park, S. Y.; Adachi, S.; Shiro, Y.; Ishimura, Y., *Journal of biochemistry* **2000**, 128, (6), 965-74.
- [66] Toy, P. H.; Newcomb, M.; Coon, M. J.; Vaz, A. D. N., *Journal of the American Chemical Society* **1998**, 120, (37), 9718-9719.
- [67] Poulos, T. L.; Finzel, B. C.; Howard, A. J., *Journal of molecular biology* **1987**, 195, (3), 687-700.
- [68] Martinis, S. A.; Atkins, W. M.; Stayton, P. S.; Sligar, S. G., *Journal of the American Chemical Society* **1989**, 111, (26), 9252-3.
- [69] Imai, M.; Shimada, H.; Watanabe, Y.; Matsushima-Hibiya, Y.; Makino, R.; Koga, H.; Horiuchi, T.; Ishimura, Y., *Proceedings of the National Academy of Sciences of the United States of America* **1989**, 86, (20), 7823-7.
- [70] Hjelmeland, L. M.; Aronow, L.; Trudell, J. R., *Biochemical and Biophysical Research Communications* **1977**, 76, (2), 541-9.
- [71] Groves, J. T.; McClusky, G. A.; White, R. E.; Coon, M. J., *Biochemical and Biophysical Research Communications* **1978**, 81, (1), 154-60.
- [72] Gelb, M. H.; Heimbrook, D. C.; Malkonen, P.; Sligar, S. G., *Biochemistry* **1982**, 21, (2), 370-7.
- [73] Ogliaro, F.; Harris, N.; Cohen, S.; Filatov, M.; de Visser, S. P.; Shaik, S., *Journal of the American Chemical Society* **2000**, 122, (37), 8977-8989.
- [74] Groves, J. T.; Adhyam, D. V., *Journal of the American Chemical Society* **1984**, 106, (7), 2177-81.

- [75] White, R. E.; Miller, J. P.; Favreau, L. V.; Bhattacharyya, A., *Journal of the American Chemical Society* **1986**, 108, (19), 6024-31.
- [76] Manchester, J. I.; Dinnocenzo, J. P.; Higgins, L. A.; Jones, J. P., *Journal of the American Chemical Society* **1997**, 119, (21), 5069-5070.
- [77] Goto, Y.; Watanabe, Y.; Fukuzumi, S.; Jones, J. P.; Dinnocenzo, J. P., *Journal of the American Chemical Society* **1998**, 120, (41), 10762-10763.
- [78] White, R. E.; Groves, J. T.; McClusky, G. A., *Acta Biologica et Medica Germanica* **1979**, 38, (2-3), 475-82.
- [79] Sligar, S. G.; Gelb, M. H.; Heimbrook, D. C., *Xenobiotica* **1984**, 14, (1-2), 63-86.
- [80] Peter, M. G.; Woggon, W. D.; Schlatter, C.; Schmid, H., *Helvetica chimica acta* **1977**, 60, (3), 844-73.
- [81] Bowry, V. W.; Luszytk, J.; Ingold, K. U., *Journal of the American Chemical Society* **1991**, 113, (15), 5687-98.
- [82] Houghton, J. D.; Beddows, S. E.; Suckling, K. E.; Brown, L.; Suckling, C. J., *Tetrahedron Letters* **1986**, 27, (38), 4655-8.
- [83] Ortiz de Montellano, P. R.; Stearns, R. A., *Journal of the American Chemical Society* **1987**, 109, (11), 3415-20.
- [84] Jamieson, C.; Walton, J. C.; Ingold, K. U., *Journal of the Chemical Society, Perkin Transactions 2: Physical Organic Chemistry (1972-1999)* **1980**, (9), 1366-71.
- [85] Bowry, V. W.; Ingold, K. U., *Journal of the American Chemical Society* **1991**, 113, (15), 5699-707.
- [86] Auclair, K.; Hu, Z.; Little, D. M.; Ortiz de Montellano, P. R.; Groves, J. T., *Journal of the American Chemical Society* **2002**, 124, (21), 6020-6027.
- [87] Choi, S.-Y.; Toy, P. H.; Newcomb, M., *Journal of Organic Chemistry* **1998**, 63, (23), 8609-8613.
- [88] Atkinson, J. K.; Ingold, K. U., *Biochemistry* **1993**, 32, (35), 9209-14.
- [89] Liu, K. E.; Johnson, C. C.; Newcomb, M.; Lippard, S. J., *Journal of the American Chemical Society* **1993**, 115, (3), 939-47.
- [90] Atkinson, J. K.; Hollenberg, P. F.; Ingold, K. U.; Johnson, C. C.; Le Tadic, M.-H.; Newcomb, M.; Putt, D. A., *Biochemistry* **1994**, 33, (35), 10630-7.
- [91] Martin-Esker, A. A.; Johnson, C. C.; Horner, J. H.; Newcomb, M., *Journal of the American Chemical Society* **1994**, 116, (20), 9174-81.
- [92] Newcomb, M.; Le Tadic, M.-H.; Putt, D. A.; Hollenberg, P. F., *Journal of the American Chemical Society* **1995**, 117, (11), 3312-13.
- [93] Newcomb, M.; Hollenberg Paul, F.; Coon Minor, J., *Archives of biochemistry and biophysics* **2003**, 409, (1), 72-9.
- [94] Newcomb, M.; Toy, P. H., *Accounts of Chemical Research* **2000**, 33, (7), 449-455.
- [95] Newcomb, M.; Aebisher, D.; Shen, R.; Chandrasena, R. E. P.; Hollenberg, P. F.; Coon, M. J., *Journal of the American Chemical Society* **2003**, 125, (20), 6064-6065.
- [96] Newcomb, M.; Chestney, D. L., *Journal of the American Chemical Society* **1994**, 116, (21), 9753-4.
- [97] Tadic-Biadatti, M.-H. L.; Newcomb, M., *Journal of the Chemical Society, Perkin Transactions 2: Physical Organic Chemistry* **1996**, (7), 1467-1473.

- [98] Newcomb, M.; Shen, R.; Choi, S.-Y.; Toy, P. H.; Hollenberg, P. F.; Vaz, A. D. N.; Coon, M. J., *Journal of the American Chemical Society* **2000**, 122, (12), 2677-2686.
- [99] Newcomb, M.; Le Tadic-Biadatti, M.-H.; Chestney, D. L.; Roberts, E. S.; Hollenberg, P. F., *Journal of the American Chemical Society* **1995**, 117, (49), 12085-91.
- [100] Ogliaro, F.; de Visser, S. P.; Cohen, S.; Sharma, P. K.; Shaik, S., *Journal of the American Chemical Society* **2002**, 124, (11), 2806-2817.
- [101] Loew, G. H.; Harris, D. L., *Chemical Reviews (Washington, D. C.)* **2000**, 100, (2), 407-419.
- [102] Kamachi, T.; Yoshizawa, K., *Journal of the American Chemical Society* **2003**, 125, (15), 4652-61.
- [103] Ruzicka, F.; Huang, D. S.; Donnelly, M. I.; Frey, P. A., *Biochemistry* **1990**, 29, (7), 1696-700.
- [104] Rollick, K. L.; Kochi, J. K., *Journal of the American Chemical Society* **1982**, 104, (5), 1319-30.
- [105] Kimata, Y.; Shimada, H.; Hirose, T.; Ishimura, Y., *Biochemical and biophysical research communications* **1995**, 208, (1), 96-102.
- [106] Vaz, A. D. N.; McGinnity, D. F.; Coon, M. J., *Proceedings of the National Academy of Sciences of the United States of America* **1998**, 95, (7), 3555-3560.
- [107] Volz, T. J.; Rock, D. A.; Jones, J. P., *Journal of the American Chemical Society* **2002**, 124, (33), 9724-9725.
- [108] Guengerich, F. P.; Vaz, A. D. N.; Raner, G. N.; Pernecky, S. J.; Coon, M. J., *Molecular Pharmacology* **1997**, 51, (1), 147-151.
- [109] Lichtenberger, F.; Nastainczyk, W.; Ullrich, V., *Biochemical and Biophysical Research Communications* **1976**, 70, (3), 939-46.
- [110] Chandrasena, R. E. P.; Vatsis, K. P.; Coon, M. J.; Hollenberg, P. F.; Newcomb, M., *Journal of the American Chemical Society* **2004**, 126, (1), 115-126.
- [111] Siegbahn, P. E. M.; Blomberg, M. R. A., *Chemical Reviews (Washington, D. C.)* **2000**, 100, (2), 421-437.
- [112] Shaik, S.; Cohen, S.; de Visser, S. P.; Sharma, P. K.; Kumar, D.; Kozuch, S.; Ogliaro, F.; Danovich, D., *European Journal of Inorganic Chemistry* **2004**, (2), 207-226.
- [113] Schoeneboom, J. C.; Cohen, S.; Lin, H.; Shaik, S.; Thiel, W., *Journal of the American Chemical Society* **2004**, 126, (12), 4017-4034.
- [114] Shaik, S.; de Visser Samuel, P.; Ogliaro, F.; Schwarz, H.; Schroder, D., *Current opinion in chemical biology* **2002**, 6, (5), 556-67.
- [115] de Visser, S. P.; Ogliaro, F.; Sharma, P. K.; Shaik, S., *Angewandte Chemie, International Edition* **2002**, 41, (11), 1947-1951.
- [116] Ogliaro, F.; Cohen, S.; Filatov, M.; Harris, N.; Shaik, S., *Angewandte Chemie, International Edition* **2000**, 39, (21), 3851-3855.
- [117] Ogliaro, F.; De Visser, S. P.; Groves, J. T.; Shaik, S., *Angewandte Chemie, International Edition* **2001**, 40, (15), 2874-2878.
- [118] de Visser Sam, P.; Ogliaro, F.; Sharma Pankaz, K.; Shaik, S., *Journal of the American Chemical Society* **2002**, 124, (39), 11809-26.
- [119] de Visser, S. P.; Ogliaro, F.; Harris, N.; Shaik, S., *Journal of the American Chemical Society* **2001**, 123, (13), 3037-3047.

- [120] Kumar, D.; de Visser, S. P.; Sharma, P. K.; Cohen, S.; Shaik, S., *Journal of the American Chemical Society* **2004**, 126, (6), 1907-1920.
- [121] Audergon, C.; Iyer, K. R.; Jones, J. P.; Darbyshire, J. F.; Trager, W. F., *Journal of the American Chemical Society* **1999**, 121, (1), 41-47.
- [122] Jones, J. P.; Korzekwa, K. R.; Rettie, A. E.; Trager, W. F., *Journal of the American Chemical Society* **1986**, 108, (22), 7074-8.
- [123] Keller, U., *Nature (London, United Kingdom)* **2003**, 424, (6950), 831-838.
- [124] Bhattacharjee, Y., *Nature* **2001**, 412, (6846), 474-6.
- [125] Stolow, A.; Jonas, D. M., *Science (Washington, DC, United States)* **2004**, 305, (5690), 1575-1577.
- [126] Zewail, A. H., *Angewandte Chemie, International Edition* **2000**, 39, (15), 2586-2631.
- [127] De Feyter, S.; Diau, E. W. G.; Zewail, A. H., *Angewandte Chemie, International Edition* **2000**, 39, (1), 260-263.
- [128] Diau, E. W. G.; Kotting, C.; Zewail, A. H., *ChemPhysChem* **2001**, 2, (5), 273-293.
- [129] Diau, E. W. G.; Kotting, C.; Zewail, A. H., *ChemPhysChem* **2001**, 2, (5), 294-309.
- [130] Diau Eric, W. G.; Kotting, C.; Solling Theis, I.; Zewail Ahmed, H., *Chemphyschem : a European journal of chemical physics and physical chemistry* **2002**, 3, (1), 57-78.
- [131] Solling, T. I.; Diau, E. W. G.; Kotting, C.; De Feyter, S.; Zewail, A. H., *ChemPhysChem* **2002**, 3, (1), 79-97.
- [132] Engel, P. S.; He, S.-L.; Banks, J. T.; Ingold, K. U.; Luszyk, J., *Journal of Organic Chemistry* **1997**, 62, (5), 1210-1214.
- [133] Horner, J. H.; Taxil, E.; Newcomb, M., *Journal of the American Chemical Society* **2002**, 124, (19), 5402-5410.
- [134] Horner, J. H.; Newcomb, M., *Journal of the American Chemical Society* **2001**, 123, (18), 4364-4365.
- [135] Choi, S.-Y.; Horner, J. H.; Newcomb, M., *Journal of Organic Chemistry* **2000**, 65, (14), 4447-4449.
- [136] Newcomb, M.; Choi, S.-Y.; Horner, J. H., *Journal of Organic Chemistry* **1999**, 64, (4), 1225-1231.
- [137] Horner, J. H.; Tanaka, N.; Newcomb, M., *Journal of the American Chemical Society* **1998**, 120, (40), 10379-10390.
- [138] Kadish, K. M.; Smith, K. M.; Guillard, R.; Editors, *The Porphyrin Handbook; Volume 10, Database of Tetrapyrrole Crystal Structure Determination*. ed.; 2000; 'Vol.' p 254 pp.
- [139] Smeets, S.; Asokan, C. V.; Motmans, F.; Dehaen, W., *Journal of Organic Chemistry* **2000**, 65, (18), 5882-5885.
- [140] Rose, E.; Quelquejeu, M.; Kossanyi, A.; Boitrel, B., *Coordination Chemistry Reviews* **1998**, 178-180, (Pt. 2), 1407-1431.
- [141] Meunier, B., *Chemical Reviews (Washington, DC, United States)* **1992**, 92, (6), 1411-56.
- [142] Traylor, P. S.; Dolphin, D.; Traylor, T. G., *Journal of the Chemical Society, Chemical Communications* **1984**, (5), 279-80.
- [143] Ostovic, D.; Bruce, T. C., *Journal of the American Chemical Society* **1989**, 111, (17), 6511-17.
- [144] Porhiel, E.; Bondon, A.; Leroy, J., *Tetrahedron Letters* **1998**, 39, (27), 4829-4830.

- [145] Lindsay Smith, J. R.; Reginato, G., *Organic & Biomolecular Chemistry* **2003**, 1, (14), 2543-2549.
- [146] Birnbaum, E. R.; Grinstaff, M. W.; Labinger, J. A.; Bercaw, J. E.; Gray, H. B., *Journal of Molecular Catalysis A: Chemical* **1995**, 104, (2), 119-22.
- [147] Wagenknecht, H.-A.; Woggon, W.-D., *Angewandte Chemie, International Edition in English* **1997**, 36, (4), 390-392.
- [148] Staeubli, B.; Fretz, H.; Piantini, U.; Woggon, W. D., *Helvetica Chimica Acta* **1987**, 70, (4), 1173-93.
- [149] Goodwin, J.; Kurtikyan, T.; Standard, J.; Walsh, R.; Zheng, B.; Parmley, D.; Howard, J.; Green, S.; Mardyukov, A.; Przybyla, D. E., *Inorganic Chemistry* **2005**, 44, (7), 2215-2223.
- [150] Aissaoui, H.; Ghirlanda, S.; Gmuer, C.; Woggon, W.-D., *Journal of Molecular Catalysis A: Chemical* **1996**, 113, (1-2), 393-402.
- [151] Aissaoui, H.; Bachmann, R.; Schweiger, A.; Woggon, W.-D., *Angewandte Chemie, International Edition* **1998**, 37, (21), 2998-3002.
- [152] Meanwell, N. A.; Roth, H. R.; Smith, E. C. R.; Wedding, D. L.; Wright, J. J. K., *Journal of Organic Chemistry* **1991**, 56, (24), 6897-904.
- [153] Clezy, P. S.; Smythe, G. A., *Australian Journal of Chemistry* **1969**, 22, (1), 239-49.
- [154] Geier, G. R., III; Littler, B. J.; Lindsey, J. S., *Journal of the Chemical Society, Perkin Transactions 2* **2001**, (5), 701-711.
- [155] Lindsey, J. S., *Porphyrin Handbook* **2000**, 1, 45-118.
- [156] Georgiadis, M. M.; Komiya, H.; Chakrabarti, P.; Woo, D.; Kornuc, J. J.; Rees, D. C., *Science (Washington, DC, United States)* **1992**, 257, (5077), 1653-9.
- [157] Kozuch, S.; Leifels, T.; Meyer, D.; Sbaragli, L.; Shaik, S.; Woggon, W.-D., *Synlett* **2005**, (4), 675-684.
- [158] Bouttemy, S.; Aubry, J.-M.; Sergent, M.; Than-Luu, R. P., *New Journal of Chemistry* **1997**, 21, (10), 1073-1084.
- [159] Cryle, M. J.; Stuthe, J. M. U.; Ortiz de Montellano, P. R.; De Voss, J. J., *Chemical Communications (Cambridge, United Kingdom)* **2004**, (5), 512-513.
- [160] Groves, J. T.; Viski, P., *Journal of the American Chemical Society* **1989**, 111, (22), 8537-8.
- [161] Serra, A. C.; Marcalo, E. C.; Gonsalves, A. M. d. A. R., *Journal of Molecular Catalysis A: Chemical* **2004**, 215, (1-2), 17-21.
- [162] Wolter, T.; Meyer-Klaucke, W.; Muther, M.; Mandon, D.; Winkler, H.; Trautwein, A. X.; Weiss, R., *Journal of inorganic biochemistry* **2000**, 78, (2), 117-22.
- [163] Meunier, B.; Robert, A.; Pratiel, G.; Bernadou, J., *Porphyrin Handbook* **2000**, 4, 119-187.
- [164] Nam, W.; Choi, S. K.; Lim, M. H.; Rohde, J.-U.; Kim, I.; Kim, J.; Kim, C.; Que, L., Jr., *Angewandte Chemie, International Edition* **2003**, 42, (1), 109-111.
- [165] Yang, J.; Breslow, R., *Angewandte Chemie, International Edition* **2000**, 39, (15), 2692-2694.
- [166] Schardt, B. C.; Hill, C. L., *Inorganic Chemistry* **1983**, 22, (10), 1563-5.
- [167] Yoshimura, T.; Toi, H.; Inaba, S.; Ogoshi, H., *Inorganic Chemistry* **1991**, 30, (23), 4315-21.
- [168] Vinhado, F. S.; Martins, P. R.; Iamamoto, Y., *Current Topics in Catalysis* **2002**, 3, 199-213.
- [169] Goh, Y. M.; Nam, W., *Inorganic Chemistry* **1999**, 38, (5), 914-920.
- [170] Geier, G. R.; Lindsey, J. S., *Tetrahedron* **2004**, 60, (50), 11435-11444.

- [171] Littler, B. J.; Ciringh, Y.; Lindsey, J. S., *Journal of Organic Chemistry* **1999**, 64, (8), 2864-2872.
- [172] Tang, S. C.; Koch, S.; Papaefthymiou, G. C.; Foner, S.; Frankel, R. B.; Ibers, J. A.; Holm, R. H., *Journal of the American Chemical Society* **1976**, 98, (9), 2414-34.
- [173] Meyer, D. N.; Woggon, W.-D., *Chimia* **2005**, 59, (3), 85-87.
- [174] Poulos, T. L.; Finzel, B. C.; Howard, A. J., *Biochemistry* **1986**, 25, (18), 5314-22.
- [175] Putnam, C. D.; Arvai, A. S.; Bourne, Y.; Tainer, J. A., *Journal of molecular biology* **2000**, 296, (1), 295-309.
- [176] Corey, E. J.; Chaykovsky, M., *Journal of the American Chemical Society* **1965**, 87, (6), 1353-64.
- [177] Enholm, E. J.; Jia, Z. J., *Journal of Organic Chemistry* **1997**, 62, (26), 9159-9164.
- [178] Li, A.-H.; Dai, L.-X.; Aggarwal, V. K., *Chemical Reviews (Washington, D. C.)* **1997**, 97, (6), 2341-2372.
- [179] Mattson, M. N.; Rapoport, H., *Journal of Organic Chemistry* **1996**, 61, (17), 6071-6074.
- [180] Blatchford, J. K.; Orchin, M., *Journal of Organic Chemistry* **1964**, 29, (4), 839-43.
- [181] Banfi, S.; Cavazzini, M.; Pozzi, G.; Barkanova, S. V.; Kaliya, O. L., *Perkin 2* **2000**, (4), 871-877.
- [182] Shaik, S.; De Visser, S. P.; Kumar, D., *JBIC, Journal of Biological Inorganic Chemistry* **2004**, 9, (6), 661-668.
- [183] Sbaragli, L.; Woggon, W.-D., *Synthesis* **2005**, (9), 1538-1542.
- [184] Parthasarathy, R.; Groves, J. T., *Proceedings of the National Academy of Sciences of the United States of America* **2004**, 101, (35), 12798-12803.

9. Curriculum Vitae

Laura Sbaragli

Date of Birth: 13 July 1971 in Italy

Nationality: Italian

Civil Status: Single

WORK ADDRESS

Institut für Organische Chemie
St. Johannis Ring 19.
4056 Basel

HOME ADDRESS

Sennheimerstr.24
CH-4054
Basel

ACADEMIC INFORMATION:

- Aug 00-May 05 **University of Basel, Switzerland**
PhD Organic Chemistry student in the research group of Prof. Dr. W. Woggon
Theme: "Radical Clock Investigation with a MetalloPorphyrin Enzyme Model"
- Jan 97-Jun 00 **University of Chemistry of Florence (Italy)**
Masters Thesis in the research group of Dr. A. Mordini
Theme: "Base promoted isomerization of aziridinyl ethers".
- Nov 91-Apr 96 **University of Chemistry of Florence (Italy)**
Majored in chemistry: Obtained 110/110 Graduated 1st in class with distinction
- Sep 85-Jun 90 **Secondary School in Florence (Italy)**
Final Exam 1990: Graduated with 58/60 Graduated 1st in class with distinction

TEACHING EXPERIENCE:

- 1997- 1999 **University of Florence**
Scientific staff member with supervision of chemistry diploma students, care and control of laboratory for students in 1st year chemistry.

INDUSTRIAL EXPERIENCE:

- Jul 90-Mar 91: **Menarini Centro di Ricerca Farmaceutica, Florence**
Responsibility for filling and cataloguing incoming chemicals in research department.

SPECIAL QUALIFICATIONS:

- Analytical Equipment:** Highly experienced in all the following: HPLC, LC/GC -MS, MALDI-ToF.
Software Knowledge: MS Office, Exel, PowerPoint, Beilstein, Chemdraw, Sci-Finder, Lotus Notes

10. Eidesstattliche Erklärung

Hiermit erkläre ich an Eides statt, dass ich meine Dissertation selbständig und nur mit den angegebenen Hilfsmitteln angefertigt habe. Ich erkläre ausserdem, dass ich diese Dissertation an keiner anderen Fakultät eingereicht habe.

Basel, den 24. May 2005

Laura Sbaragli